

CHARACTERISTICS OF ABNORMALLY-PRESSURED GAS  
COMPARTMENTS, AND POTENTIAL SEALING  
MECHANISMS IN THE SPIRO SANDSTONE:  
ARKOMA BASIN, OKLAHOMA

By

RODNEY FELLER

Bachelor of Science

Oklahoma State University

Stillwater, Oklahoma

1993

Submitted to the Faculty of the  
Graduate College of the  
Oklahoma State University  
in partial fulfillment of  
the requirements for  
the Degree of  
MASTER OF SCIENCE  
July, 1995

CHARACTERISTICS OF ABNORMALLY-PRESSURED GAS  
COMPARTMENTS, AND POTENTIAL SEALING  
MECHANISMS IN THE SPIRO SANDSTONE:  
ARKOMA BASIN, OKLAHOMA

Thesis Approved:

*Zuhair al-Hajri*

\_\_\_\_\_  
Thesis Adviser

*Jordan Genev*

*Gary J. Jewell*

*Thomas C. Collins*

\_\_\_\_\_  
Dean of the Graduate College

## PREFACE

This investigation provides some plausible explanations for generation of abnormal pressures in Spiro sandstone reservoirs of the Arkoma Basin. These reservoirs are thrust and completely sealed compartments. A better understanding of the geometry and sizes of these compartments may lead to a more accurate estimate of the basin's natural-gas reserves. In addition, the findings may also lead to significant decreases in the risk involved in exploring for natural gas in such a tectonic setting.

Compartmentation processes and sealing mechanisms were studied by integrating various geological and geophysical models and information. These include, structural and tectonic framework of the basin, depositional setting, diagenetic patterns, and pressure regimes. The significant source of information was produced by modeling of the Wilburton area in the Ouachita fold and thrust belt. Chamosite-bearing facies were identified as being the best reservoir quality in the Spiro sandstone. The spatial relationships of the models and information was used to model basin diagenesis.

Diagenetic patterns observed were greatly influenced by mechanical as well as chemical processes involved in the basin evolution. For example, diagenetic cements from various pore fluids, and shale smears from fault actions. These patterns were useful in evaluating various hypotheses related to the development of seals and the preservation and/or destruction of primary porosity.

## ACKNOWLEDGEMENTS

I wish to express sincere appreciation to my primary advisor, Dr. Zuhair Al-Shaieb for his intelligent supervision, constructive guidance and inspiration. My sincere appreciation extends to my other committee members Dr. Ibrahim Cemen and Dr. Gary Stewart, whose guidance, assistance, encouragement, and friendship are also invaluable. I would like to thank Dr. Zuhair Al-Shaieb and the Department of Geology for providing this research opportunity, and their generous financial support, made possible with a grant from the Oklahoma Center for the Advancement of Science and Technology.

Moreover, I wish to express my sincere gratitude to those who provided suggestions and assistance for this study: Dr. Arthur Cleaves, James Puckett, Forrest Hess, Chris Cambell, Salim Aktar and Ata Sagnat. Thanks must also go to my parents for their support and encouragement, throughout my entire college career.

Finally, I would like to thank the School of Geology and staff for their support during these two years.



## TABLE OF CONTENTS

Chapter	Page
I. INTRODUCTION	
Background.....	1
The Problem.....	1
Purpose of the Study.....	1
Objectives of the Study.....	1
Significance of the Study.....	4
Scope and Limitations.....	4
Outline of Work.....	4
II. GEOLOGICAL SETTING	
Geologic History.....	4
History of Gas Production.....	6
Stratigraphy.....	8
Structural Geology.....	8
III. METHODOLOGY	
Data Bases.....	12
Data Sources.....	12
Pressure Data.....	12
Log Data.....	14
Seismic Data.....	18
Core Sampling.....	19
Thin Sections.....	20
X-Ray Diffraction.....	20
Cathodoluminescence.....	20
Fluid Inclusions.....	20
IV. PETROLOGY AND PETROGRAPHY	
Constituents.....	20
Porosity.....	25
Depositional Environments.....	25

Chapter	Page
<b>V. STRUCTURAL GEOLOGY</b>	
Structural Features .....	31
Fault Components .....	32
<b>VI. PETROLEUM</b>	
Kerogen .....	32
Generation .....	36
Pressure Regimes .....	38
<b>VII. RESERVOIR QUALITY</b>	
General Description .....	40
Effect of Clays .....	44
<b>VIII. DIAGENESIS FROM BASIN EVOLUTION</b>	
Diagenetic Minerals .....	46
Compartmentation .....	46
Formation of Abnormal Reservoir Pressures .....	61
<b>IX. SUMMARY, CONCLUSIONS AND RECOMMENDATIONS</b>	
Summary of Findings .....	62
Conclusions .....	64
Recommendations for Further Studies .....	67
BIBLIOGRAPHY .....	68
APPENDICES .....	74
APPENDIX A: PRESSURE DATA TABLES .....	75
APPENDIX B: X-RAY DIFFRACTOGRAMS .....	90
FLUID-INCLUSION DATA	
APPENDIX C: WELL-LOG DATA .....	102
PETROLOGS	
FORMATION DATA	
APPENDIX D: PLATES I-IV .....	109

## LIST OF TABLES

Table	Page
I. Pressure Data Wells 1960-1969 .....	76
II. Pressure Data Wells 1960-1979 .....	78
III. Pressure Data Wells 1960-1989 .....	80
IV. Pressure Data Wells 1960-1994 .....	83
V. Potentiometric Data .....	89
VI. X-ray Diffraction Pan American 1 Reusch .....	91
VII. Fluid-inclusions Pan American 1 Reusch .....	101
VIII. Well-log Evaluations of Spiro Zones .....	103
IX. Formation Lithologies and Thicknesses .....	108

## LIST OF FIGURES

Figure	Page
1. Map of Natural Gas Production in the Arkoma Basin .....	2
2. Map of the Arkoma Basin Showing the Study Area .....	3
3. Regional Province Map of Eastern Oklahoma and Western Arkansas .....	5
4. Generalized Surface-structure Map of Arkoma Basin .....	7
5. Generalized Stratigraphic Column of Arkoma Basin .....	9
6. Generalized block-diagram of structure and facies through Wilburton Area .....	10
7. Tear-fault Compartmentation Model .....	11
8. Generalized Pressure-gradient Map of Wilburton Area .....	13
9. Pan Am #1 Reusch: Well-log Curves .....	15
10. King 1-3 Layden: Well-log Curves .....	16
11. Arkoma #1 Cindy: Well-log Curves .....	17
12. Seismic Cross-section through Wilburton Area .....	19
13. Shell 1 Mabry: Well-log Curves .....	26
14. Isopach Map of the Atokan Spiro Sandstone .....	28
15. Paleogeographic Map of Atokan Arkoma Basin Area .....	29
16. Diagram of Depositional Environments .....	30
17. Generalized Diagram of Imbricate Complex .....	33
18. Thermal Maturity and Kerogen Types of Arkoma Basin .....	35

Figure	Page
19. Burial and Maturation Curves, Arkoma Basin.....	37
20. Pressure-Depth Plots, Spiro Sandstone.....	39
21. 3-D Potentiometric Plot, Arkoma Basin.....	110
22. Lithologic Map, Spiro Sandstone.....	42
23. King #1 Layden: Well-log Curves.....	43
24. Plot of Percent Chamosite v. Percent Porosity.....	47
25. Model for Spiro Compartmentation.....	48
26. Photomicrographs from the Pan American 1 Reusch Core.....	50
27. Photomicrographs from the Pan American 1 Reusch Core.....	51
28. SEM Photographs of Chamosite in the Pan American 1 Reusch Core.....	52
29. Cathodoluminescence Photomicrographs of Pan American 1 Reusch Core.....	54
30. Photomicrographs of Fluid Inclusions in the Pan American 1 Reusch Core.....	56
31. Plot of Pressure v. Depth, Fluid Inclusions.....	58
32. Calculated Burial History with Diagenetic History.....	59
33. Diagram of Pressure Differences, Spiro Sandstone.....	63

## ABBREVIATIONS

Ro	vitrinite reflectance
psi	pressure per square inch
$\phi$	porosity of rock
Den	density porosity of rocks
S	sonic porosity of rocks
MMcf	gas production totals in million cubic feet
whsip	well-head shut-in pressure
IBHP	initial bottom-hole pressure
BHT	bottom-hole temperature
perf	interval of perforated rock
TTI	time-temperature index

## INTRODUCTION

The Arkoma basin of southeastern Oklahoma contains some of the most productive gas fields in the region. Some fields have been producing since the late 1950s (Figure 1). New wells are currently being completed. One of the most productive target zones in the Arkoma basin of Oklahoma is the Atokan Spiro Sandstone. In Oklahoma, cumulative gas production from wells that produce only from the Spiro total more than 1.6 billion cubic feet, as of 1994.

Production and exploration in the Arkoma basin has not been successful everywhere. Much of the problem is related to discontinuities in reservoirs, due to the complex geometry of structural features and an extensive diagenetic history. These reservoir qualities have led to dry holes and wells abandoned due to poor production, as places where other geologic variables were favorable.

The purpose of this study has been to provide an explanation as to the structural style and diagenetic patterns that explain the formation of abnormally pressured reservoir compartments, in the Wilburton area (Figure 2). The resulting model may provide information as to how to reduce the risk involved with gas exploration and production within the Arkoma basin or in other basins with similar features.

The objectives outlined for the study, which included:

1. Identification of local areas where pressure gradients are abnormal.
2. Explanation of localized abnormal-pressure gradients.
3. Identification of various mechanisms of compartmentation.
4. Implications of reservoir continuity
5. Modeling of a diagenetic and tectonic history for the basin

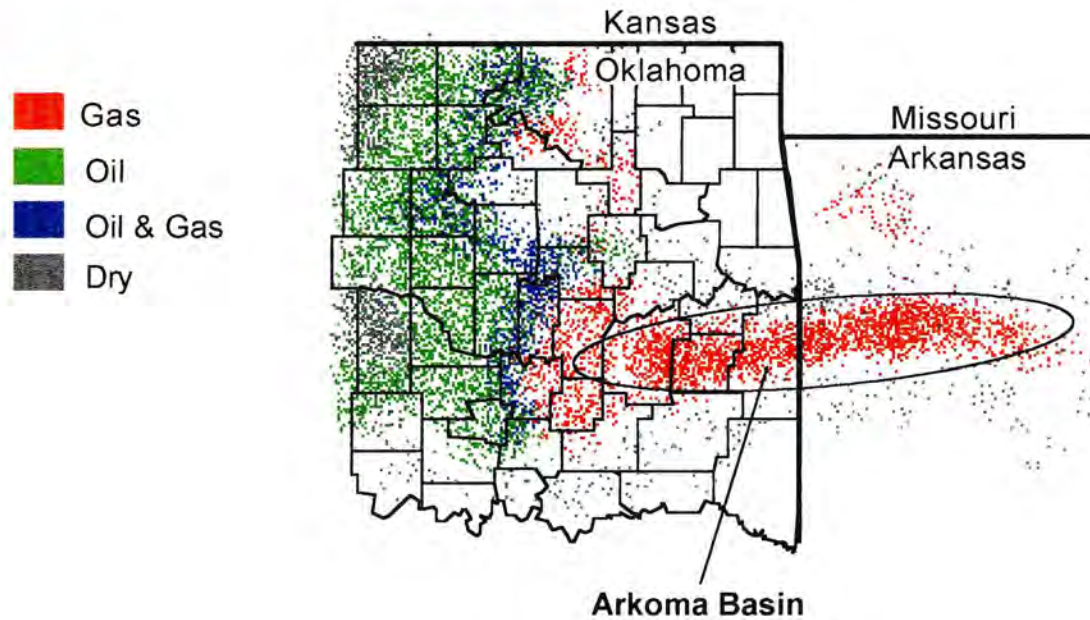
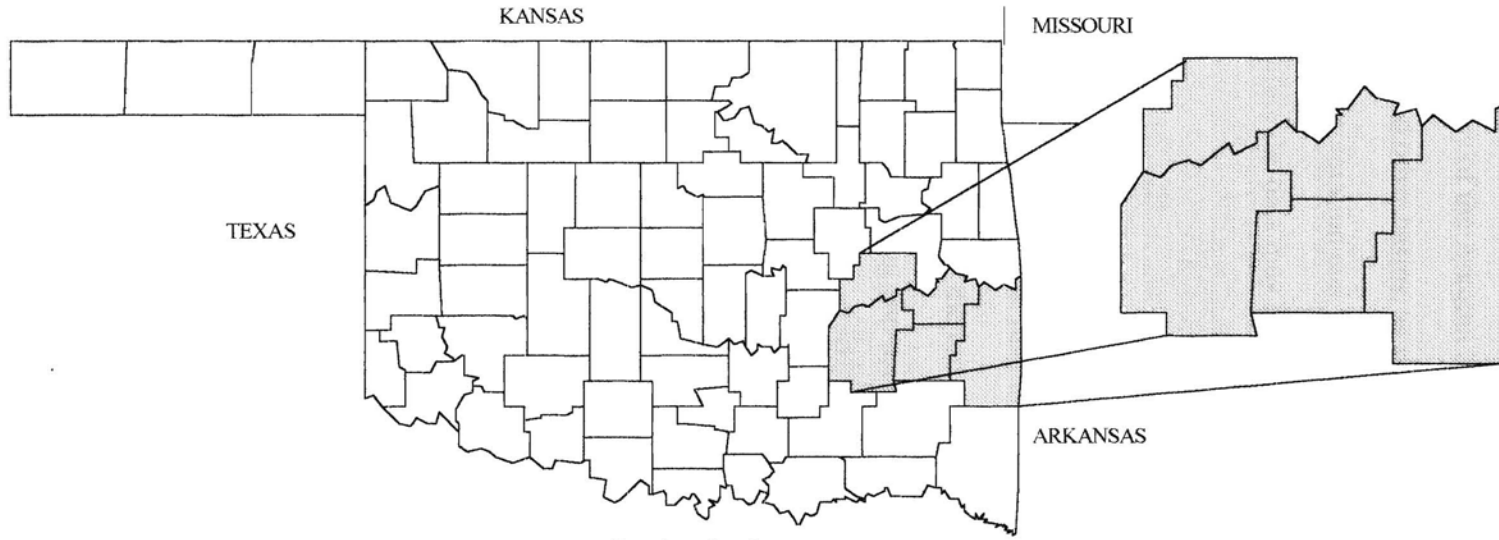
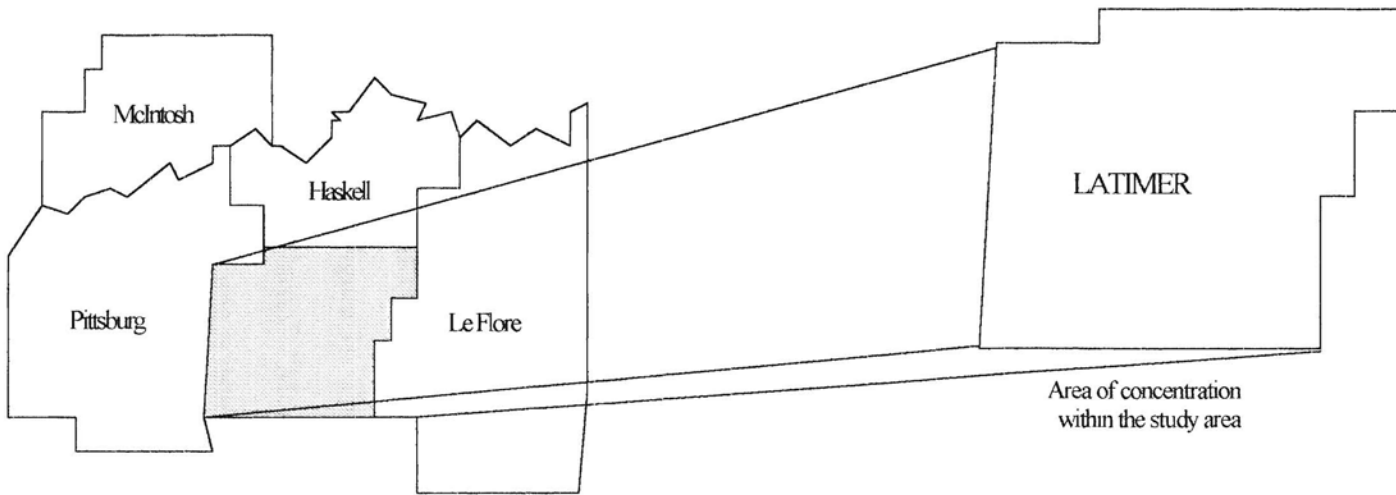


Figure 1. A map of localities where petroleum has been produced in the Arkoma basin region. Gas production in southern Oklahoma follow the trend of the Frontal Fold and Thrust Belt (source: U.S. Geologic Survey).





Regional location of study area.



Area of concentration within the study area

Through the integration of current study and previous work on the Spiro Sandstone, a model has been proposed to give a more refined and detailed explanation of the geology of the Arkoma basin. The investigation may provide data for further studies of this and other basins, as well as for use by the petroleum industry to reduce economic risks in exploration and production. The reserves of all hydrocarbon reservoirs are finite. Therefore the data may also be of significant benefit in secondary recovery, of oil and gas.

This study has been limited to the data available to the public and to gracious donations of proprietary work by various organizations. Many technological advances have been made since the initial production in the Arkoma basin, which accounts for the difficulty in obtaining and using data from early production wells. The localization of oil and gas fields necessitates “gaps” in well control across the basin, which has been compensated in some areas, by estimation of circumstances.

## GEOLOGIC SETTING

The term “Arkoma basin” was introduced in the late 1950s for the asymmetric structural depression between the south flank of the Ozark Uplift (the Boston Mountains) and the thrust front of the Ouachita Mountains (Cline, 1960, p.16)(Figure 3). The new name replaced terms used earlier in Oklahoma, terms such as “Coal basin”, “McAlester basin” and “McAlester coal fields”. The northern boundary in Oklahoma is usually drawn at the Mulberry fault, a major south dipping normal fault. The tectonic southern boundary of the Arkoma basin is well defined in Oklahoma as the outcrop trace of the Choctaw fault (Arbenz, 1989, p.623).

The ancient Oklahoma embayment was the predominant sedimentary feature of Oklahoma and Arkansas, until the post-Hunton (Devonian) orogeny changed sedimentary

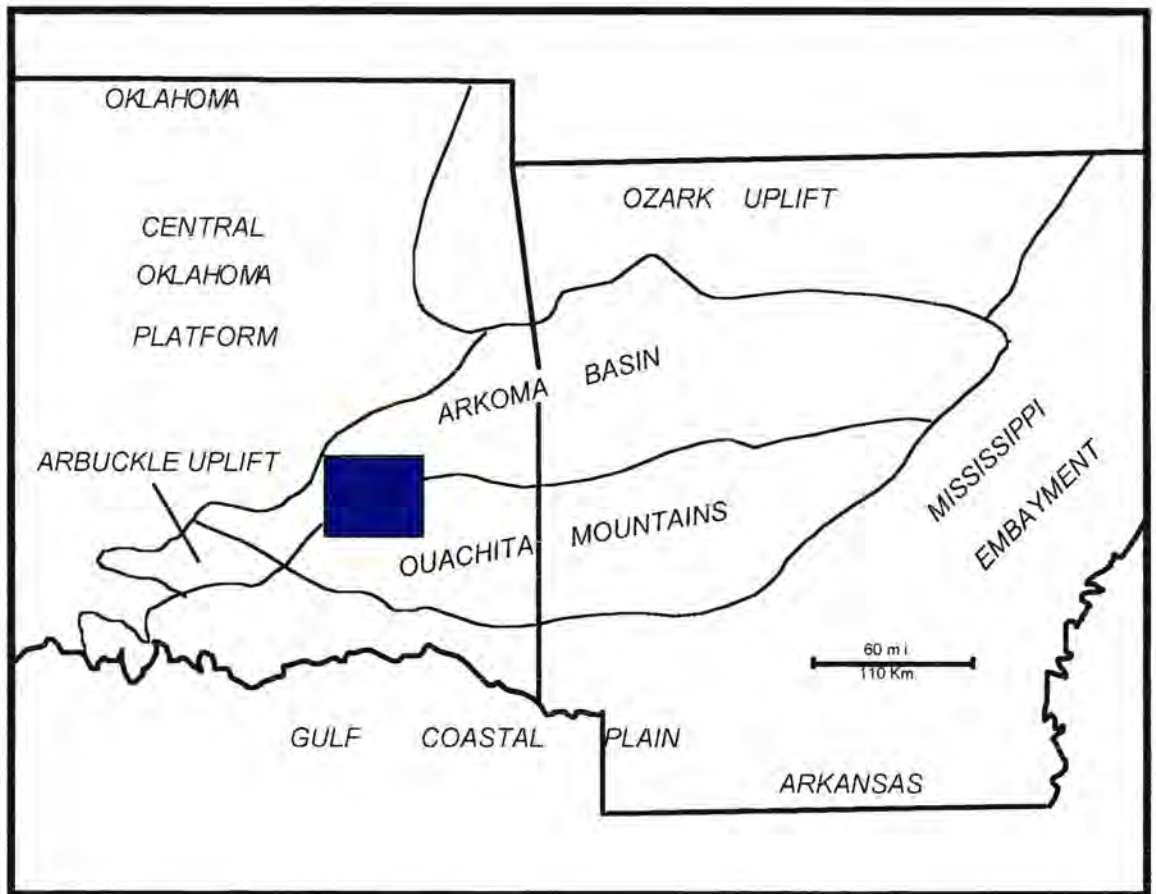


Figure 3. Geologic Provinces of Eastern Oklahoma and Western Arkansas.  
 (After Camp and Ratliff, 1991).

patterns. In the Arkoma basin, beds below the Mississippian System thicken to the south-southeast. At the beginning of the Mississippian Period, a large part of what is now the deeper part of the basin was very high. This is made evident by the Silurian-Devonian limestone of the Hunton Group on the basin shelf, whereas in much of the deep basin the Hunton is thinner or absent by truncation before deposition of Mississippian strata. The arch began to subside during Mississippian time; maximal subsidence was during the Early and Middle Pennsylvanian in the Atokan and Early Desmoinesian Epochs (Branan, 1966). During the Pennsylvanian Period, the southern mid-continent region included the margin of the Paleozoic continent Laurasia. This portion of the Laurasian continental margin was initially an Atlantic-type passive margin, as the distal end of the Southern Oklahoma Aulacogen. The assembly of Pangea by the collision of Laurasia and Gondwana resulted in a transition to a convergent margin. The Pennsylvanian was a period of accelerated subsidence, due in part to the convergence. Sedimentation continued until the Late Pennsylvanian Arbuckle orogeny of southern Oklahoma. This orogeny uplifted the Tishomingo anticline in south-central Oklahoma and separated the subsident Arkoma basin from the Fort Worth basin, south of the uplift. During the late Atokan to Permian, the Ouachita Mountain orogeny developed as an incipient uplift (Figure 4). During this period sedimentary patterns of the Middle to Late Pennsylvanian were affected, but little effect was made on the structural framework of the basin. The Permian movement modified the entire province. In the Arkoma basin compressional forces caused crustal shortening and folding with thrust faulting. The Arkoma basin was tilted westward after the Ouachita folding, presumably by the later Appalachian movements. The Late Permian and the Cretaceous Laramide orogeny had minor influence on the basin. The basin is still active with small earth shocks recorded in the area (Branan, 1966).

During formation of the basin, extensive heat flow as a consequence of basin formation and surrounding orogenies matured organic material within the Spiro

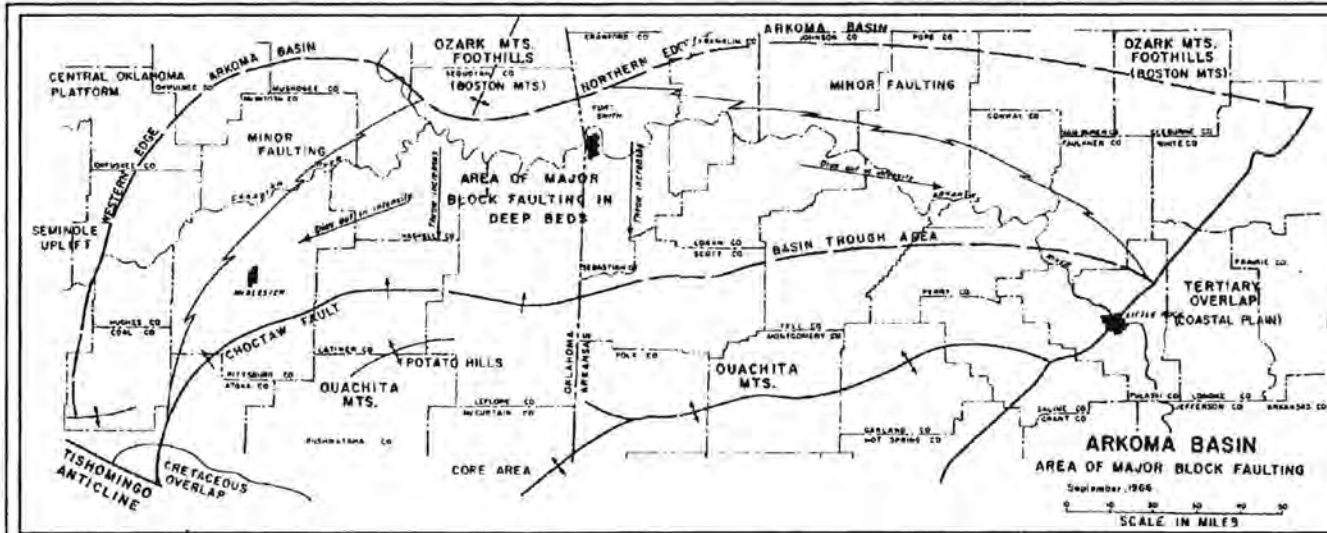
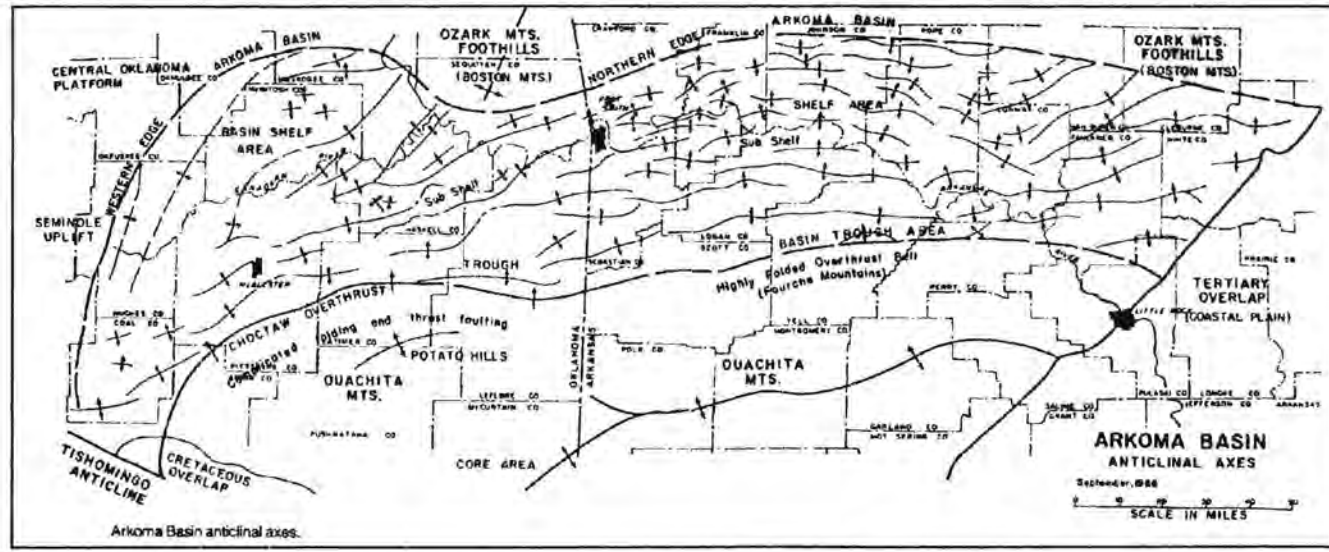


Figure 4a. Location and trend of block-faulting in the Arkoma basin of Oklahoma and Arkansas. (after Branan, 1966)

Figure 4a. Anticlinal axes at the surface in the Arkoma basin of Oklahoma and Arkansas. (after Branan, 1966)



Arkoma Basin anticlinal axes.

Sandstone, as well as thick shale sequences below the Spiro. The Type III kerogens passed quickly into the gas window to produce dry gas. This natural gas has been produced in the Arkoma basin more than forty years. The cumulative production for the entire Arkoma basin in Oklahoma and Arkansas is about 3 trillion cubic feet.

The Stratigraphy of the Arkoma basin begins with Cambrian units that were deposited upon PreCambrian Washington Volcanic Group basement. Rock-stratigraphic units at the surface are of Late Pennsylvanian age. It has never been fully established whether units younger than the Pennsylvanian/ Permian were ever deposited, or whether these units have been deposited and removed over time. The Spiro Sandstone is the lowermost Atokan formation of Pennsylvanian strata in the Arkoma basin (Figure 5). The Atokan Formation unconformably overlies the Morrowan Wapanucka Limestone, and is overlain throughout the axial part of the basin by Hartshorne Sandstone and McAlester Formation of Desmoinesian age (Zachry and Sutherland, 1984).

Probably the most controversial component of the Arkoma basin is the subsurface structural geology. Figure 6 shows a generalized cross-section through the Wilburton area. The Arkoma basin north of the Choctaw fault is composed of normal block faulting formed as an integral part of the Southern Oklahoma Aulacogen. These blocks acted as ramps for the thrust faulting that makes up the major structure of the basin. The most significant aspect for thrusting in the Arkoma basin for the purpose of this study has been the formation of stacked sheets of Spiro Sandstone. These are formed by a complex of imbricate thrust faults; in turn may be acting as a ramp for the Choctaw fault, forming the frontal Ouachita boundary. Differential thrusting has resulted in tear-faulting, which has added a shear component to the imbricate complex (Figure 7). This model helps explain discontinuity in the imbricate complexes, as the amount of stacked sheets decreases to the east and west from the Wilburton area.

SYSTEM/SERIES		GROUP/FORMATION/BED	ROCK TYPE	PAY ZONE	
PENNSYLVANIAN	DESMOINSIAN	Boggy Fm.	Shale		
		Savanna Fm.	Shale		
		McAlester Fm.	Shale	☀	
		Hartshorne Fm.	Shale	☀	
	ATOKAN	UPPER	Atoka Fm.	Shale	
			M	Shale	
			L	Shale	
			K	Shale	
			J	Shale	
			I	Shale	
		MIDDLE	Fanshawe	Shale	☀
			Red Oak	Shale	☀
			Panola	Shale	☀
			Brazil	Shale	☀
			Cecil	Shale	☀
			Shay	Shale	☀
		LOWER	C	Shale	
	B		Shale		
	A		Shale		
	<b>Spiro</b>		Sandstone	☀	
	MORROWAN	Wapanucka Fm.	Limestone	☀	
		Union Valley Fm.	Limestone		
		Cromwell Fm.	Sandstone	☀	
MISSISSIPPIAN	Caney Fm.	Shale			
DEVONIAN	Woodford Fm.	Shale			
SILURIAN	Hunton Gp.	Limestone	☀		
ORDOVICIAN	Sylvan Fm.	Shale			
	Viola Gp.	Limestone			
	Simpson Gp.	Sandstone			
CAMBRIAN	Arbuckla Gp.	Dolomite	☀		
	Regan Fm.	Sandstone			
PRECAMBRIAN	Washington Volcanic Gp.	Igneous			

SANDSTONE   
 LIMESTONE   
 DOLOMITE   
 SHALE  
 IGNEOUS

Figure 5. Stratigraphic column Arkoma basin (after Camp and Ratliff, 1991).



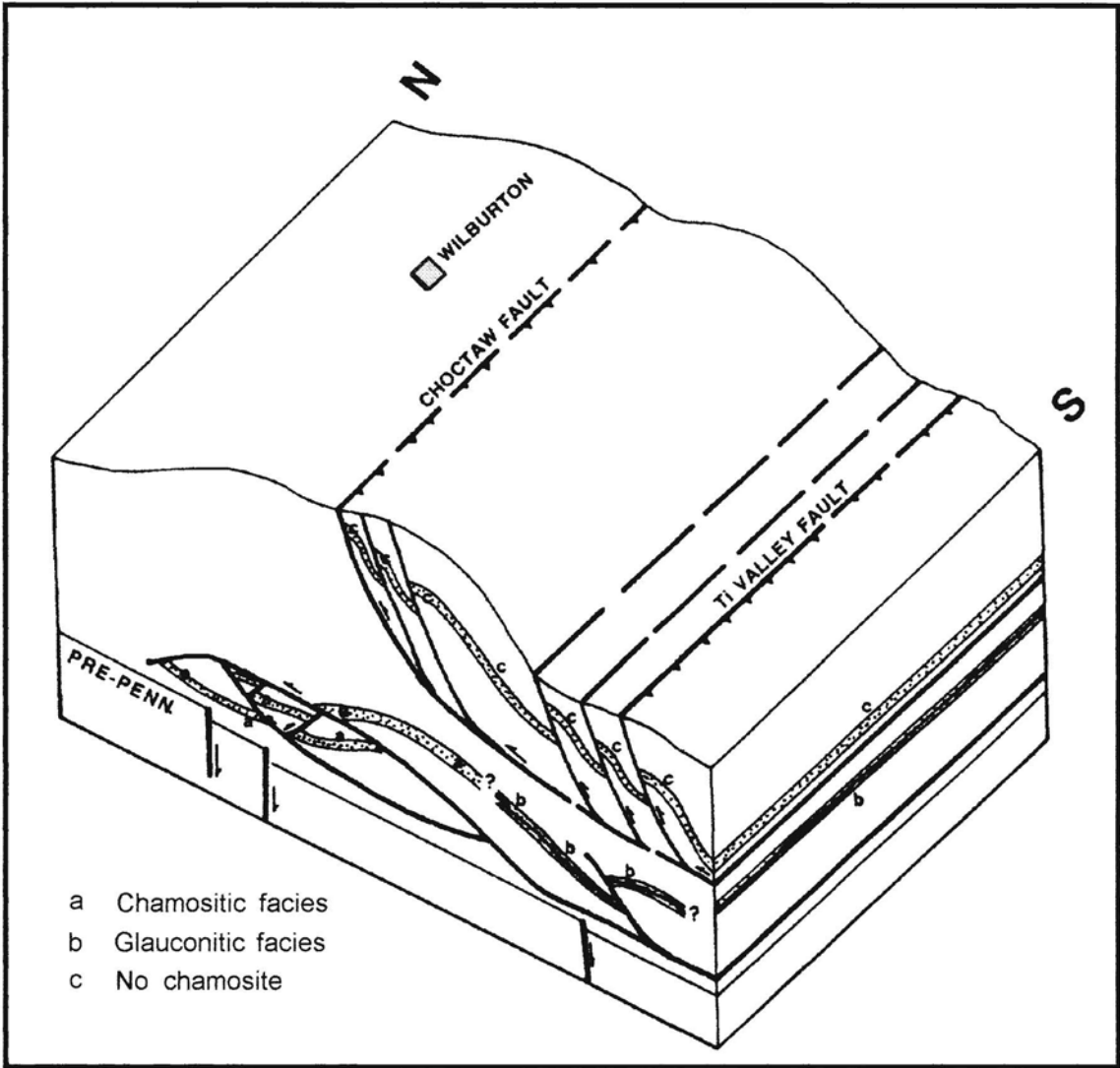


Figure 6. Block Diagram, structure and facies in the Wilburton area (after Cemen, 1993).



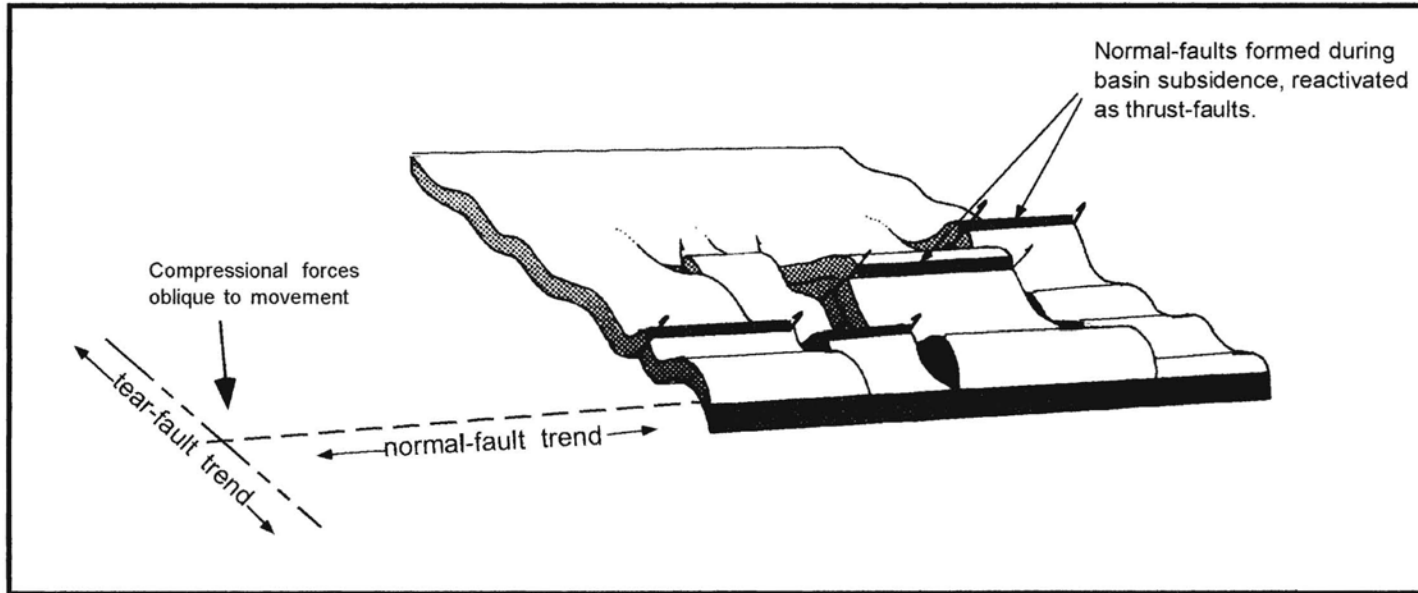


Figure 7. Schematic block diagram, illustrating compartmental shear faulting model for the Wilburton area (after Davis, 1991).

## METHODOLOGY

The presence of compartmentation, and sealing mechanisms were studied by integrating various geological and geophysical models and information. The study included the structural and tectonic framework of the basin, depositional setting, diagenetic patterns, and pressure regimes.

Data about formation pressures and production-totals used in the study were obtained from Dwights Natural Gas Well Production Histories. The data have been tabulated by well, for single completions in Spiro Sandstone. This data was used to map Initial Bottom Hole Pressures (IBHP), and calculating pressure gradients and cumulative productions.

Initially, more than 500 wells were selected as single-Spiro Sandstone completions for the Arkoma basin in Oklahoma (Table 1, Appendix). A generalized pressure-gradient map was constructed using all Spiro wells reported since 1960. From this map the area of abnormally pressured Spiro reservoirs was identified as being confined to the Wilburton area, which includes the Wilburton and South Panola Fields (Figure 8). The study area was reduced to the Wilburton area for more detailed investigation of Spiro pressure-regimes.

The well data for the study area were tabulated by several means in order to compare the pressure data over time (Appendix). Data was tabulated with pressure data from 1960 to 1994 (most current), then tabulated by year in ten-year blocks for comparison of bottom-hole pressures over time. Tabulated data for each ten year block was plotted in pressure-depth plots which show decline in bottom-hole pressures over time. A decline analysis by well was not prepared, due to the fact that bi-yearly tests were 24-hour tests, therefore, data obtained may not be accurate pressure data for the area drained by production. Due to differences in porosity and permeability across the Wilburton area, 24 hours may not be adequate time for pressure build-ups in wells with

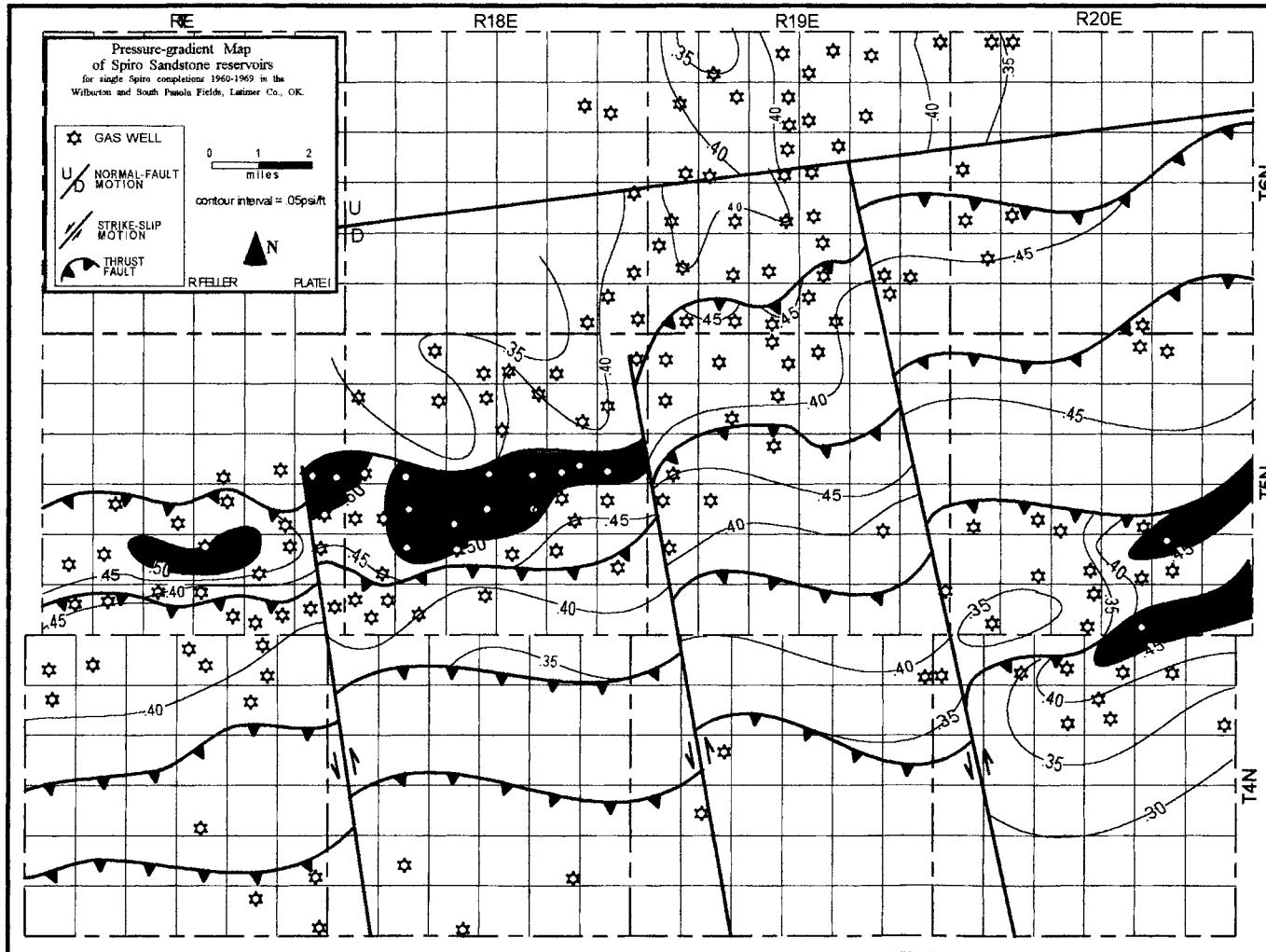


Figure 4. Pressure-gradient map with general areas of abnormal-gradients, Wilburton ■ and South Panola ■ Fields.

low permeabilities. Therefore, initial-bottom-hole pressures were the only data deemed reliable for estimation of declines in reservoir pressures.

Well logs for the equivalent pressure data were gathered from several sources. Gamma-ray logs, resistivity logs and porosity logs were used for identification and correlation of zones within the Spiro. The correlation of zones identified in the Spiro across the Wilburton area was the basis for mapping of continuity of diagenetic-seal zones and reservoir porosities. Two type-logs used for the area were the Pan American 1 Reusch, Sec. 3, T. 4N., R. 19E.(Figure 9), King 1 Layden, Sec. 3, T. 4N., R. 17E. (Figure 10), and An Son 1-21 Cindy, Sec. 21, T. 5N., R. 20E. (Figure 11).

Because porosities and permeabilities of the Spiro sandstone are due to preservation of porosity by chamosite (Al-Shaieb and Lynch, 1989), porosity logs were used to correlate the chamosite facies across the area. Logs of wells with available cores were correlated with logs of other wells to map lithologic zones within the Spiro. Wells with gamma-ray and porosity logs were used to identify lithologies in wells without core data. The variation in age and types of porosity logs used by logging companies posed the problem of measuring reliability of reported porosities. Density-porosity and bulk-density logs were the porosity logs preferred for the study, as they are the most consistent in light of lithologic changes and presence of hydrocarbons. The incorporation of sonic, neutron, and bulk- density porosity logs required adjustments, to fit density-porosity log data better. Where core porosity has been tested, and more than one kind of porosity log has been run in the same well, a correction factor can be calculated (Feller, Exxon unpublished). However, no such data was available for this study. Upon mapping of the Spiro-zone porosities, anomalous data were ignored or adjusted to fit the surrounding values.

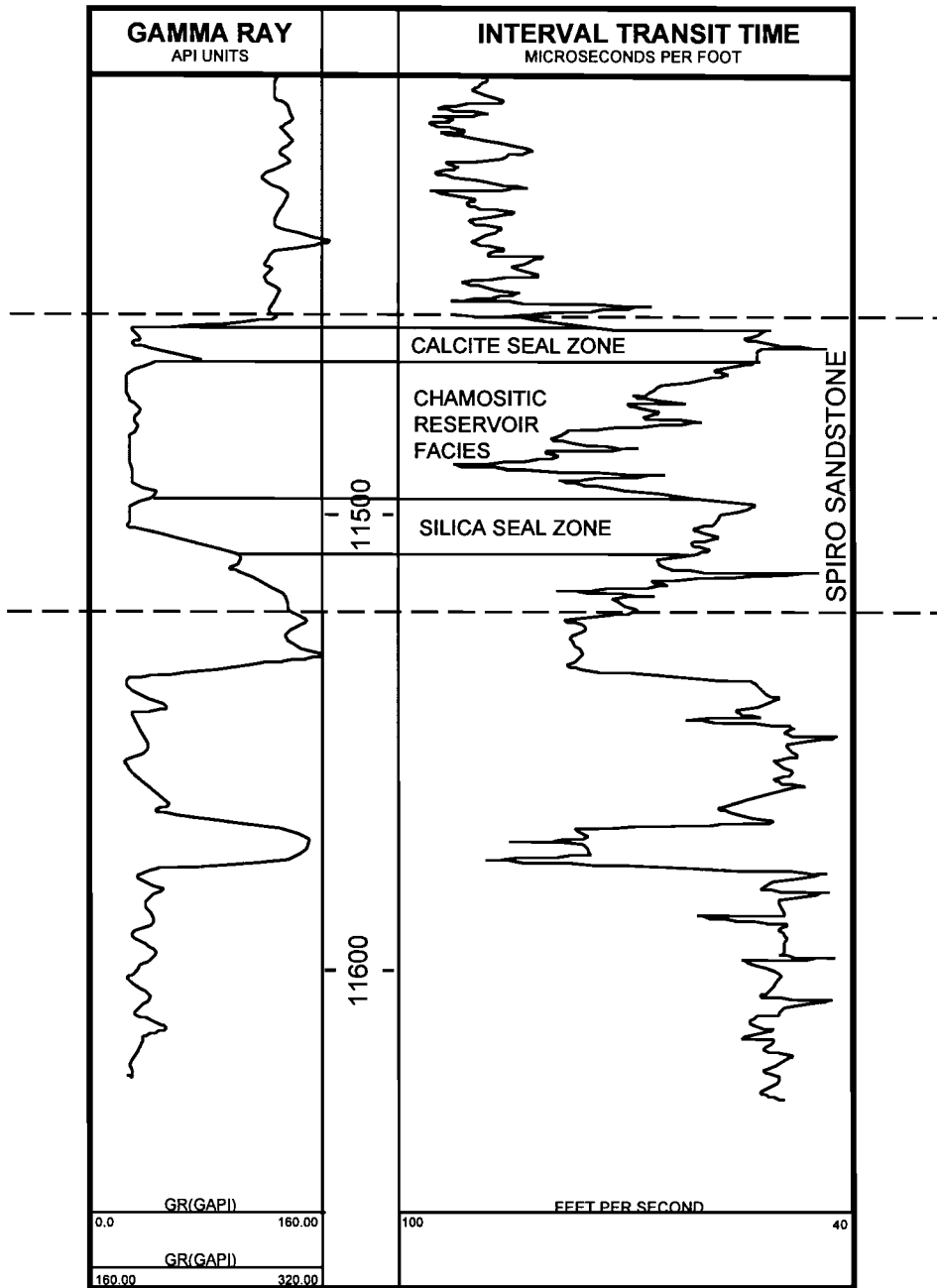


Figure 9. Gamma-ray and interval transit-time logs, Spiro Sandstone, Pan American 1 Reusch, Sec. 3, T. 5N., R. 19E.

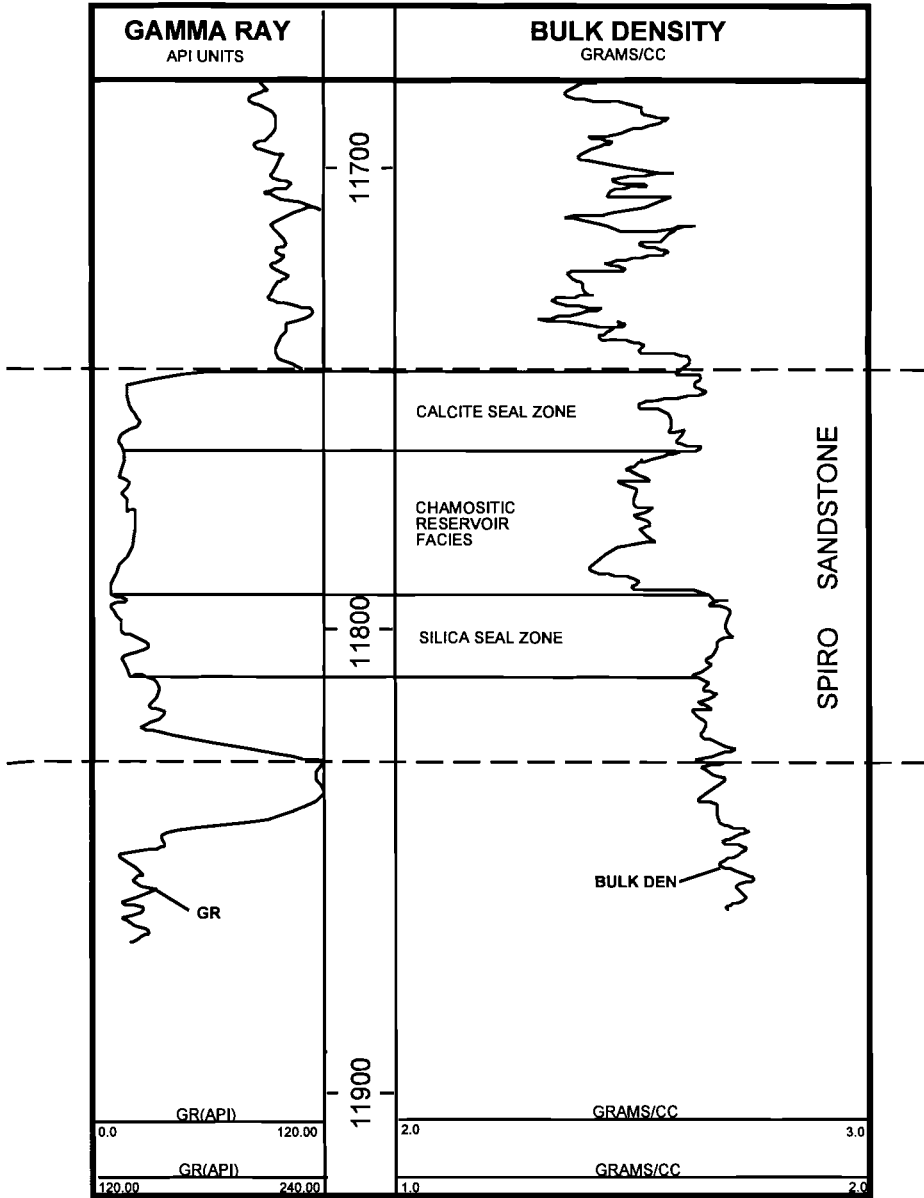


Figure 10. Gamma-ray and bulk-density logs, Spiro Sandstone, King 1 Layden Sec. 3, T. 4N., R. 17E.

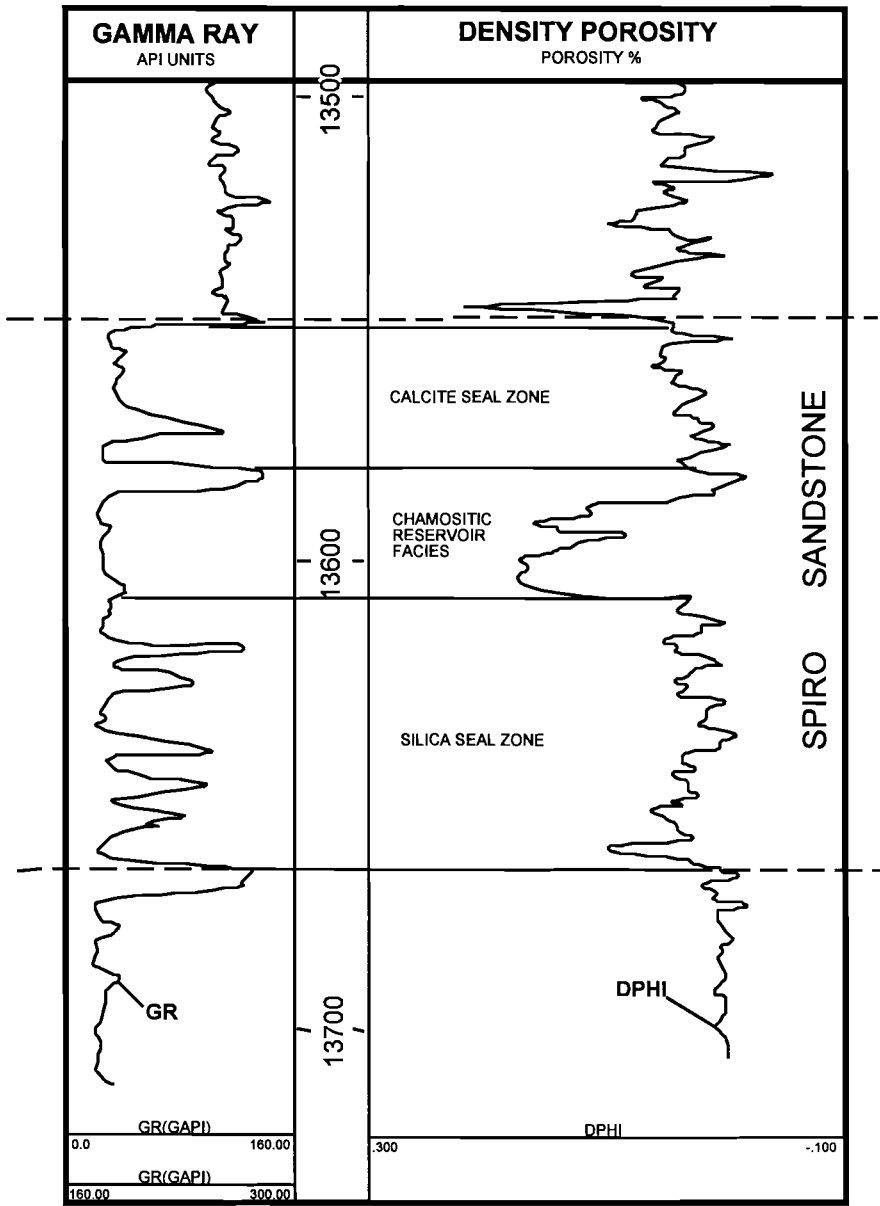


Figure 11. Gamma-ray and density-porosity logs, Spiro Sandstone, An Son 1-21 Cindy Sec. 21, T. 5N., R. 20E.

Seismic lines that aided in the interpretation of structural geology were taken from the area were obtained from published works (Wilkerson and Wellman, 1993., Valderrama and others, 1994) and were donated by Exxon USA. The primary seismic line used in this study (Figure 12) is a migrated line through the Wilburton area. The seismic lines were used to verify the imbricate structure in the Wilburton area.

Cores were sampled from wells close to the abnormal pressure zones, the wells included Pan American 1 Reusch Sec. 3, T. 5N., R. 19E., Shell 1 Mabry Sec. 9, T. 4N., R. 18E. and Amoco 25-1 Erlaine Wheeler Sec. 36, T. 5N., R. 19E. (thins-section samples only). The cores were examined by hand samples to identify lithologic changes, sedimentary structures, and to correlate with well logs. From visual inspection, contacts and lithologic changes were marked for thin-section sampling. These cores were logged on a prepared report sheet; where and observations were also noted. Samples taken for thin sections were also used for x-ray-diffraction evaluation, cathodoluminescence, and for identification of fluid inclusions, to identify types and timing of potential seals and chamosite zones.

Samples from the cores used in the study were analyzed by x-ray-diffraction in order to identify mineral constituents. Preparation of samples consisted of crushing and pulverizing for bulk runs. Powdered samples were bathed in dilute acid while being heated to remove calcium carbonate. Then clays were extracted by centrifuging, and by rinsing the samples to settle quartz grains, leaving clay particles in suspension. Porcelain tiles were heated and the solution containing suspended clays was spread on the tiles, water evaporated, depositing the clay. Three tiles were used for each sample; one sample was heated to collapse expandable clays, another sample was glycolated to expand the clay, and the third tile was regarded as the normal sample.





Thin-sections from the Pan American 1 Reusch and Shell 1-9 Mabry were also studied by cathodoluminescence to identify the stages of diagenesis in the seal-zones. The samples were placed into a vacuum stage on a petrographic microscope and bombarded with electrons. Photomicrographs were taken during the process. The purpose of analysis by cathodoluminescence was to evaluate stages of diagenesis in various zones of the Spiro.

Fluid inclusions in samples taken from the Pan American 1 Reusch were studied to estimate the temperature of formation in the upper calcite and lower quartz-overgrowth zones in the Spiro. Doubly polished (polishing of both sides of the sample) plates of the core samples are necessary for microthermometry, to prevent pits in samples; the pits limit the effectiveness of the microscope and prevent seeing into the inner layers of samples. For study of phenomena of diagenesis, the plates are cut thin ( $\sim 50\mu\text{m}$ ) so as to allow the appropriate amount of light to pass through. Some techniques consist of leaving the thin-section attached to the glass slide used in making the sample. However, in this study an adhesive was used that allowed the grinding of the samples, but that was dissolved with acetone to separate the sample from the glass. The proper preparation of samples allows the study of phase changes in small inclusions ( $<2\ \mu\text{m}$ ).

## PETROLOGY AND PETROGRAPHY

The Spiro Sandstone in the Wilburton area is very-fine to medium-grained and moderately well sorted quartz arenite, sub-litharenite and calcareous sandstone. Quartz is the major constituent; feldspar, rock fragments, and skeletal fragments are present in various amounts (Al-Shaieb, Shelton, and Puckette, 1989).

The most abundant quartz grains in the Spiro Sandstone are well rounded; some show uniform extinction, while others show undulose extinction. Monocrystalline quartz is most common; polycrystalline quartz is present in much lesser amounts. Samples taken from fault zones in the Wilburton area include fractured quartz grains.

Plagioclase and K-feldspar are of minor amounts. Plagioclase grains are easily identified by their albite twinning. Orthoclase is identified by the cloudy or dirty appearance due to alteration, and is untwinned. Perthite and microcline are less common than orthoclase in the Spiro (Al-Shaieb, Shelton, and Puckette, 1989).

Metamorphic and sedimentary rock fragments are minor constituents. Sedimentary rock fragments consist mostly of clay or mudstone, while others consist of carbonate-rock fragments are a minor component.

Other minor constituents include skeletal fragments that range in type and abundance depending on position of the Spiro interval. The various types of fossil fragments include bryzoans, echinoderm plates and stems, and fusulinids. Muscovite, biotite, zircon, and rutile are present as exotic grains.

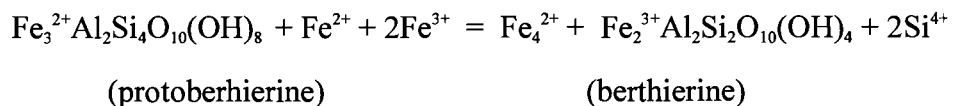
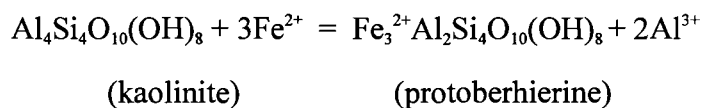
Diagenesis of the Spiro Sandstone produced authigenic constituents such as clays and cements. Illite and kaolinite are present in some wells, and occur as pore-filling or pore-lining materials. Chamosite is in sandstone from wells in the northern part Wilburton area, whereas in the southern part chamosite is absent. Glauconite is the dominant clay in the southern part (Al-Shaieb and Lynch, 1989). Pressure solution is evident from extensive stylolitization of quartz grains. Pyrite is restricted mostly to fracture-fillings; however, nodules of pyrite were recorded in many samples.

Formation of authigenic micas and clay minerals occurs mainly at temperatures and pressures higher than those that exist at the Earth's surface, although glauconite commonly forms under comparatively low-pressure and low-temperature conditions on the sea floor. Montmorillonite, or other smectite clays, contain interlayer water that can be lost during diagenesis. Loss of water, combined with replacement of sodium by potassium and replacement of some silicon by aluminum, convert montmorillonite to illite. Dehydration of montmorillonite is temperature-dependent, and the threshold temperature required for alteration to illite ranges from about 70°C to more than 150°C (Bruce, 1984). Temperatures in the range of 100°C to 150°C are most common.

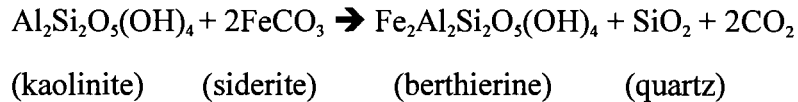
Kaolinite also breaks down at about the same temperatures, although kaolinite and illite can coexist. Thus, illite and chlorite tend to increase during deep burial, at the expense of montmorillonite and kaolinite. Dehydration of montmorillonite releases pore waters that may differ in chemical composition from pore waters of adjacent sediments. The escape of these waters during diagenesis is believed to be an important mechanism for flushing petroleum from shales into permeable sandstones or limestones (Boggs, 1987).

The iron-silicate minerals chamosite and glauconite are restricted to marine continental-shelf environments (Porrenga, 1967). These minerals form in areas of low sedimentation, and in the presence of some organic matter, primarily by alteration of other minerals at the sediment-water interface or at very shallow burial depths. Therefore, these authigenic minerals are fairly reliable indicators of marine conditions (Selley, 1978). Curtis and Spear (1968) indicate initial precipitation of berthierine as a mixed gel, stable at positive Eh, with subsequent transformation to chamosite.

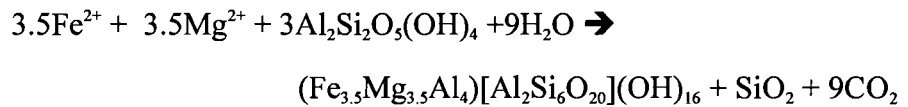
Chamosite has also been defined as diagenetic in origin. Bhattacharrya (1983) suggests that the chamosite precursor berthierine, is diagenetically related to a detrital precursor. In experimental conditions, pH= 7 and Eh= -250 to -350 mv, berthierine has been precipitated.



Iijima and Matsumoto (1982) proposed the transformation of siderite and kaolinite to berthierine, under reducing conditions and temperatures between 65 and 150° C under burial conditions of 2-5 km.



Boles and Franks (1979) advocated the formation of iron-rich chlorite by the reaction of kaolinite, Fe, and Mg, released by during illitization processes.



Diagenetic origin of chamosite from berthierine combined with authigenic deposition of a gelatinous berthierine/chamosite, supports the presence of coated quartz grains and pore-linings.

In the Spiro, calcite is the more dominant cement in the upper zones and silica in the lower zones. Calcite cement is syntaxial overgrowths or rims in some areas; elsewhere drusy mosaic calcite fills pores.

Calcite cements are deposited mainly by formation waters with high pH. Calcite is one of the common cements in sandstones. Syntaxial overgrowths occur as large singular crystals in which many sand grains are enveloped. Drusy calcite mosaics consist of equant crystals that fill pores, and that typically show increase in crystal size toward centers of pores. During precipitation of calcite, grains commonly are displaced, so that some grains appear to "float" in cement. Apart from pore filling, calcite replaces grains. Quartz grains cemented by calcite commonly are etched and corroded at their margins (Tucker, 1991).

Calcite cements are common in grain-supported sandstones, such as quartz arenites, arkoses and litharenites. Early precipitation of calcite can result in total loss of porosity and permeability.  $\text{CaCO}_3$  precipitation, taking place when the solubility product

is exceeded, often occurs through an increase in activity of the carbonate ion. At varied subsurface depths (depending on location), precipitation of carbonate can be brought about by an increase pH and/or temperature. The source of  $\text{CaCO}_3$  may be pore water itself, but in marine sandstones, much probably is derived from dissolution of carbonate skeletal grains (Tucker, 1991).

Silica occurs as overgrowths and as minor chalcedony in sandstone of the Spiro. Quartz overgrowths are one of the most common types of silica cements. Silica is precipitated around the quartz grain and is in optical continuity with the grain, so that the grain and cement extinguish together under crossed nicols. In many cases the shape of the original grain is delineated by a thin "dust rim" of minerals or clays present at the time of cementation (Moncure, Lahann and Siebert, 1984).

Silica in the Spiro sandstone may have come from two major sources. The first being from pressure-solution attendant to compaction during basin deformation. The second from generation of hydrocarbons, which produced fluids of low pH. Sources of silica may include pressure solution, alterations of montmorillonite to illite, alterations of feldspars to kaolinite, and silt particles from interbedded shales. An important characteristic of quartz cementation of sandstones is hardness to better withstand the effects of compaction and pressure dissolution during further burial.

Dolomite is early, formed small hypidiotopic rhombohedra that replaced authigenic clays, and are pore lining material, and detrital grain coatings. Late-stage dolomites are ankerite, which may be of hydrothermal origin.

The most common crystal shape of dolomites in the Spiro Sandstone is well-formed rhombohedra, .10-.06mm in size. Dolomite mostly is iron-rich, and may have been derived from clays or other iron-rich minerals that are minor constituents of the Spiro. With the high temperatures present during basin subsidence in the Arkoma Basin,

these alterations may have occurred at depth. Thus these rhombs should be classified as thermal dolomites (ankerites).

Porosity in the Spiro is preserved-primary porosity, and secondary porosity from dissolution of grains or from enlargement of pores. Where chamosite coats grains primary porosity has been preserved. Strata with chamosite-preserved porosity can be identified from core samples; these strata can be identified in porosity logs, and they can be correlated across the study area. The production of hydrocarbons in the Spiro created charged reservoirs during basin deformation. This may have acted to oppose compactional forces, to preserve primary porosity in the chamositic zones.

In strata where chamosite is not present, mostly in the southern part of the study area, porosity has not been preserved. Chamosite has been replaced by the formation of discrete glauconitic grains, and has allowed extensive cementation, thus decreasing primary and the formation of secondary porosity. Spiro Sandstone penetrated by the Shell 1-9 Mabry is an example of Spiro facies with no porosity; these strata can be correlated with and compared to chamosite facies to the north (Figure 13). Core samples verified the glauconite and the absence of chamosite.

Depositional environments of the Spiro Sandstone are still a matter of great debate. Exum and Harms (1968) pointed out that the vertical sequence of offshore shelf marine bars is characterized by a coarsening-upward pattern. This contrasts markedly with the fining upward sequence that distinguishes channel-fill deposits further north in the study area. Grayson and Hinde (1987) recognized three siliclastic facies: 1) bar-crest, 2) bar-flank, and 3) bar-margin (Figure 14). Grayson (1980) discussed Spiro sandstone bar facies in terms of tidal sand waves and ribbons.

From study of cores of Spiro Sandstone in the Wilburton area, and from study of previous works, depositional environment of the sandstone is inferred. Houseknecht

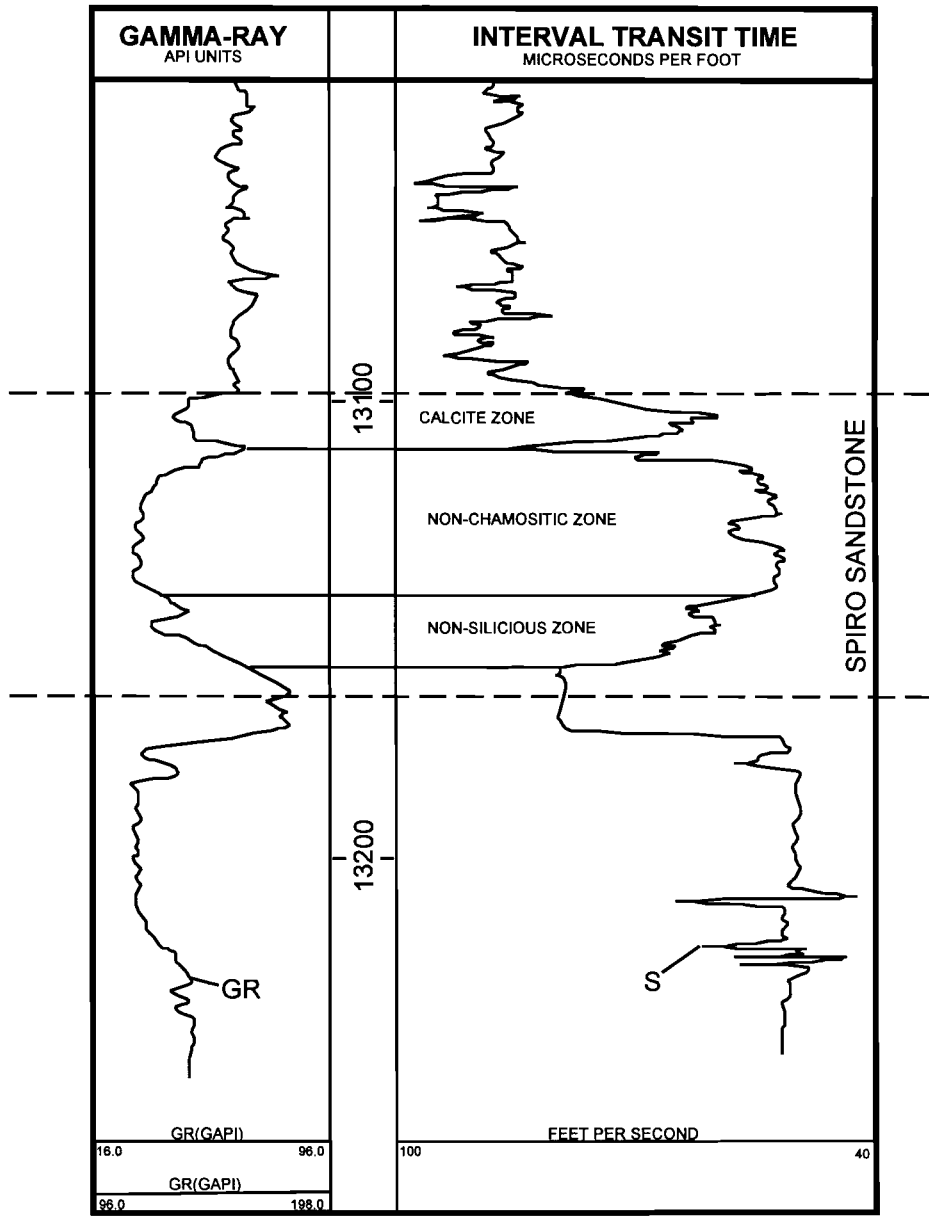


Figure 13. Gamma-ray and interval transit time curves, Spiro Sandstone, Shell 1-9 Mabry, Sec.9, T. 4N., R. 17E.



(1987) suggests that the main source of sediment for the Spiro was to the east, in terrain that is in Arkansas. A change in lithology of the Spiro consists of clean sandstone to the east, to increasingly carbonate-rich sandstone westward, to shale southward (Lumsden, Pittman and Buchanan, 1971). The Foster channels identified by Lumsden and others (1971), suggest a sediment source to the north across tidal flats. This source area draining across the tidal flat area, rich in organic matter, such is the case of the Foster channels during a reduction in sediment input, has been identified as a depositional environment of chamosite (an iron rich chlorite)(Boggs, 1987).

One interpretation suggests that the source from Arkansas consists of the reworking of a delta complex (Figure 15). Sediments from the delta were reworked to the west by longshore drift, depositing the cleaner sands to the east of the study area. This may represent the deposition of sheet sand deposits (Figure 16). Some of these sediments brought by long shore drift to the area of chamosite deposition are rolled through a gelatinous accumulation, coating the sand grains with clay platelets tangential to the grain surface. After the deposition of zone 1, a reduction in the long shore source reduces sediment influx. Primary depositional source was then supplied by the Foster channels. Carroll (1958) concluded that clay from the source area can carry enough absorbed iron oxide to provide the iron needed for the deposition of berthierine and chamosite. Within pores these accumulations, berthierine (7 Å) probably is the first-formed iron-rich clay mineral, chamosite (14 Å) deposits syndepositionally with the berthierine (Odin and Matter, 1981; Velde et al., 1974). It is this deposition of chamosite which produces clay platelets normal to the quartz grains as seen in the SEM photos from the Reusch core. The mapping of the areal extent of the chamosite facies shows that it has a limited distribution in the Wilburton area. However, without a regional study of the depositional patterns, the only confirmation of depositional environment comes from Spiro Sandstone constituents. Glauconite minerals deposited in deeper waters on the

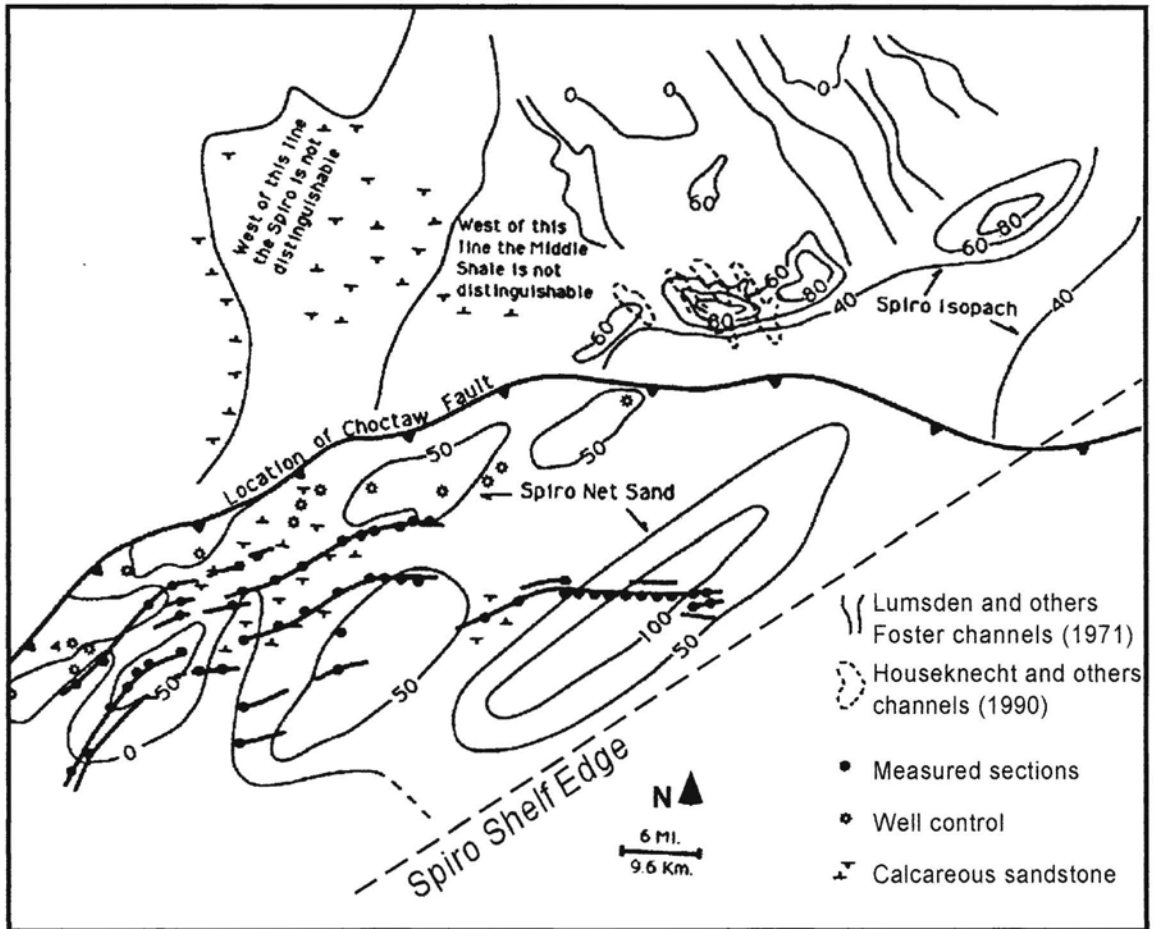


Figure 14. Thickness of Spiro Sandstone, including Foster and Houseknecht Channels (after Grayson and Hinde, 1992).

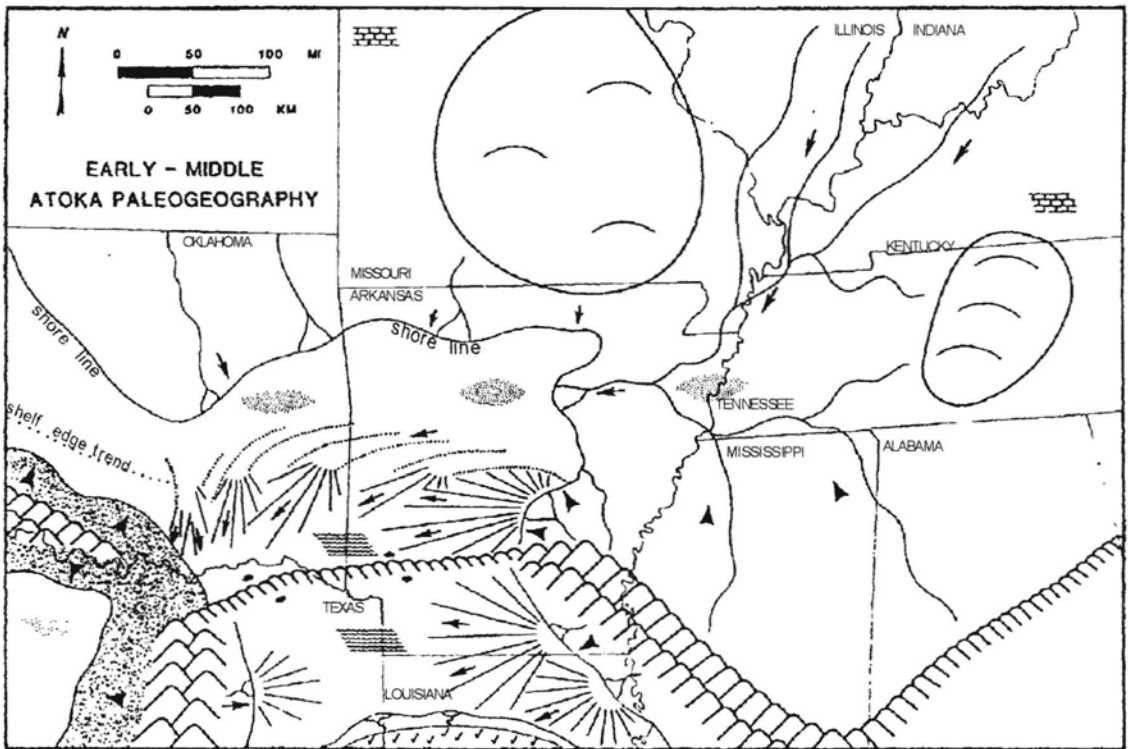


Figure 15. Atokan paleogeography map of the Arkoma Basin Area (modified after Houseknecht and Kacena, 1983).

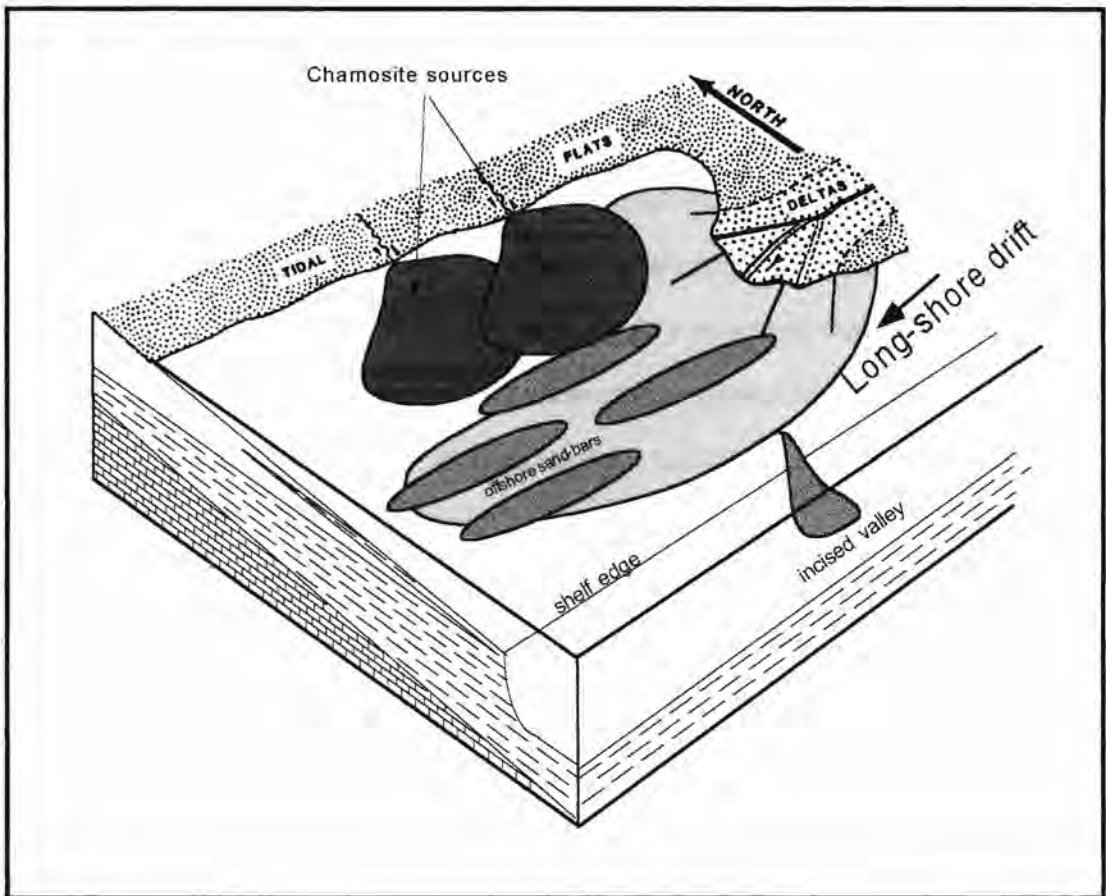


Figure 16. Inferred depositional environments of Spiro Sandstone.

shelf, favor high Si and K content are probably largely a product of neof ormation by the replacement of several kinds of substrates or by filling voids, as in tests of microfauna (Van Houten and Purucker, 1984). The presence of chamosite suggests a shallow marine environment, whereas glauconite suggests a deeper marine environment.

## STRUCTURAL GEOLOGY

Structure geology of rocks exposed in the Ouachita Mountains, where strata of Spiro Sandstone and Wapanucka Limestone dip steeply, is indicative of the complex subsurface structure. Study of the Spiro in the subsurface has led to multiple interpretations, of course. However, the incorporation of well-log and seismic data has provided cross-sections in the Wilburton area that are more accurate than cross-sections of previous studies. Ulrich (1927) and Drake (1921) suggested that the juxtaposition of the drastically different facies required northward transport of the interior portions of the Ouachita thrust belt. Other geologists nevertheless hypothesize a basically in situ, pseudo-autochthonous deformation style for the province. An upswing in seismic exploration and drilling activity for the Arkoma basin contributed to new insights regarding structural style for the Arkoma basin, leading to detailed cross-sections that were published in the 1968 guidebook of the Oklahoma City Geological Society (Buchanan and Johnson, 1968; Berry and Trumbly, 1968; Hopkins, 1968). The collective conclusion showed that folds observed at the surface in the Arkoma basin are detached from their substrate by a decollement zone in lower Atokan rocks, and that the lowermost Atokan strata, including the Spiro Sandstone and underlying strata, displays an extensional, basement block-faulted style that includes high-angle normal faults.

A frontal imbricated zone is well defined between the Choctaw fault to the north and the Windingstair fault to the south, this belt is 2.4 to 19 km wide and comprises closely-spaced, north-vergent set of thrust slices. This imbricate complex composes the "over-thrusted Spiro", exposed surface outcrops.

The subsurface structure in the Wilburton area of the Arkoma basin consists of normal faults overridden by thrust faults. The normal-faulting is restricted to north of the Choctaw fault, formed as a result of the basin formation. Block-faulting later served as a ramp for the lower Springer detachment, and a zone of imbricate thrust faults, in what is known as the "underthrust Spiro Sandstone" formed. Normal-fault movement of fault-blocks could have been reactivated as thrust-faults, creating the imbricate complex. This may explain why the imbricate complexes are localized and discontinuous, owing to tear faulting from differential faulting. Spiro imbricate complex consist of two to five stacked thrust sheets. However, some areas may include subsurface anticlines. The highest concentration of Spiro thrust-sheet stacking is in the Wilburton area. The underthrust Spiro imbricate complex is the focus of production in the Arkoma basin (Figure 17). Block-faulting north of the Choctaw fault, later acted as a ramp for the lower Springer detachment surface, creating imbrication of Spiro thrust sheets. Block-faults that has functioned as a ramp for the detachment also may have contributed to differential faulting, as the direction of thrusting was at an angle to the strike of the normal-faults. Differential thrusting in the lower imbricate complex has incorporated shear components to create localized concentrations of thrust sheet stacking. The lower Spiro imbricate complex may have in turn served as a ramp for the "overthrust Spiro sandstone" imbricate complex of major thrust-faults exposed at the surface in the Choctaw, Ti Valley and other major thrust faults.

## PETROLEUM

David White (1915) was the first geologist to observe a relationship between coal rank (thermal maturity) and petroleum in associated strata. He observed that low, intermediate, and high coal rank coincided with oil, gas, and no petroleum, respectively

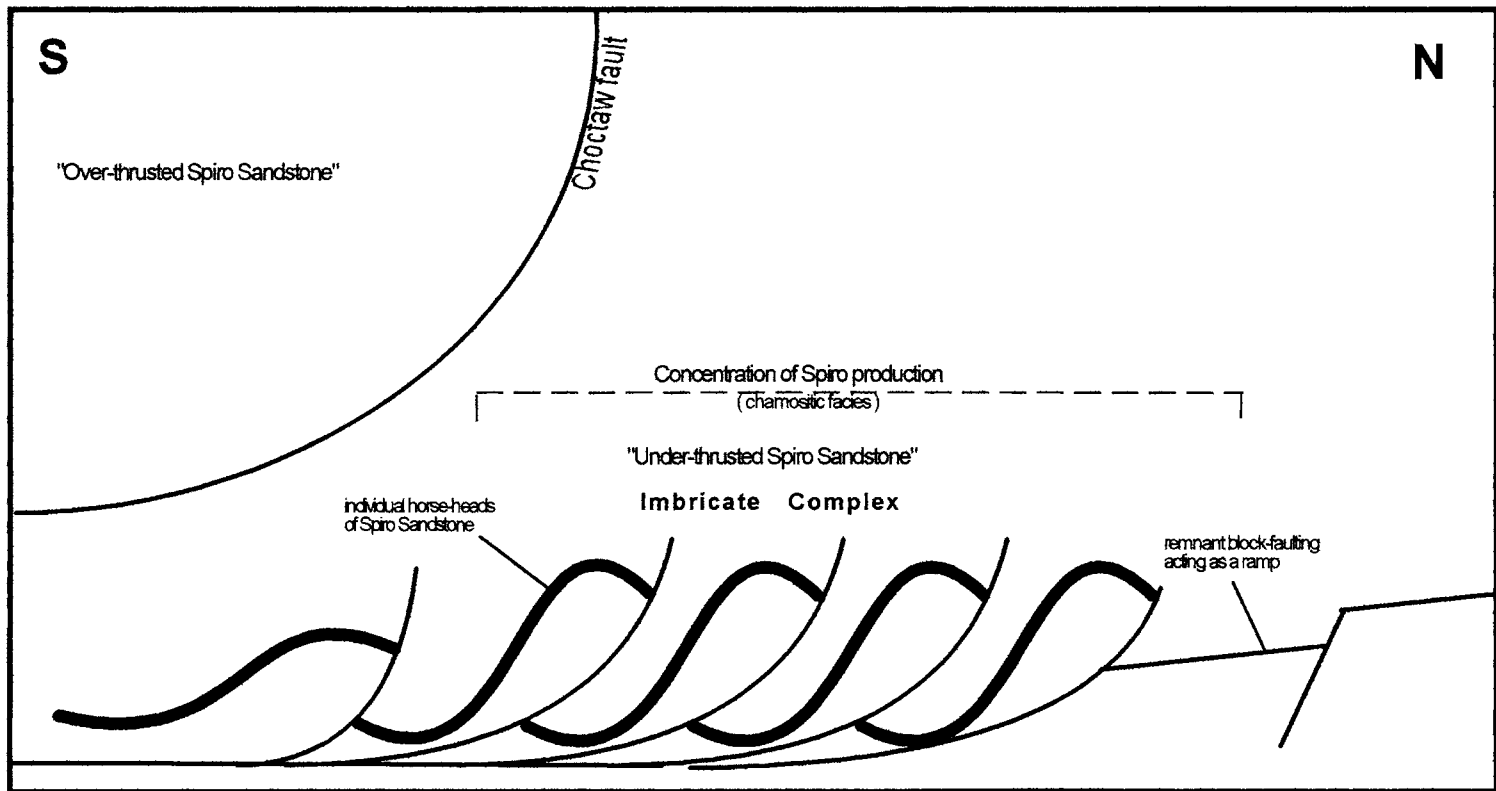


Figure 17. Location of the imbricate complex within the subsurface geology in the Wilburton area.

(summarized by Landes, 1967). In the 1970's and 80's, much research on thermal generation and thermal destruction of hydrocarbons led to the concept of hydrocarbon windows, specific ranges of thermal maturity within which oil, wet gas, and dry gas develop. Dow's (1977) correlation of thermal maturity and hydrocarbon windows is illustrated in Figure 18.

Within the Spiro sandstone are numerous thin intervals of shale, which increase in number to the north. These shales are suggested to have been a source rock for some of the petroleum within the Spiro. Samples taken from outcrop sections comprising Middle Pennsylvanian Atoka (including Spiro) Formation contains gas-generative, Type III Kerogen (Curiale, 1983; Curiale and others, 1984; Fowler and Douglas, 1984; Zemmels and others, 1985; Guthrie and others, 1986). On the basis of plots of extractable organic matter (EOM  $\geq$  60ppm) vs. total organic carbon (TOC  $\geq$  0.5 wt%), Weber (1992) concluded that of samples collected at the surface, one sample from the Atoka Formation had fair to good oil-source potential. However, these outcrop-sample, organic-richness measurements may be minimal values (Clayton and Swetland, 1978).

Houseknecht and Matthews (1985) illustrated an isorefectance map of the Ouachita Mountains based on 89 surface samples, primarily of Carboniferous strata. Thermal maturity of the Oklahoma segment, based on 32 samples, was shown by Ro values ranging from 0.24% in the west to 3.96% in the core area (Matthews, 1982). Carrot (1994) calculated vitrinite-reflectance values from 0.24% to 1.16%. Houseknecht and Matthews (1985, p. 344) concluded that "in the Oklahoma portion of the Ouachitas, thermal maturity increases with the stratigraphic age, thermal-maturity contours parallel structural grain, and older strata on upthrown sides of thrust faults are more thermally mature than younger strata on downthrown sides. Sedimentary burial appears to have exerted a dominant influence on thermal maturation, although tectonic burial was also important."



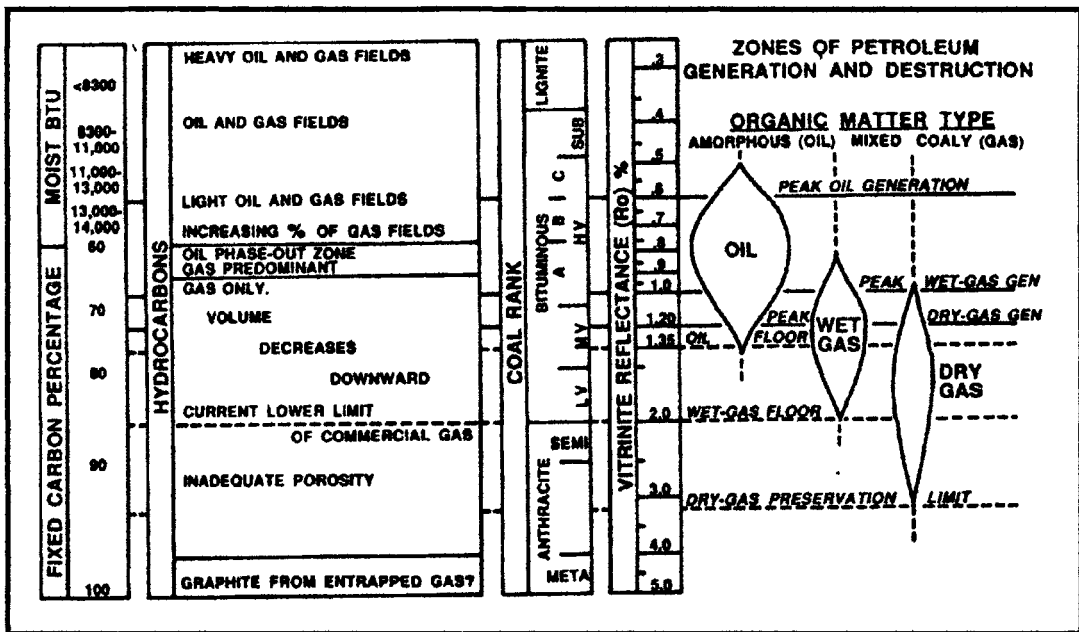


Figure 18. Relationship between thermal maturity and occurrence of petroleum. Left two columns summarize knowledge as of 1967 (Landes, 1967). Right part summarizes more recent concepts regarding zones of hydrocarbon generation and destruction (hydrocarbon windows), expressed in terms of coal rank and vitrinite reflectance (Dow, 1977).

From the study by Carrot (1994), the mean reflectance values vary spatially as a result of thrusting. There is a general trend of increased thermal maturity from west to east in the northern part of the Arkoma/Ouachita system in Oklahoma. However, a general trend of increasing thermal maturity with increasing age, as reported by Houseknecht and Matthews (1985) was not found (Carrot, 1994). In addition to attributing these reflectance values to depositional and tectonic burial (pre-orogenic and syn-orogenic coalification), the abundance of high-gray vitrinite in the Pennsylvanian samples could have skewed the mean vitrinite reflectance to a higher value (Carrot, 1994).

From the vitrinite-reflectance data, thermal history, and burial history documented from previous work, a model of the Arkoma basin in Oklahoma was constructed (Figure 19). The curves model the burial history of the stratigraphic section that includes Upper Pennsylvanian strata exposed at the surface, to Reagan Sandstone that lies upon igneous basement rock.

Depressions in the curve represent periods of basin subsidence, whereas orogenic events are marked by positive slope. During the Middle Pennsylvanian the basin subsided rapidly; subsidence climaxed at the beginning of the Permian. The Permian marked the beginning of gradual tectonic rise in the basin, with eventual erosion of strata above the Pennsylvanian.

Thermal maturities of kerogens within the basin (Figure 19) is plotted over the burial history curves; these show that the Spiro passed through the gas window during the Early Pennsylvanian. With high thermal flow in the Paleozoic, the gas window in the Spiro occurred relatively shallow (~ 7500-8500ft). The comparatively low thermal conductivity of shale facies traps extra heat. This increases the geothermal gradient; fluid pressures in a well-isolated system cannot be dissipated effectively. Trapped heat causes thermal expansion of pore fluids, reinforcing the fluid-pressure system (Luo, Baker and

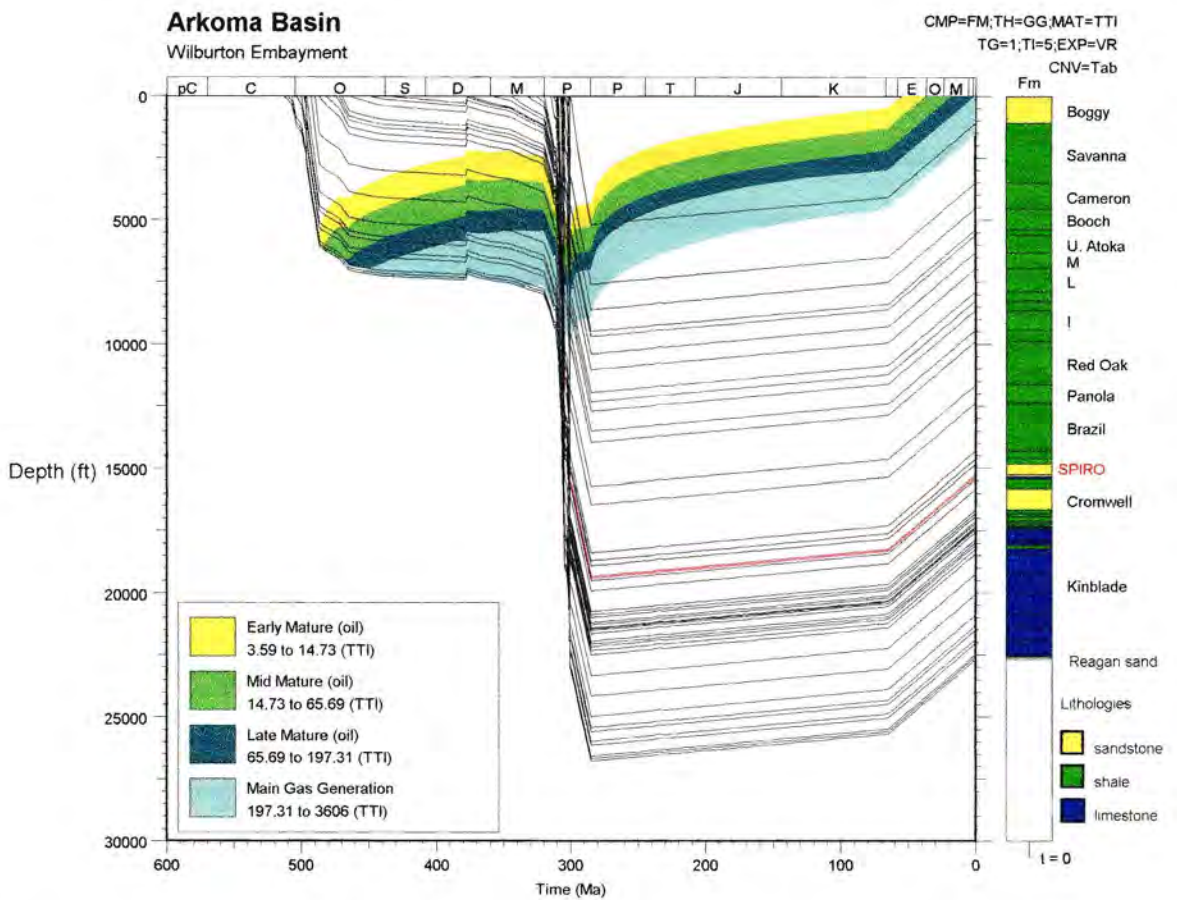


Figure 19. Calculated burial history with thermal maturation of kerogens, Arkoma Basin, Latimer County, Oklahoma. Spiro Sandstone history highlighted in red.

LeMone, 1994, p. 1399). Thick shales in the Upper and Middle Atoka may have acted so, to trap heat.

Houseknecht (1992) believed that the high absolute values of thermal maturity are partly the result of anomalous heat flow along Atokan syndepositional normal faults. He believed that such faults would have enhanced heat flow in the basin, in the same way that heat flow is enhanced by growth faults of the modern Gulf Coast basin (e.g., Bodner and Sharp, 1988). In recent years, lateral thermal-maturity gradients within individual formations have been explained by means of "hydrothermal" fluid migration within foreland basin strata. Three general mechanisms have been proposed to provide the head for such fluid migration: overpressuring of thick foreland-basin strata, due to rapid sediment accumulation (e.g., Cathles and Smith, 1983), gas generation (e.g., Spencer, 1987), loading of thick foreland-basin strata by advancing thrust sheets (e.g., Garven and Freeze, 1984; Bethke and Marshak, 1990).

Enhanced heat flow along basement-rooted normal faults, combined with hydrothermal fluid migration away from the Ouachita orogenic belt, provides an explanation for the high levels of thermal maturity and the lateral thermal-maturity patterns in the basin.

Published pressure-data was gathered for single Spiro completions across the Wilburton area. Initial bottom hole pressures (IBHP) of wells completed from 1960 through 1994 were used to calculate pressure-gradients. Owing to depletion of the gas reservoirs from production over time (Figure 20), the primary well data used in the study were initial production wells completed in the 1960's. However, in the South Panola field, well data are more recent, because the field has been active only for three to four years.

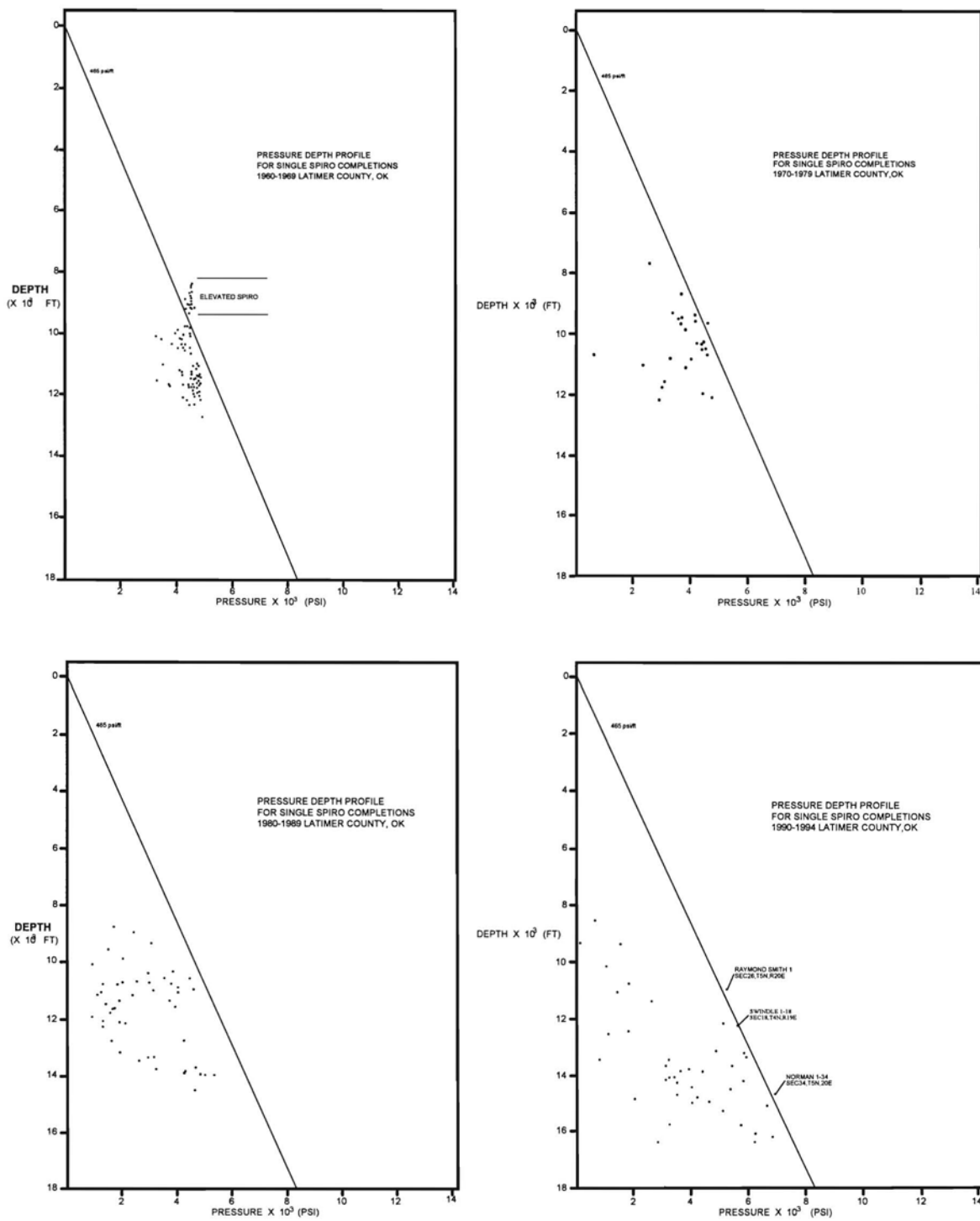


Figure 20. Pressure-depth plots, Spiro Sandstone, Wilburton area, ten-year blocks.

Pressure-gradients are calculated by dividing IBHP by the Spiro reservoir depth, and is therefore depth-dependent. The normal pressure-gradient in a formation is equivalent to the pressure exerted at any given depth by a column of 10-percent-salt water extending from that depth to the surface (0.465 pounds per square inch per foot) (Dictionary for the Petroleum Industry, 1994). Mapping of the pressure-gradient values with an isobar contour map revealed distinctive patterns and compartments (Plate 1). These patterns identify pressure regimes within the individual compartments. Maps illustrate that the compartments are comprised of a central trend of highest pressure-gradients, and that the gradients decline away the central trend.

Another isobar contour map of the IBHP of the data wells shows very little variation in pattern (Plate 2). The IBHP reported for the wells drilled in the 1960's averages 4500psi. Because the IBHP averages 4500psi and the average depth of the Spiro reservoirs in the Wilburton area is 10-12,000ft, none of the wells would be considered overpressured.

A third type of map was created to outline abnormally pressured and compartmented Spiro reservoirs was a three-dimensional potentiometric-surface plot. The potential of a fluid is represented by the level (generally expressed in feet or meters above a surface) to which the pressure of a column of gas would rise if unconfined. Figure 21 is a plot of well data (all wells dated 1960-1994) in the Wilburton area. By overlaying this plot on the pressure-gradient map, areas of abnormal-pressure compartments coincide. As with the calculation of pressure-gradient, fluid potential is dependent upon the depth of the reservoir.

## RESERVOIR QUALITY

Within the Spiro Sandstone variations occur in reservoir quality westward from Arkansas in the Arkoma basin of Oklahoma. Lumsden and others (1971) identified

changes in the Spiro east-to-west and north-to-south (Figure 22). Spiro Sandstone of the eastern Arkoma basin in Oklahoma consists of relatively clean sandstone that grades westward into limy-sand. Southward the Spiro becomes shaly and grades into shale toward the shelf edge; Northward multiple bodies of Spiro channel-fill sandstone are separated by shale.

From analyzing declines in IBHP observed between offset wells (completed ten or more years after nearby well completion) and initial wells, higher rates of reservoir depletion are noticed to the east, where Spiro Sandstone is cleaner, more porous and more permeable.

By well-log evaluation of the Spiro intervals, the formation was divided into five general zones, based on gamma-ray curves and porosity curves (Figure 23). The King 1 Layden was used as a type log for the study (Figure 23). Zone 1 is the lower part of the Spiro Sandstone. Zone 1 is made up of thin sand bodies, perhaps stacked channels, and is the lower silica-cemented zone. Correlated to units in outcrops, zone 1 is a ridge-former, being very resistive. Zone 2 is the lowest unit of the massive Spiro Sandstone. Zones 2,3 and 4 are the chamosite/reservoir interval, with the most porosity. Correlated to units in outcrop, the rock is friable. Zone 5 is the uppermost interval of the Spiro; it is a tightly cemented calcite zone, potentially a seal.

Authigenic clay minerals are particularly important because since they occupy pores and pore-throats and have large surface areas. Their crystalline morphology influences their distribution habits within the pore geometry. Most of the clay minerals have exposed charged surfaces that are available for interaction with polar fluids.

Chamosite, illite, and kaolinite are the common authigenic clays in the Spiro Sandstone. Each of these minerals show different morphologies, surface areas, cation-exchange capacities, and presents specific problems during well-completions.

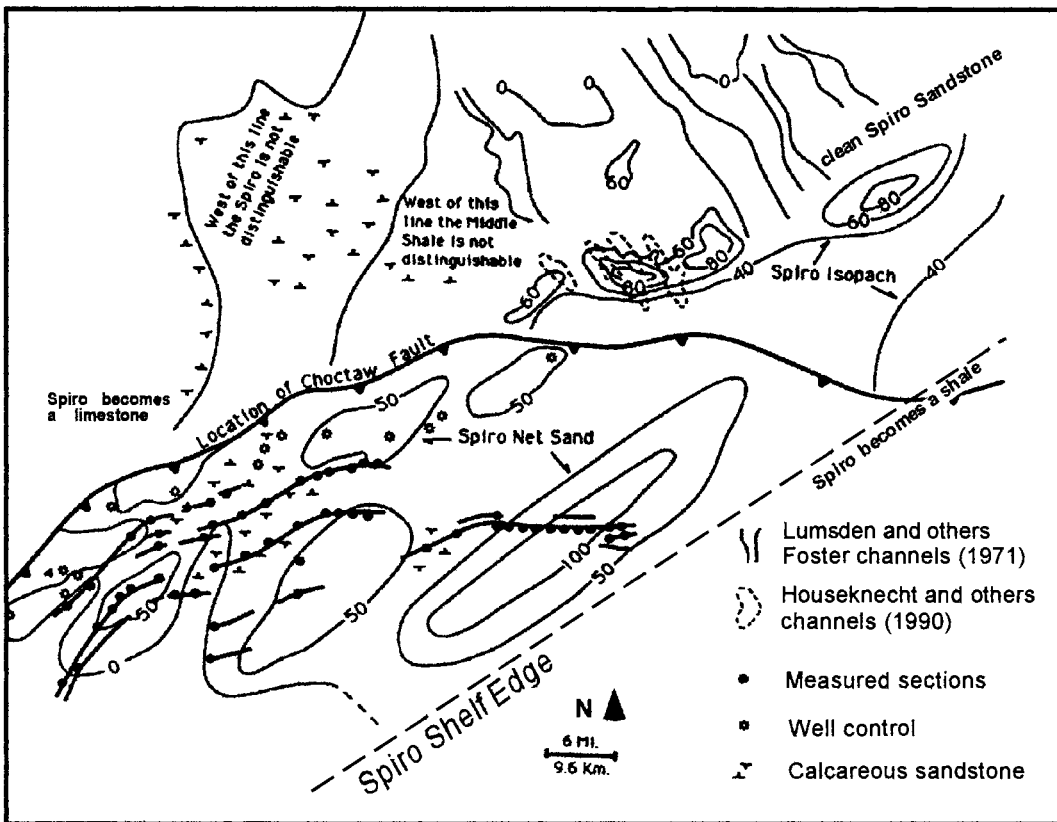


Figure 22. Lithologic changes of Spiro Sandstone across the Wilburton area (after Grayson and Hinde 1992).



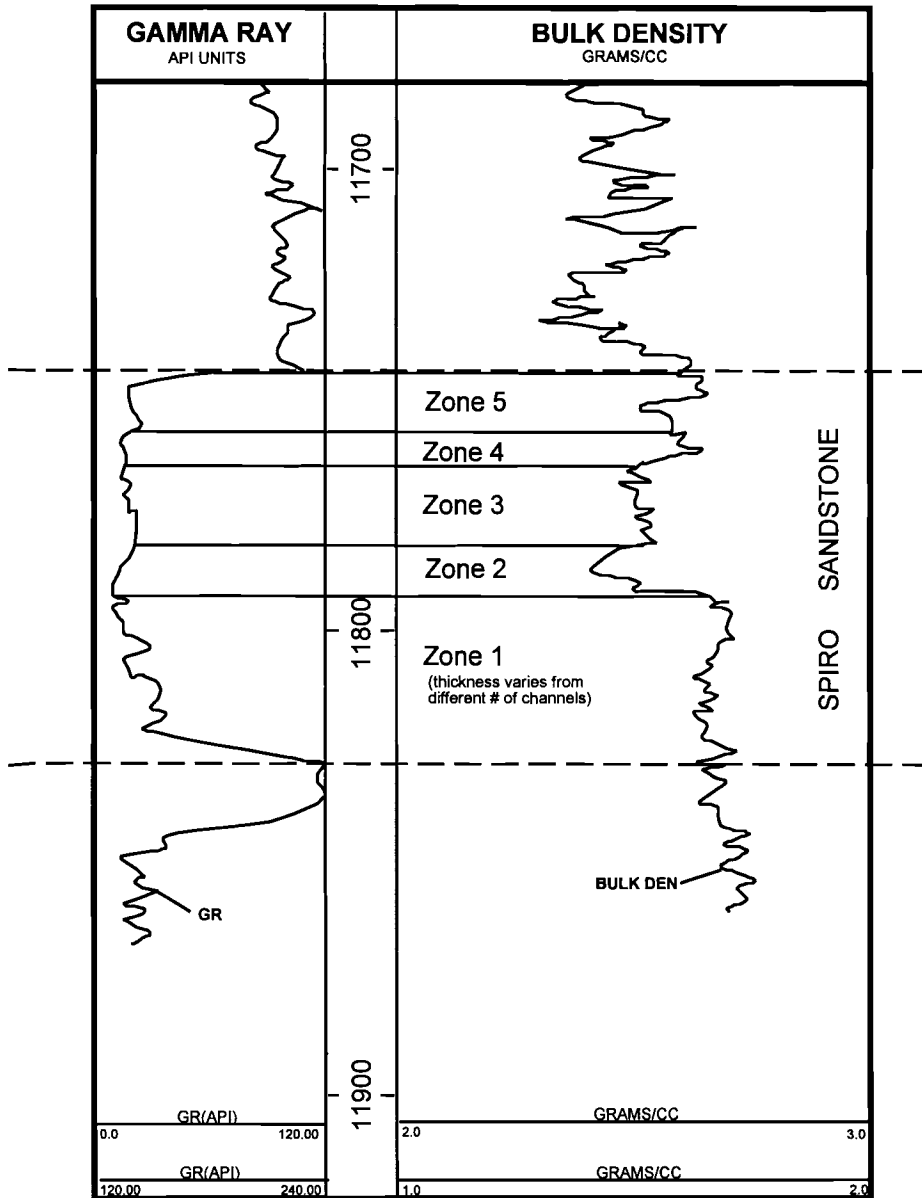


Figure 23. Gamma-ray and density-positivity curves for the King 1-3 Layden Sec. 3, T. 4N., R. 17E., divided into five zones, based on lithology, log signature and porosity.

All chamosite observed in the Spiro Sandstone is iron-rich. Chamosite is soluble in acids and forms ferric hydroxide  $\text{Fe}(\text{OH})_3$  upon reaction with oxygenated solutions. The resultant colloidal material may precipitate in pore throats, reducing permeabilities and reducing reservoir quality. This problem usually can be avoided by using either an oxygen scavenger or chelating agent for iron ions, to prevent formation of iron hydroxide.

The breaking of lath-shaped illite crystals may result in closing of pore throats and a corresponding decrease in permeability. In some cases HF is helpful in dissolving illite and cleaning pore throats. However, silica may be a precipitant in this treatment, with reduction in sizes of pore throats.

Kaolinite and/or dickite occur only as loosely discrete particles filling pore spaces. They are relatively less soluble than other clays and generally do not have any significant chemical reactivity with fluid. However, because of their size and loose packing, turbulent flow will detach kaolinite "booklets" and move them toward pore throats. Kaolinite occurs in trace quantities in the Spiro Sandstone, therefore migration of kaolinite is rather insignificant.

The content of authigenic and diagenetic clays within the Spiro varies from eastward to westward in the Arkoma basin of Oklahoma. The detrital shale and clay pellets, with compaction, undergo ductile deformation, in some cases filling the pore spaces, and damaging reservoir quality.

Diagenetic clay minerals can present problems in wire-line log interpretation. Their charged-surface-area to pore-volume ratio affects the responses of wire-line logs.

The natural radioactivity measured by the gamma-ray log is due primarily to  $\text{K}^{40}$ , Th, and U. In the Spiro Sandstone, detrital or diagenetic illite and muscovite are the sources of gamma radiation because of their high potassium content. Therefore, in order to evaluate gamma-ray logs effectively, several considerations should be noted:

1. Chlorite-rich sandstone may not appear to be shaley on gamma-ray logs, because chlorite does not contain potassium ions and uranium-thorium minerals.

2. Gamma-ray logs can be used to evaluate the degree of "shaliness" in a sandstone-shale sequence; although rock fragments (particularly, metamorphic rocks and clay/shale) and illite as matrix may lead to errors in interpretation. Problems include; low gamma-ray log response in shale, and high gamma-ray response with feldspars, metamorphic rock fragments, and glauconite (Asquith, 1982, p.91).

Therefore, evaluating the degree of "shaliness" and "cleanliness" of sandstones, based on gamma-ray logs, requires calibration.

Authigenic clay minerals in sandstones affect the electric-log response because of their negatively charged surfaces and large surface areas. The spontaneous potential (SP) log may show suppressed responses in strata with high clay content; however, the amount of suppression will depend upon the type of clay. Decrease in resistivity, due to the low resistivity of authigenic clays, causes certain producing intervals to show high values of water saturation. Spiro Sandstone contains large amounts of clays, which presents a problem in calculating water saturations from electric logs.

With high chamosite pellet and other clay content, the density log calibrated for sandstone ( $2.65 \text{ gm/cm}^3$ , assuming quartz arenite) may give higher density values. Therefore, a correction factor or correction curve is needed to calculate porosities in the Spiro accurately.

The greatest effect on reservoir quality in the Spiro Sandstone comes from chamosite grain-coatings and the generation of hydrocarbons, preserving primary porosity.

Generally, authigenic and diagenetic clay minerals inhibit porosity and permeability. Unless grains are directly deposited into a clay-rich environment, the clay minerals form on available grain surfaces. Chamosite-coated quartz grains are observed

in the gas productive intervals of the Spiro. Coating of most types of grains, with clay platelets, requires some form of agitation or rolling of the grains through deposits of clay. This is a possible explanation for ooids found in the Spiro. Clay platelets that are normal to grain-surfaces, are identified as pore lining, opposed to grain-coating. Syn-depositional with the sand grains, pore lining is the dominant occurrence of chamosite in reservoir facies. Chamosite-linings have protected the quartz grains from dissolution and cementation, preserving most primary porosity. Where pores of the Spiro are not lined by chamosite, no primary porosity remains; these sandstones were susceptible to diagenesis. Figure 24 is a plot of percent-chamosite v. percent-porosity, from samples of cores of Spiro Sandstone.

Hydrocarbons of Spiro reservoirs, in conjunction with the chamosite coatings, preserved primary porosity. Pore fluids provided hydrostatic resistance, inhibiting further compaction by overburden, that destroys porosity and alter grains (Atwater and Miller, 1965).

## DIAGENESIS FROM BASIN EVOLUTION

Chemical diagenesis has modified the Spiro Sandstone significantly, with various episodes of cementation and dissolution. Although these are common diagenetic phenomenon, local variations may be related to the original sediment composition and textures.

The most abundant and important diagenetic minerals in Spiro Sandstone of the Wilburton area include; calcite cement, silica cement, and dolomite/ ankerite. These minerals form the diagenetic seals. They are in Spiro Sandstone where chamosite grain-coatings are sparse or nonexistent. The timing of formation of these minerals and their extents were key evidence in the interpretation of sealing mechanisms.

Diagenesis and tectonic evolution of the Arkoma basin have produced reservoir compartments in the Spiro Sandstone. Figure 25 illustrates characteristics of the

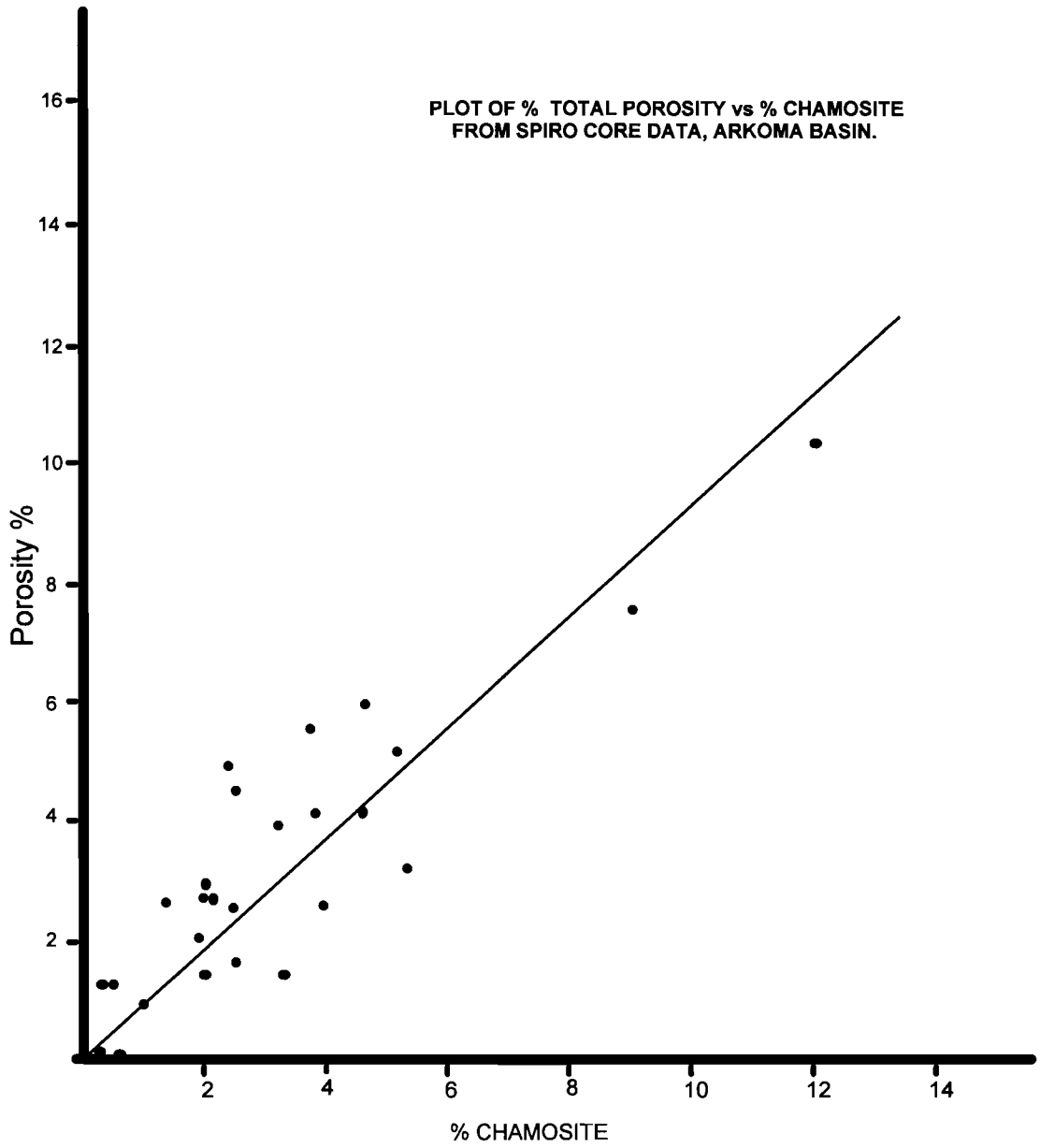


Figure 24 Plot of % chamosite pore-lining v. % primary porosity from Spiro Core samples in the Wilburton Area.

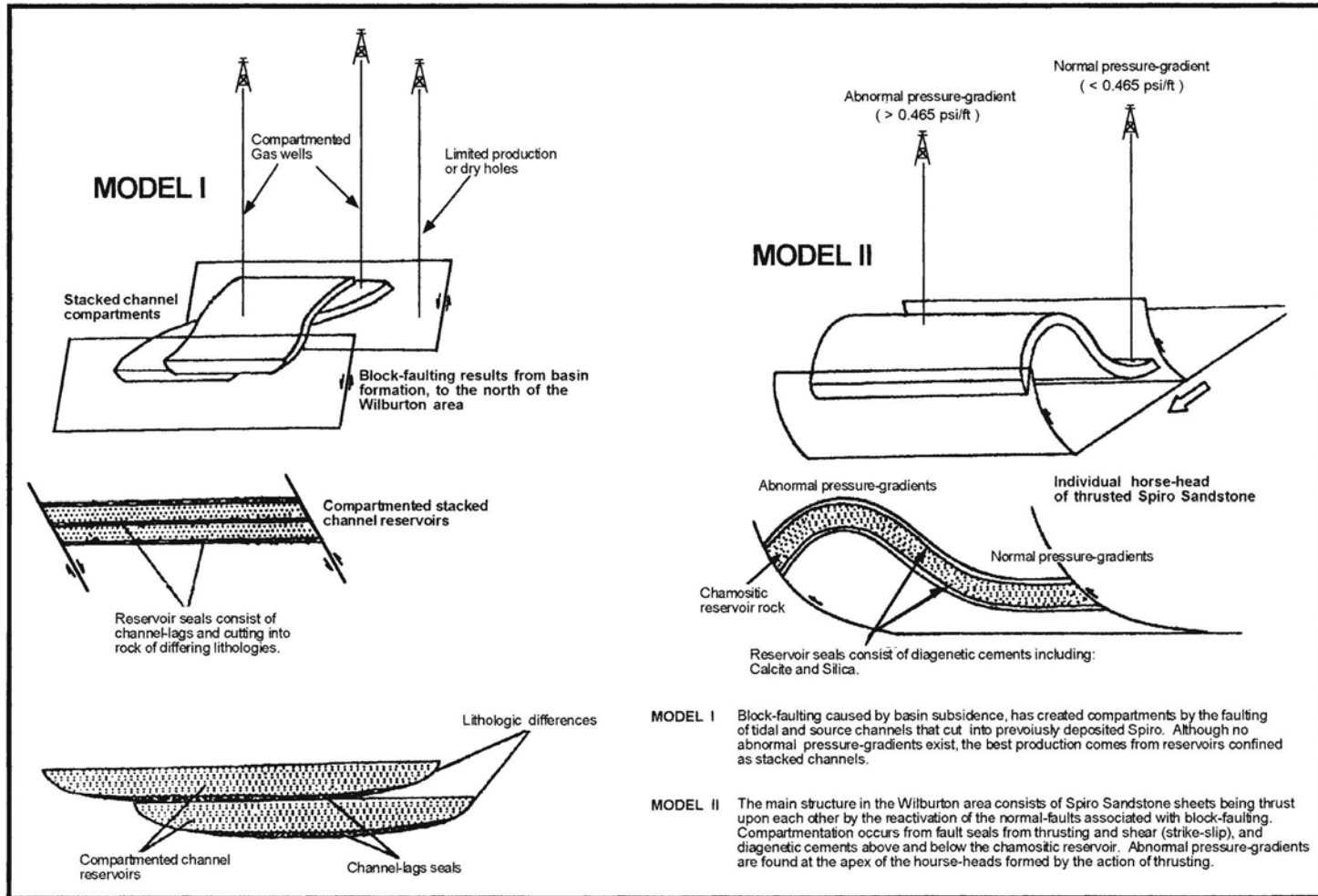


Figure 25. Compartmentation models of Spiro Sandstone reservoirs in the Wilburton area

independent compartments sealed. These compartments were sealed by diagenetic cements, lithologic differences, and stacked channel-lag deposits. Diagenetic cements were examined by means of thin-sections, x-ray diffraction, cathodoluminescence, and analysis of fluid inclusions, to delineate the timing of the diagenetic events.

The Pan American 1 Reusch well was used as the type well for the study. Samples from core were taken at several intervals for evaluation. A core evaluation sheet with observations made is tabulated in the Appendix. Zone 1 (Figure 23) is not productive in any well. Photograph 1 (Figure 26) is a photomicrograph of Zone 1 (silica-cemented seal). The photograph shows quartz overgrowths as the dominant cement; however, remnant calcite cement can be seen in the fragment of bryzoan. X-ray-diffraction examination of Zone 1, showed silica, calcite, and dolomite/ ankerite (Appendix). Chamosite is absent from Zone 1 and the first stage of diagenesis was extensive calcite cementation, as made evident by remnant fossil-fragments. Zone 1 consistently is the zone of lowest porosity in the Spiro, across the Wilburton area.

Zones 2,3 and 4 are the best reservoirs in the Spiro; in these zones, pores are chamosite-lined (Photomicrograph 2-Figure 26, Photomicrograph 3a & b, Figure 27). X-ray diffraction of samples from these zones (Appendix) indicate that chamosite and quartz are the major constituents. Evidence of calcite is explained by fragments of fossils.

Zone 5 is the uppermost interval of Spiro Sandstone it is the upper diagenetic seal (Photomicrograph 4, Figure 28). X-ray diffraction of samples from this interval indicated that quartz and calcite are constituents; chamosite is absent (Appendix). Correlated across the Wilburton area, Zone 5 consistently is a low-porosity zone; serving as a reservoir seal.

Cathodoluminescence can be an invaluable analytical method in petrographic studies. It provides information on the spatial distribution of trace elements in terrigenous clastic grains and in cements. The cause of fluorescence by cathodoluminescence is



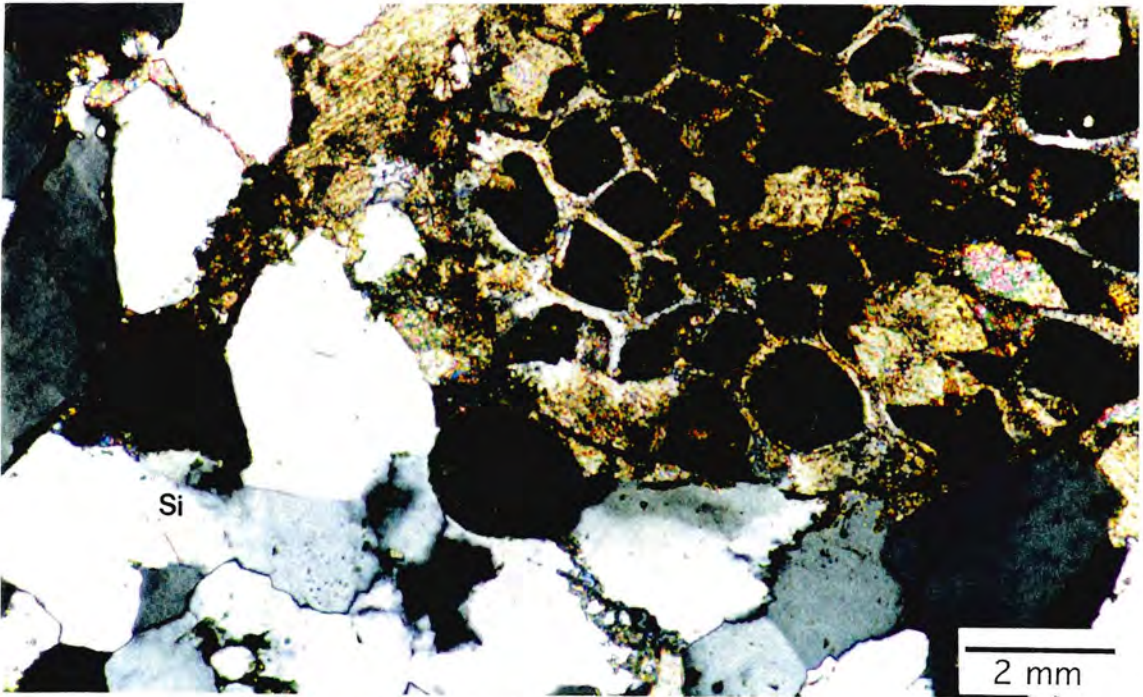


Photo 1 Photomicrograph of Zone 1 in the Pan Am Reusch Core.

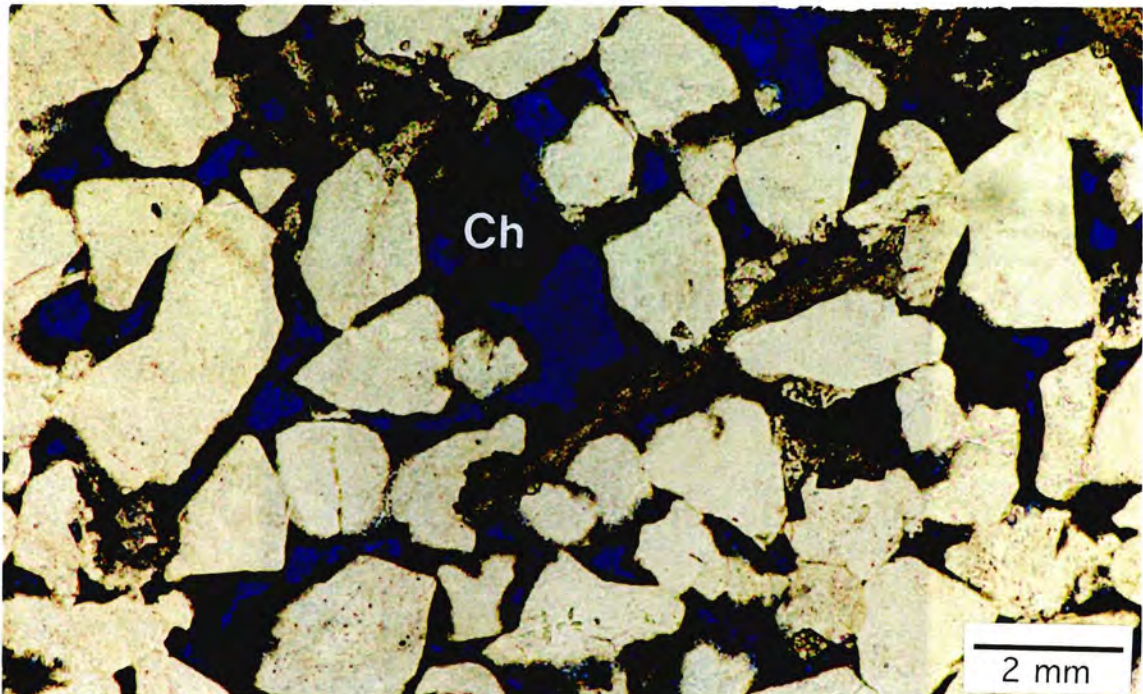


Photo 2 Photomicrograph representing Zones 2,3 and 4, showing Chamosite Coatings.

Figure 26. Pan American 1 Reusch, Spiro Sandstone.



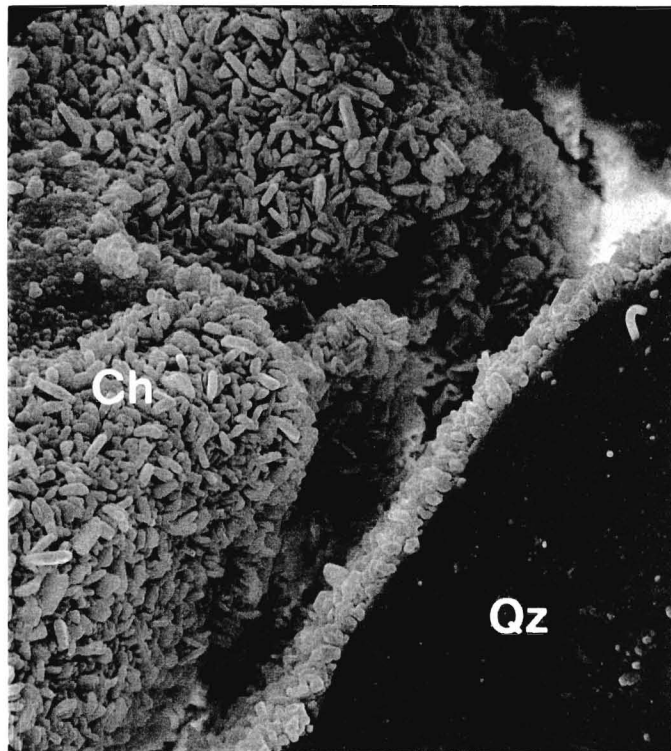
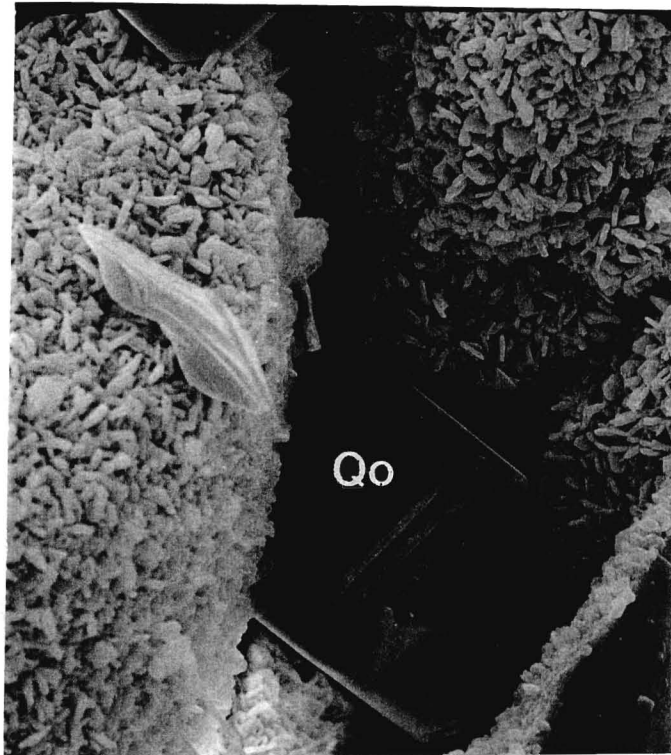
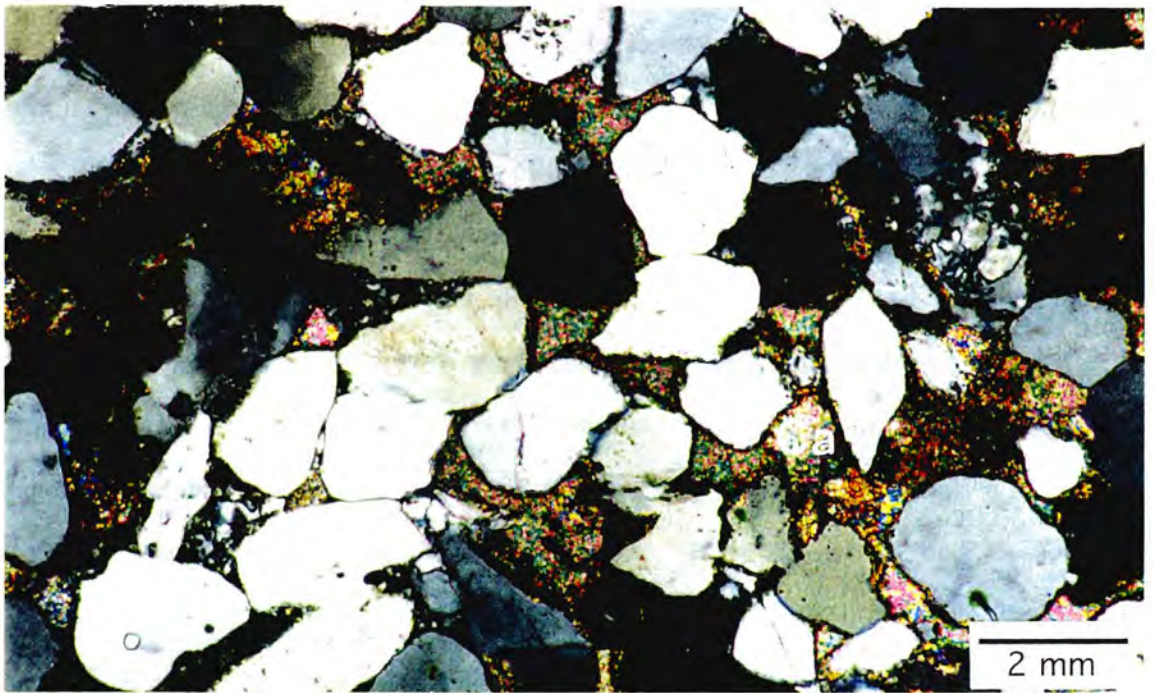


Photo 3a & b SEM Photos of Chamosite Grain Coatings in the Pan Am Reusch Core.

Figure 27. Pan American 1 Reusch, Spiro Sandstone.



Photomicrograph 4. Representing zone 5, calcite seal.

Figure 28. Pan American 1 Reusch, Spiro Sandstone.

similar to the cause of color, and ions of the transition metals are effective activators. Electrons excited by the invisible short radiation are raised to higher energy levels. When they fall back to their initial (ground) state, they emit visible light. Because some of the excited energy is lost to heat, the radiation emitted is less energetic and thus of longer wavelength. The color of the emitted light varies considerably with wavelengths or source of ultraviolet light (Klein and Hurlbut, 1977). Cathodoluminescence used to identify the number of stages of diagenetic cementation.

Zones 1 and 5 were identified as potential reservoir seals of the Spiro Sandstone. Samples of core from the Pan American 1 Reusch, and the Shell 1 Mabry were examined under luminescence. Upon examination of thin sections from Zone 1 of the Pan American 1 Reusch, quartz overgrowths and remnant calcite (within fossil fragments) cement were identified. In the Shell 1 Mabry samples of Zone 1 showed dominance of multiple stages of cementation, with minor inclusions from other stages. Photomicrograph 5 (Figure 29) showed that, variations in color identify multiple stages of diagenesis. However, cathodoluminescence analysis of zone 5 indicates only a single stage of diagenetic cementation (Photomicrograph 6, Figure 29) in both the 1 Reusch and 1 Mabry.

Evaluation of fluid inclusions can be used to estimate the temperature and pressure of formation of various minerals. When a crystal precipitates from a fluid, the surface of crystal growth commonly is imperfect. Imperfections on the crystal surface are engulfed by the surrounding crystal, producing a vacuole within the crystal, which contains the fluid present at the moment of sealing. These *primary* fluids are samples of solutions that existed during diagenesis; fluids from which the diagenetic minerals evolved (Goldstein and Reynolds, 1994).

When observed at room temperature using a transmitted-light microscope, most fluid inclusions have rather sharp outer boundaries that mark the edges of the inclusion-cavities. This boundary is visible because of a significant difference in refractive index



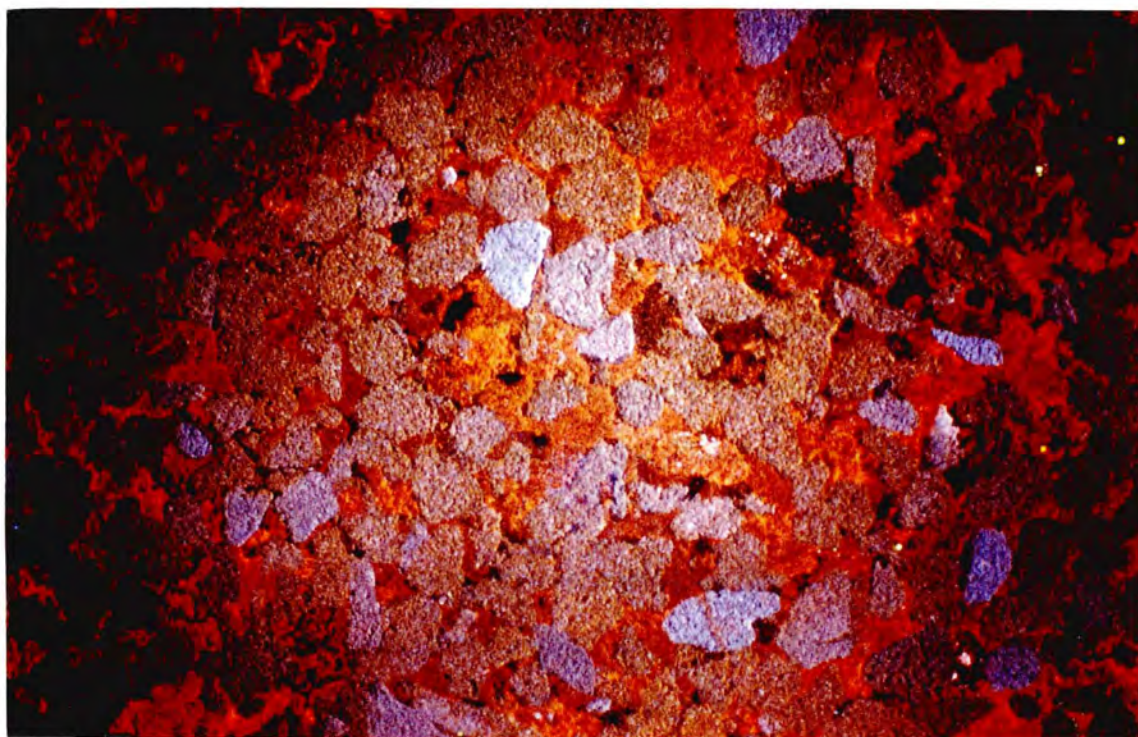


Photo 5. Cathodoluminescence Zone 1, multiple stage diagenesis.

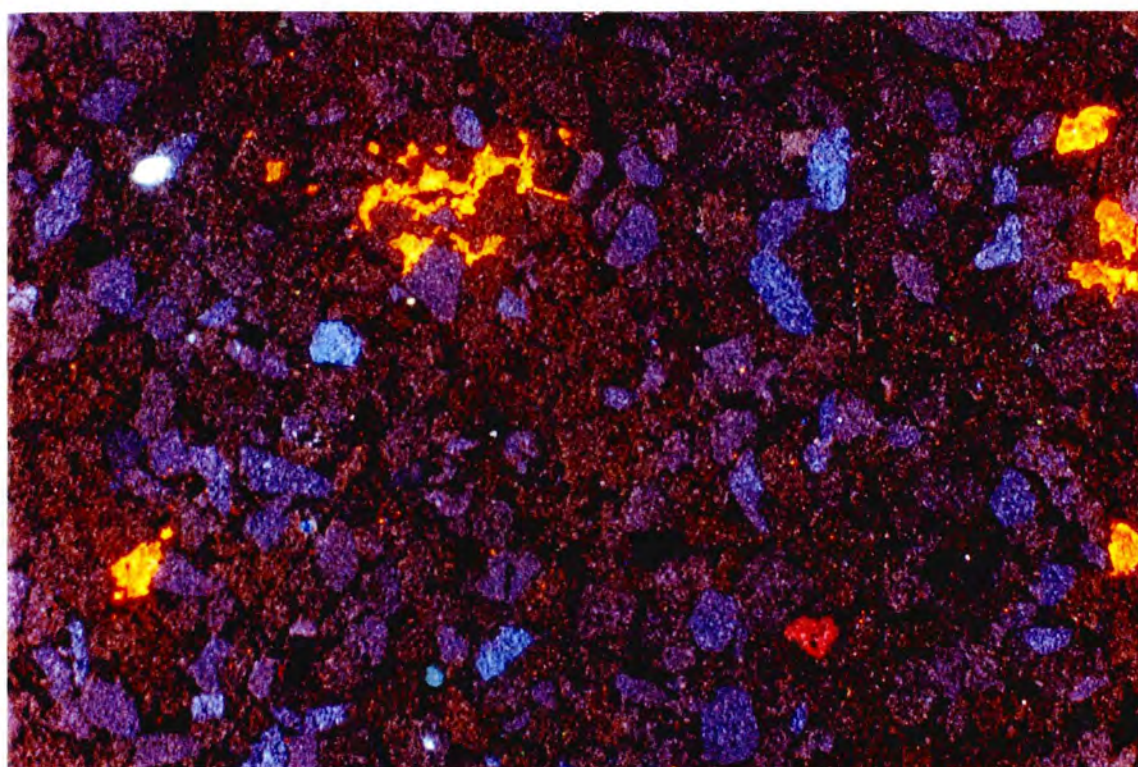


Photo 6 Cathodoluminescence Zone 5, single stage of diagenesis.

Figure 29. Pan American 1 Reusch, Spiro Sandstone.

between inclusion fluids and their mineral host: most aqueous fluids have refractive indices between 1.33 and 1.45, whereas the minerals in which they are included have refractive indices of 1.43 to 3.22 (Goldstein and Reynolds, 1994).

Primary fluid inclusions in calcite may have a variety of shapes, ranging from negative crystal to globular (smoothed surfaced) to irregular. However, there is no general correlation between inclusion shape and origin. The most useful criterion is fluid inclusions confined by growth-zone boundaries, growth zones that are defined by a single sheet of fluid inclusions, producing a cloudy crystal (Photomicrographs 7a & b, Figure 30).

Quartz-overgrowth primary inclusions are common along the surfaces ("dust rims") that separate detrital grains from authigenic overgrowths, and are also within the overgrowths. Inclusions along the detrital grain/overgrowth boundary typically parallel the boundary. Commonly they are small (<2 $\mu$ m diameter), but are rarely large (>10 $\mu$ m diameter) (Goldstein and Reynolds, 1994).

In diagenetic systems as those of the Spiro Sandstone, environments above 50°C occurs at significant burial depths and is commonly dominated by a single aqueous phase. Trapped at elevated temperatures, and in a one-phase environment, inclusions generate small vapor bubbles (less than 15 vol.% ) after temperatures fall below temperature of formation. All inclusions trapped under the same conditions have the same liquid-to-vapor ratio, and homogenize at the same temperature when heated. In some inclusions, the bubble is in constant motion ("active" ) within the vacuole. Roedder (1984) explained that the movement is due to extremely rapid flow at the bubble's surface from surface-tension contrasts caused by infinitesimally small thermal gradients. However, some bubbles remain stationary until the temperature reaches the temperature of formation.

A less conservative approach for temperature of heating ( $T_h$ ) is to determine the temperature of entrapment by applying a pressure correction to the  $T_h$  data from



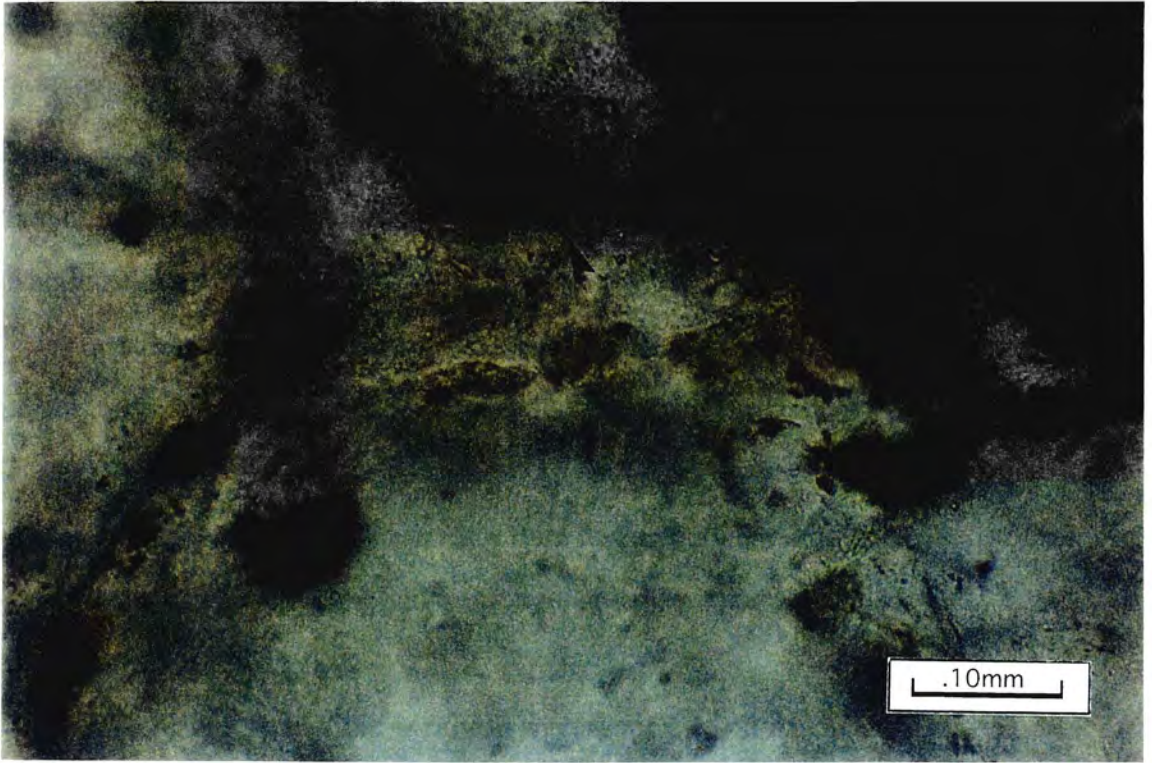


Photo 7a. Fluid inclusion Zone 1, quartz overgrowths.

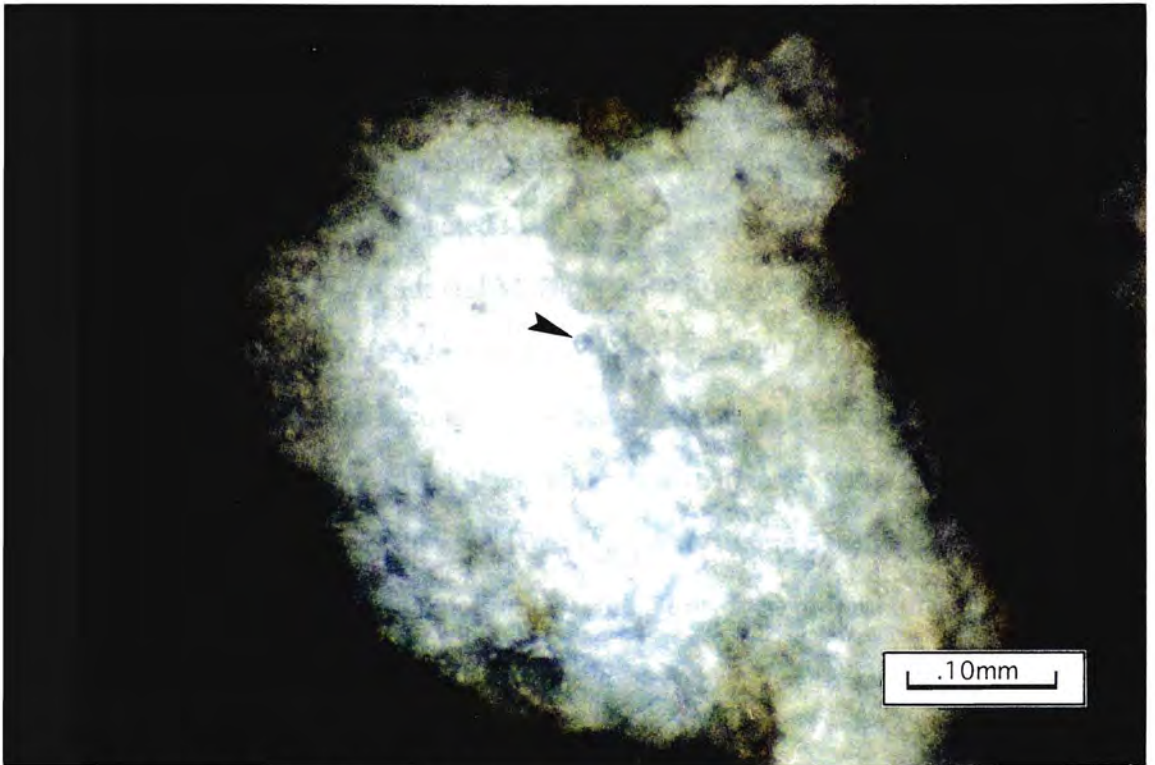


Photo 7b. Fluid inclusion Zone 5, calcite cement.

Figure 30. Pan American 1 Reusch, Spiro Sandstone.

consistent fluid-inclusion analysis. To apply the correct pressure correction, first, enough must be known about the composition of the inclusion fluid so that the appropriate phase diagram can be selected. Then the pore fluid pressure that existed at the time of inclusion entrapment must be determined independently. However, this type of analysis is beyond the applications for this study.

For the purpose of this study, depth-temperature point at which the temperature intersects the paleo-temperature gradient, yields depth of entrapment (Figure 31). However, such high-temperature and depth of entrapment for calcite cement, it may be assumed this may be a reset-temperature from deeper burial. Although, in subsurface depths, carbonate precipitation can be brought about by an increase in the pH and/or temperature (Tucker, 1991).

With results of the fluid-inclusion analysis of the Pan American 1 Reusch core from Zones 1 and 5, the following conclusions are proposed: The initial diagenetic-cementing stage involved deposition of calcite cement in Zones 1 and 5, at approximate temperature of 120°C and approximate depth of 8200ft (Figure 31a). As a result of hydrocarbon generation within the Spiro sandstone, acidic fluids leached into the lower calcite zones. The acidic solution acted to dissolve the calcite and deposit silica (Al-Shaieb and Walker, 1987; Schmidt and McDonald, 1979).

The silica deposited in the form of quartz overgrowths, leaving remnant calcite within fossil fragments, as the second stage of diagenesis in zones 1 and 2. Zone 1 silica diagenetic-cementing stage involved deposition of quartz overgrowths, formed at approximately 140° C and approximate depth of 9750ft (Figure 31a). Later diagenesis of ferroan minerals deposited thermal dolomites, which however, did not affect the sealing properties. Figure 32 shows the approximate timing of cementation episodes.

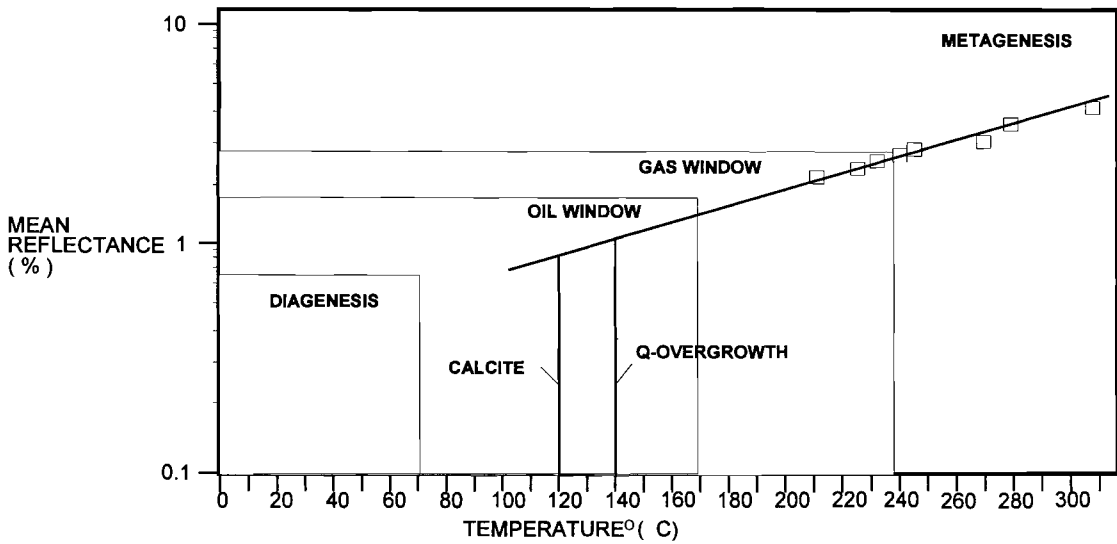
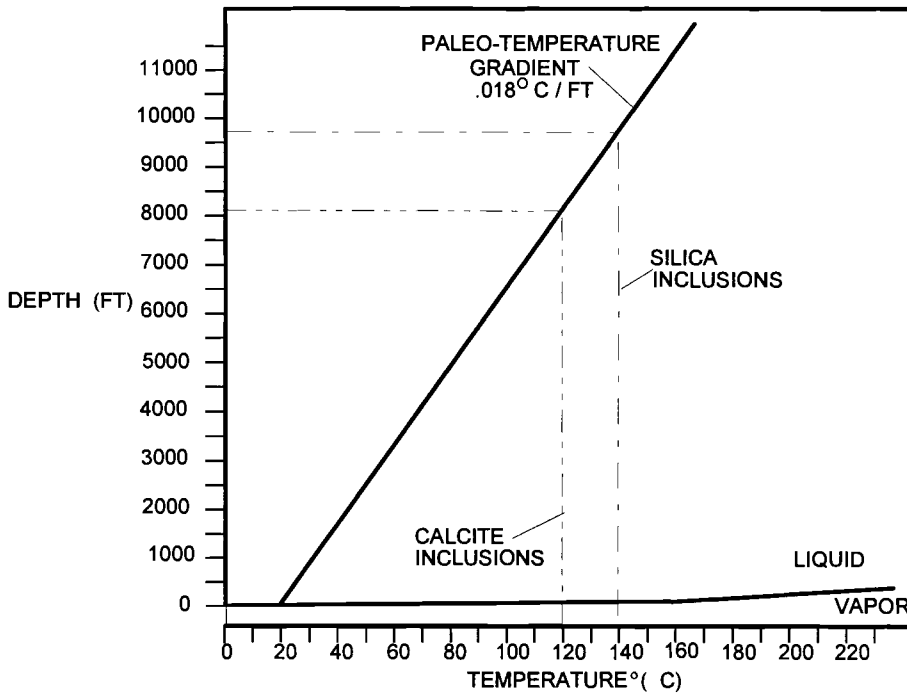


Figure 31a. Plot of burial-depth v. temperature of formation. Figure 31b. Vitrinite-reflectance v. temperature.



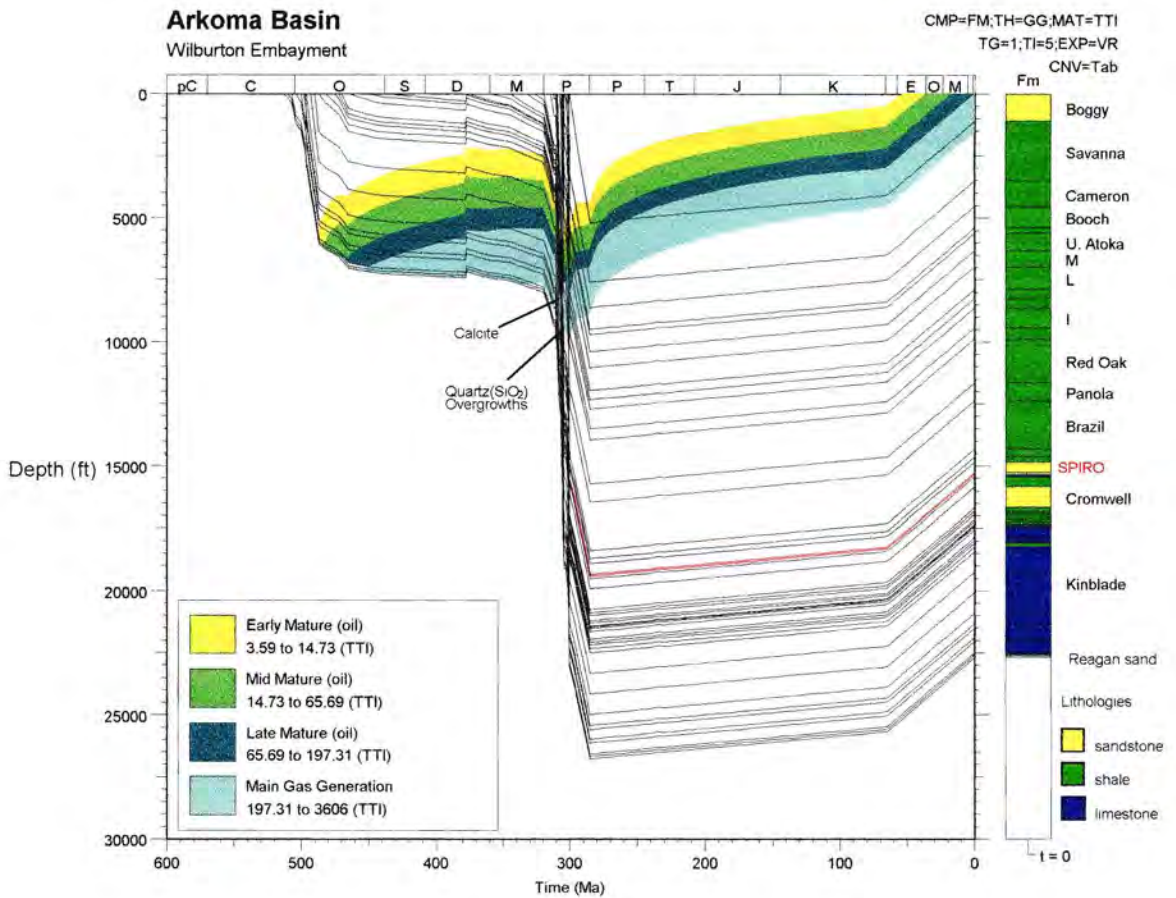


Figure 32. Calculated burial curve, and approximate cementation depth, Arkoma basin.

The diagenetic-cement zones can be correlated across the study area, they are reservoir seals in the Spiro Sandstone in the Wilburton area. These zones are consistently of very low porosity; they seal compartments from top and bottom. Plate 4 shows evidence that the seal zones are continuous, with thickening due to variation in the thickness of the Spiro, within the lower Spiro imbricate complex.

An argument in favor of the effectiveness of diagenetic seals in the presence of thrust faulting, and resistance to failure of seals can be explained with reference to extensive high heat flow that has been identified in the Arkoma basin. Upon extensive heating the minerals become ductile, allowing the seal zones to flow with faulting. Therefore, the seals remained effective throughout the basin deformation.

Diagenetic cements that form seals above and below the Spiro reservoir, but a mechanism is required for lateral seals to complete the compartmentation. Lateral seals may be fault seals. Thrusting of the imbricate complex, brings the Spiro reservoir into contact with impermeable beds, along with generation of mylonites, creates fault block compartments. Shale smears as a consequence of faulting, where shale smears with the greatest spatial distribution occur where the shale comprises at least 25% of the stratigraphic section displaced across the entire termination of a reservoir sandstone. The lack of permeability and porosity across the smear can be interpreted most simply to represent the mechanical collapse porosity and permeability under the influence of increased stresses (Gibson, 1994).

Strike-slip components of tear faulting also provide lateral fault seals for compartmentation. Suneson (1992) identified evidence of strike-slip motion in the Spiro, as well as surface expressions of strike-slip motion in the Wilburton area. The plan-view expression of overthrust belts commonly is marked by transverse strike-slip faults. These tear faults form as a result of the impossibility of transporting a huge masses of rock as single units. A miogeoclinal wedge hundreds of kilometers wide, and kilometers thick

simply cannot be moved along thrusts of unlimited length. Instead, large masses are broken into smaller units bounded by thrust faults and tear faults (Dahlstrom, 1969).

Tear faults have been described as compartmental faults. Recognized by Brown (1975) in the Wyoming foreland province, these serve as partitions between domains of rocks in which a common magnitude of shortening has been achieved in different ways. A given compartmental fault might separate a fold-dominated compartment from another that is fault-dominated. Compartmented faults are unlike classic strike-slip faults in that the sense of slip need not be uniform along the length of the fault. Moreover, compartmental faults are short compared to the magnitude of slip they accommodate (Davis, 1984).

Lithologic differences and stacked channels acting as sealing mechanisms, are restricted to areas north of the Wilburton area, where block-faulting dominates. Figure 25 illustrates compartments formed by the faulting of stacked channel-fill sandstones. Tidal or distributary channels across the tidal flats, have cut down into previously deposited sediments. Down-cutting and deposition of channel-lags, act as reservoir seals.

Based on the assumption that the Spiro reservoir within the individual compartments is continuous and completely sealed, a tectonic cause of abnormal pressures may be advanced as an explanation. Normal Spiro IBHP, as compared to average Spiro depth do not meet the requirements necessary for the reservoirs to be considered as overpressured. Because pressure-gradients are depth-dependent and typical Spiro gradients have normal pressure-gradients (0.465 psi/ft), an explanation of the abnormal pressure-gradients is that thrust faulting brought the Spiro reservoirs to a structurally higher position (Figure 33). The increase in structural elevation increases the pressure-gradient. However, the question remains "How is pressure maintained after being brought to shallower depths?". If the compartments are truly completely sealed and

there is continuity within the compartment, the pressure of the gas should be equal throughout the reservoir. However, an argument may be related to the tectonic activity. Tectonic stresses within the imbricate complex, may replace overburden stresses to maintain reservoir pressures.

## SUMMARY, CONCLUSIONS AND RECOMMENDATIONS

The Spiro Sandstone Formation of the Arkoma basin within Oklahoma has been a major gas source for over 40 years. However, an understanding of the geometry and characteristics of compartmented gas reservoirs has never been established for the Arkoma basin. The complex structural geology and lack of an accurate depositional model across the Wilburton area, have resulted in numerous dry holes. In some gas wells, abnormal pressure-gradients have been observed within imbricate-thrust complexes.

The purpose of this study was to provide plausible explanations for the generation of abnormal pressures in Spiro Sandstone reservoirs in the Arkoma basin. These reservoirs have been thrust; they are completely sealed compartments. Findings of the study may decrease the risk of exploration and may outline new areas for production of gas from the Spiro.

Mechanisms of compartmentation and sealing were studied by integrating various geological and geophysical data and information, concerning structural framework, depositional setting, diagenetic settings and patterns, and pressure regimes. The spatial examination of these lines of evidence aided in proposing a model for diagenesis of the Spiro sandstone in the Arkoma basin.

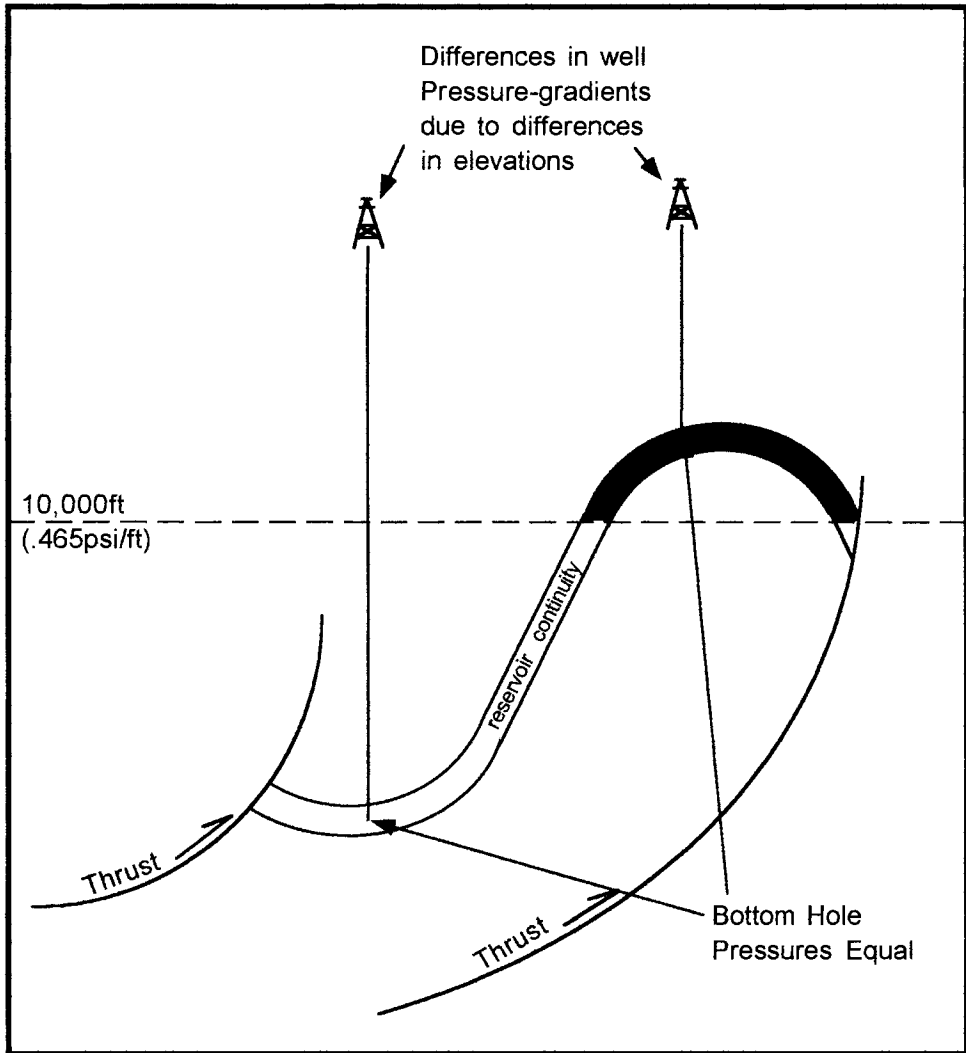


Figure 33 Diagram illustrating the model of Spiro Sandstone reservoirs elevated, increasing pressure-gradients when the reservoir is elevated above 10,000ft. With bottom-hole pressures  $\geq 4500$ psi, pressure-gradients are above 0.465psi/ft.

Patterns of diagenesis observed were influenced greatly by mechanical as well as chemical processes involved in evolution of the basin. These patterns were useful in evaluating various hypotheses related to development of seals and preservation and/or destruction of primary porosity.

From the evaluation of several cores of Spiro Sandstone within the Wilburton area, and from previous works, descriptions of the Spiro petrology, depositional environment, and porosity of the Spiro provided the following observations:

Quartz arenite, sublitharenite, and calcareous sandstone are the major lithologies observed. Quartz is the most abundant constituent; rock and fossil fragments are minor clasts. Diagenetic constituents include chamosite grain-coatings in the northern Arkoma basin, and glauconite in the southern Arkoma basin. Further to the south, the Spiro grades into a shale. There is a marked change in lithology across the basin from east to west. Sandstone is “cleaner” to the east, toward proposed sources of detrital material, whereas to the west the Spiro is increasingly calcareous.

Zones of highest porosity in the Spiro are in intervals where percentages of chamosite grain-coatings are great. Where chamosite is not present in the Spiro, reservoir-zone porosity is low as in the Shell 1-9 Mabry. Chamosite, combined with generation of hydrocarbons, preserved porosity, despite forces associated with compaction. Secondary porosity, due to chamosite and tightly cemented zones, is minimal, restricted primarily to moldic porosity in the Spiro, within the Wilburton area.

Proposed herein is a simplified depositional model for the Spiro Sandstone in the Wilburton area. Most works on the deposition of the Spiro have interpreted the major source of sediment to have been in Arkansas. Deltas to the east may have supplied the sediment, which was reworked by longshore drift westward down the paleo-coast. Tidal-flats to the west, coursed by distributary-channels supplying a wave-dominated delta system, mixed with the reworked sediments. Tidal flats and distributary-channels were a

sources of chlorite and chamosite; for a gelatinous-ooze and pore lining material. During low influx of sediment from the east, chamosite deposited as pore linings. The depositional system was in place while basin subsidence was increasing.

Structural geology of the Wilburton area consists of a system of imbricate thrust sheets that override an area of extensive normal block-faulting. The imbricate system is composed of upper and lower imbricate complexes, the upper complex having surface expressions of the major thrust faults. The thrust mass created a shear-component in the form of tear faults due to differential faulting.

Source rock of gas may have more than one source including intra-Spiro shale interbeds, migration along the basin trend from Arkansas, and migration from lower shale units prior to the formation of the lower seal. Production from the Spiro consists of dry gas with very minor oil production northwest of the Arkoma basin. Kerogen from various source rock in the Arkoma basin, has been classified as Type III. A burial and thermal maturation plot for the Arkoma basin in Oklahoma, showed that the Spiro passed through the gas window early in basin deformation, therefore, producing only gas.

Generation of hydrocarbons produced a pressured reservoir within the Spiro sandstone, which was compartmented later. Bottom-hole pressures across the Wilburton area consistently average 4500lb/psi. Pressure gradients vary greatly however, and the largest gradients are confined to the location of the imbricate complexes.

Diagenetic minerals in the Spiro have greatly influenced trapping of gas in the reservoir facies. The first stage of diagenetic cementation consisted of abundant calcite, in strata above and below the reservoir facies. A second stage of diagenesis consisted of the leaching of acidic fluids attendant to generation of hydrocarbons in the Spiro. These fluids dissolved calcite from the lower part of the Spiro and deposited silica as quartz overgrowths, the dominant cement in the lower Spiro. These two diagenetic zones are continuous across the Wilburton area.

With diagenetic cements that sealed the Spiro from the top and bottom, another mechanism of seal was required to complete the compartmentation. Lateral sealing was developed as tear-fault and thrust-fault components. Mylonites and shale smears provided low porosities and permeabilities to complete compartmentation.

Combining data from various characteristics of Spiro sandstone in the Arkoma basin provided the basis for possible explanations of abnormal-gas-pressure compartments in the Wilburton area.

Petrological characteristics and structural geology components of compartmentation developed in various stages of basin genesis. Diagenetic-cementation reduced porosity in parts of the Spiro where grains were not coated by chamosite. Calcite cement produced initial zones of low porosity; the lower calcite zone then underwent dissolution, replaced by quartz overgrowths. At this stage the hydrocarbons in the reservoir facies is confined by the lateral extent of the chamosite facies. With the approach of the South American Plate, thrust faulting produced imbricate thrust sheets which included the Spiro formation. Differential faulting produced strike-slip motion that along with the thrust faults, provided lateral seals to complete compartmentation.

After analyzing pressure data from the Arkoma basin, initial bottom-hole pressures of wells drilled in the 1960s averaged 4500psi. However, upon calculating pressure-gradients, variations arise across the Wilburton area. The average pressure gradient of oil and gas reservoirs is 0.465psi/ft, and the average depth Spiro Sandstone is more than 10,000ft, therefore, if undeformed, the Spiro would not be considered as an overpressured reservoir. Because pressure-gradients in some reservoirs of the Spiro exceed 0.465psi/ft computed by (initial-bottom-hole pressure) X (reservoir depth), these reservoirs must have been elevated structurally, with preservation of reservoir pressure. Comparison of the pressure-gradient map and the Spiro sandstone structural contour map shows that the area of the imbricate complexes (where the Spiro has been elevated)



coincides with the abnormal pressure-gradients. The preservation of the reservoir pressure upon being brought to environments of reduced overburden, is compensated by the stresses produced from thrusting action and thrust sheet stacking.

A summary of the model states that compartmentation of the Spiro sandstone in the Wilburton area is due to diagenetic cements and faulting, the combination of which formed reservoir seals. Abnormal pressure regimes are due to structural elevation of some Spiro reservoirs, by thrusting that formed the Arkoma basin.

Future studies of the Spiro sandstone could be concentrated on the detailed structural geology of the Wilburton area. The South Panola field is a second area of abnormal pressures; bottom-hole pressures are higher than in the Wilburton field.

## SELECTED BIBLIOGRAPHY

- Abeegg, F. E., (1990), Fluid-inclusion Analysis of Dolomite in the Lithoclasts from the Morgan Creek Limestone (Upper Cambrian) of Central Texas: The Compass, vol. 67, p. 135-146.
- Al-Shaieb, Z., and Walker, P., (1987), Evolution of Secondary Porosity in Pennsylvanian Morrow Sandstones, Anadarko Basin, Oklahoma: Geology of Tight Gas Reservoirs: American Assoc. Petrol. Geol. Studies in Geology no.24, p. 45-67.
- Al-Shaieb, Z., Shelton, J., and Puckette, J., (1989), Sandstone Reservoirs of the Mid-Continent: American Assoc. of Petrol. Geologists: 1989 Meeting, p. 59-72.
- Al-Shaieb, Z., and Lynch, M., (1989), Chamosite: Critical ingredient in diagenetic differentiation of sandstone reservoirs, Abstract: AAPG Annual Convention, San Antonio, vol. 73-3, p. 326-327.
- Arbenz, J. K., (1968), Structural Geology of the Potato Hills, Ouachita Mountains, Oklahoma, *in* Cline, L. M., ed., A Guidebook to the Geology of the Western Arkoma Basin and Ouachita Mountains, Oklahoma: Oklahoma City Geological Society, p. 109-121.
- Asquith, G., (1982), Basic Well Log Analysis for Geologists: American Association of Petroleum Geologists, Tulsa, Ok., p. 91, 216.
- Barker, C. E., and Halley, R. B., (1988), Fluid Inclusions in Vadose Cement with Consistant Vapor to Liquid Ratios, Pleistocene Miami Limestone, Southeastern Florida: Geochimica et Cosmochimica Acta, vol. 52, p. 1019-1025.
- Berry, R. M., and Trumbly, W. D., (1968), Wilburton Gas Field, Arkoma Basin, Oklahoma, *in* Cline, L. M., ed., A Guidebook to the Geology of the Western Arkoma Basin and Ouachita Mountains, Oklahoma: Oklahoma City Geological Society, p. 86-103.
- Boggs, S., Jr., (1987), Principles of Sedimentology and Stratigraphy: New York, N.Y., Macmillan, 313 p.
- Branan, C. B., (1960), Tectonics of the Ouachita Mountains of Oklahoma and Arkansas: 7th Bienn. Geological Symposium, Norman, Oklahoma University., p. 3-28.

- Briggs, G., (1974), Carboniferous Depositional Environments in the Ouachita Mountains: Arkoma Basin Area of Southeastern Oklahoma: in Briggs, G. (ed.) Carboniferous of the Southeastern United States: Geol. Soc. of America Special Paper no. 148, p. 225-240.
- Brown, W. G., (1975), Casper Wyoming area (Wyoming)--Structural Model of Laramide Deformation (abs): American Association of Petroleum Geologists Bulletin, vol. 59, p. 906.
- Bruce, C. H., (1984), Smectite Dehydration-- Its Relation to Structural Development and Hydrocarbon Accumulation in Northern Gulf of Mexico Basin: Am. Assoc. Petroleum Geologists Bulletin, vol. 68, p. 673-683.
- Buchanan, R. S., and Johnson, F. K., (1968), Bonanza Gas Field; A Model for Arkoma Growth Faulting, in Cline, L. M., ed., A Guidebook to the Geology of the Western Arkoma Basin and Ouachita Mountains, Oklahoma: Oklahoma City Geological Society, p. 75-85.
- Burley, S. D., Mullis, J., and Matter, A., (1989), Timing Diagenesis in the Tartan Reservoir (UK North Sea): Constraints from Combined Cathodoluminescence Microscopy and Fluid Inclusion Studies: Marine and Petroleum Geology, vol. 6, p. 98-120.
- Carrot, B. J., (1994), Thermal Maturity of Surface Samples from the Frontal and Central Belts, Ouachita Mountains, Oklahoma: Geology and Resources of the Eastern Ouachita Mountains Frontal Belt and Southeastern Arkoma Basin, Oklahoma: Oklahoma Geological Survey, vol. 29, p. 271-276.
- Cemen, I., Al-Shaieb, Z.; Hess, F.; Akthar, S., And Feller, R., (1995) Geometry of Thrusting in the Wilburton Gas Field and Surrounding Areas, Arkoma Basin, Oklahoma: Implications for Gas Exploration in the Spiro Sandstone Reservoirs: Unpublished, Oklahoma State University.
- Cline, L. M., (1960), Stratigraphy of the Late Paleozoic Rocks of the Ouachita Mountains. Oklahoma: Oklahoma Geological Survey Bulletin 85, p.113.
- Curiale, J. A., (1983), Petroleum Occurrences and Source Rock Potential of the Ouachita Mountains, Southeastern Oklahoma: Oklahoma Geological Survey Bulletin, vol. 135, p. 65.
- Davis, G. H., (1984), Structural Geology of Rocks and Regions: New York, N. Y. p. 285.
- Dow, W. G., (1977), Kerogen Studies and Geological Interpretations: Journal of Geochemical Exploration, vol. 7, p. 79-99.

- Exum, F. A., and Harms, J. C., (1968), Comparison of Marine Bar with Valley Fill Stratigraphic Traps, Western Nebraska: American Association of Petroleum Geologists Bulletin, vol. 52, no. 10, p. 1851-1868.
- Feller, R. B., (1994), Reevaluation of the Geologic Model of the Deep Rock Glorietta Formation for Secondary Recovery: Exxon USA, Unpublished, p. 10.
- Gibson, R. G., (1994), Fault-Zone Seals in Siliclastic Strata of the Columbus Basin, Offshore Trinidad: AAPG Bulletin, vol. 78/9, September 1994, p. 1372-1386.
- Grayson, R. C., and Hinde, L. K., (1988), Lower Atokan Group (Spiro Sand), Stratigraphic Relationships, Depositional Environments, and Sand Distribution, Frontal Ouachita Mountains, Oklahoma: Unpublished, Baylor University.
- Goldstein, R. H., (1994), Systematics of Fluid Inclusions in Diagenetic Minerals: Society for Sedimentary Geology, Short Course 31.
- Goldstein, R. H., (1986a), Reequilibrium of Fluid Inclusions in Low-Temperature Calcium-Carbonate Cement: Geology, vol. 14, p. 792-795.
- Goldstein, R. H., Franseen, E. K., and Mills, M. S., (1990), Diagenesis Associated with Subareal Exposure of Miocene Strata, Southeastern Spain: Implications for Sea-Level Change and Preservation of Low-Temperature Fluid Inclusions in Calcite Cement: Geochimica et Cosmochimica Acta, vol. 54, p. 699-704.
- Gregg, J. M., and Sheldon, K. L., (1990), Dolomitization and Dolomite Neomorphism in the Back Reef Facies of the Bonnetterre and Davis Formations (Cambrian), Southeast Missouri: Journal of Sedimentary Petrology, vol. 60, p. 549-562.
- Guscott, S. C., and Burley, S. D., (1993), A Systematic Approach to Reconstructing Paleofluid Evolution from Fluid Inclusions in Authigenic Quartz Overgrowths, *in* Parnell, J., and others, eds., Conference Proceedings, Geofluids, vol. 93, p. 323-328.
- Hopkins, H. R., (1968), Structural Interpretation of the Ouachita Mountains, *in* Cline, L. M., ed., A Guidebook to the Geology of the Western Arkoma Basin and Ouachita Mountains, Oklahoma: Oklahoma City Geological Society, p. 104-108.
- Houseknecht, D. W., (1987), The Atoka Formation of the Arkoma Basin: Tectonics, Sedimentology, Thermal Maturity, and Sandstone Petrology: Tulsa Geol. Soc., Short Course, Note, p. 1-72.
- Houseknecht, D. W., and Mathews, S. M., (1985), Thermal Maturity of Carboniferous Strata, Ouachita Mountains: American Association of Petroleum Geologists Bulletin, vol. 69, p. 335-345.

- James, N. P., and Bone, Y., (1992), Synsedimentary Cemented Calcareous Layers in Oligo-Miocene Coolwater Shelf Limestones, Eucla Platform, Southern Australia: Journal of Sedimentary Petrology, vol. 62, p. 860-872.
- Janssen-Van Rosmalen, R., and Bennema, P., (1977), The Role of Hydrodynamics and Supersaturation in the Formation of Liquid Inclusions in KDP: Journal of Crystal Growth, vol. 42, p. 224-227.
- Klein, G., (1977), Clastic Tidal Facies: Continuing Education Publication Co., Champaign, Ill., p. 149.
- Lumsden, D. N.; Pittman, E. D., and Buchanan R. S., (1971), Sedimentology and Petrology of the Spiro and Foster Sands (Pennsylvanian), McAlester Basin, Oklahoma: American Association of Petroleum Geologists Bulletin, vol. 55, no. 1, p. 254-266.
- Luo, M., Baker, M. R., and LeMone, D. V., (1994), Distribution and Generation of the Overpressured System, Eastern Delaware Basin, Western Texas and Southern New Mexico: American Association of Petroleum Geologists Bulletin, vol. 78/9, p. 1386-1404.
- McLimans, R. K., (1987), The Application of Fluid Inclusions to Migration of Oil and Diagenesis in Petroleum Reservoirs: Applied Geochemistry, vol. 2, p. 585-603.
- Powers, S., (1928), Age of the Oklahoma Mountains--The Ouachita, Arbuckle and Wichita Mountains of Oklahoma and Llano-Burnet and Marathon Uplifts of Texas: Geological Society of America Bulletin, vol. 39, p. 1031-1072.
- Porrenga, D. H., (1967), Glauconite and Chamosite as Depth Indicators in the Marine Environment: Marine Geology, vol. 5, p. 495-501.
- Roedder, E., (1984), Fluid Inclusions: Mineralogical Society of America, Reviews in Mineralogy, vol. 12, p. 644.
- Selley, R. C., (1978), Ancient Sedimentary Environments: 2nd edition, Cornell University Press, Ithaca, N.Y., 287 p.
- Tucker, M. E., (1991), Sedimentary Petrology: An Introduction to the Origin of Sedimentary Rocks: 2nd edition, Cambridge, Mass., p. 57-58.
- Ulrich, E. O., (1927), Fossiliferous Boulders in the Ouachita Caney Shale and the Age of the age of the Shale Containing Them: Oklahoma Geological Survey Bulletin, vol. 45, 48 p.

- Walker, G., and Burley, S. D., (1991), Luminescence, Petrology and Spectroscopic Studies of Diagenetic Minerals, *in* Barker, C. E., and Kopp, O., eds., Luminescence Microscopy: Quantitive and Qualitive Aspects: Society of Economic Paleontology and Minerology Short Course Notes, vol. 11, p. 83-96.
- White, D., (1915), Some Relations in Origin Between Coal and Petroleum: Journal of the Washington Academy of Sciences, vol. 5, p. 189-212.
- Zachary, D. L., and Sutherland, P. K., (1984), Stratigraphy and Depositional Framework of the Atoka Formation, Arkoma Basin of Arkansas and Oklahoma; *in* The Atoka Series (Pennsylvanian) and its Boundaries-- A Symposium: Oklahoma Geological Survey Bulletin 136, p. 9-19.

## REFERENCES

1. A Dictionary for the Petroleum Industry. Petroleum Extension Service Division of Continuing Education, University of Texas at Austin, 1991
2. Dwights' Natural Gas Well Production Histories. Richardson, Tx., 1994.
3. Dwights' Natural Gas Well Production Histories. Richardson, Tx., 1989.
4. Dwights' Natural Gas Well Production Histories. Richardson, Tx., 1979.

## APPENDICES



APPENDIX A  
PRESSURE DATA TABLES

PRESSURE DATA TABLE OF 24 HOUR TEST  
FOR WELLS COMPLETED AND PRODUCING 1960-69  
ARKOMA BASIN OKLAHOMA  
(source DWGHTS)

COMP - YEAR PRODUCTION BEGAN  
WHISP - WELL HEAD SHUT IN PRESSURE (PSI)  
BHT - BOTTOM HOLE TEMPERATURE ( DEG F)  
IBHP - INITIAL BOTTOM HOLE PRESSURE (PSI)  
PGR - PRESSURE GRADIENT(PSI / FT)  
PROD - CUMULATIVE PRODUCTION AS OF 1994 (MMCF- MILLION CUBIC FEET)

COMP	OPERATOR	WELL	LOCATION	WHSIP	PERF	BHT	IBHP	PGR	PROD
1964	Arco	Dunagan ASE#A1	13-5N-17E	3859	8434-8455	188	4560	.54	16.0
1966	Mobile	Kent Heirs#1	14-5N-17E	2503	9975-10017	212	3291	.33	1.1
1968	Arco	Bowman Pauline 1	20-5N-17E	3662	9270-9317	202	4494	.48	18.1
1967	Arco	Bowman Pauline 1	21-5N-17E	3732	9630-9668	207	4588	.48	8.4
1966	Mobil	Sivil Gol 1	22-5N-17E	3558	9177-9221	200	4320	.47	9.3
1965	Mobile	Darby UN#1	23-5N-17E	3787	9946-9986	212	4529	.45	9.5
1964	Marathon	Fabro NW SE	24-5N-17E	3846	9126-9150	199	4591	.50	8.9
1965	Arco	Henley JL#1	25-5N-17E	3756	10022-10052	213	4536	.45	7.4
1965	Amoco	Caudron U#1	26-5N-17E	3542	9774-9788	209	4347	.44	1.8
1966	Arco	Parker Alfred#1	27-5N-17E	3804	9121-9140	198	4557	.50	10.4
1967	Arco	USA 1	28-5N-17E	3640	9707-9757	208	4428	.45	5.1
1968	Arco	Bowman 1	29-5N-17E	3650	10553-10606	221	4512	.43	2.6
1969	Arco	Richards Edith 1	30-5N-17E	3786	11030-11055	228	4636	.42	5.3

PRESSURE DATA TABLE OF 24 HOUR TEST  
FOR WELLS COMPLETED AND PRODUCING 1960-69  
ARKOMA BASIN OKLAHOMA  
(source DWIGHTS)

COMP - YEAR PRODUCTION BEGAN  
WHISP - WELL HEAD SHUT IN PRESSURE (PSI)  
BHT - BOTTOM HOLE TEMPERATURE ( DEG F)  
IBHP - INITIAL BOTTOM HOLE PRESSURE (PSI)  
PGR - PRESSURE GRADIENT(PSI/ FT)  
PROD - CUMULATIVE PRODUCTION AS OF 1994 (MMCF- MILLION CUBIC FEET)

COMP	OPERATOR	WELL	LOCATION	WHSIP	PERF	BHT	IBHP	PGR	PROD
1964	Arco	Dunagan ASE#A1	13-5N-17E	3859	8434-8455	188	4560	.54	16.0
1966	Mobile	Kent Heirs#1	14-5N-17E	2503	9975-10017	212	3291	.33	1.1
1968	Arco	Bowman Pauline 1	20-5N-17E	3662	9270-9317	202	4494	.48	18.1
1967	Arco	Bowman Pauline 1	21-5N-17E	3732	9630-9668	207	4588	.48	8.4
1966	Mobil	Sivil Gol 1	22-5N-17E	3558	9177-9221	200	4320	.47	9.3
1965	Mobile	Darby UN#1	23-5N-17E	3787	9946-9986	212	4529	.45	9.5
1964	Marathon	Fabro NW SE	24-5N-17E	3846	9126-9150	199	4591	.50	8.9
1965	Arco	Henley JL#1	25-5N-17E	3756	10022-10052	213	4536	.45	7.4
1965	Amoco	Caudron U#1	26-5N-17E	3542	9774-9788	209	4347	.44	1.8
1966	Arco	Parker Alfred#1	27-5N-17E	3804	9121-9140	198	4557	.50	10.4
1967	Arco	USA 1	28-5N-17E	3640	9707-9757	208	4428	.45	5.1
1968	Arco	Bowman 1	29-5N-17E	3650	10553-10606	221	4512	.43	2.6
1969	Arco	Richards Edith 1	30-5N-17E	3786	11030-11055	228	4636	.42	5.3
1968	Oryx	Casteel 1	32-5N-17E	3786	11380-11420	233	4674	.41	4.2
1969	Arkoma	Potichny 1	33-5N-17E	3784	11054-11098	229	4635	.42	5.0
1969	Arkoma	Whitney#1	34-5N-17E	3450	11162-11268	231	4291	.38	2.8
1966	Arco	Lerblance#1	36-5N-17E	3577	10554-10572	221	4338	.41	1.2

1964	Arco	USA Jarq Anderson#1	1-5N-18E	3965	11414-11435	234	4764	.42	8.7
1963	Arco	Davis James#1	2-5N-18E	3621	11682-11710	238	4481	.38	2.8
1963	Arco	Pate Kinnikin#1	3-5N-18E	3800	11660-11700	238	4632	.40	4.3
1963	Arco	#1 Edgar S Woods	4-5N-18E	3360	11671-11684	238	4251	.36	1.5
1963	Arco	Sawyer Lela#1	5-5N-18E	3527	11646-11686	237	4425	.38	1.4
1963	Arco	Gardner 1	7-5N-18E	3288	11998-12033	243	4227	.35	.08(69)
1963	Arco	Raunika 1	8-5N-18E	2918	11653-11691	238	3753	.32	.20(70)
1963	Arco	State Topping#1	9-5N-18E	3691	11712-11739	238	4542	.39	1.3
1963	Arco	MCalister A#1	10-5N-18E	3840	11757-11793	239	4670	.40	2.4
1963	Arco	Davis A#1&2A	11-5N-18E	3528	11912-12132	244	4406	.36	.60
1963	Arco	Robinson#1	12-5N-18E	4015	11980-12004	242	4824	.40	10.2
1963	Arco	Austin Wayne	13-5N-18E	3975	9083-9136	198	4669	.51	15.0
1963	Arco	Costilow PE#1	14-5N-18E	3701	8568-8605	190	4432	.52	.90
1963	Arco	Yourman#1	15-5N-18E	3830	8754-8802	193	4573	.52	10.8
1963	Arco	Kilpatrick#1	16-5N-18E	3766	8576-8614	190	4488	.52	5.9
1963	Arco	Fazekas Steve#1	17-5N-18E	3862	8784-8833	193	4597	.52	22.5
1963	Arco	Hampton Bub#1	18-5N-18E	3867	9030-9069	197	4581	.51	16.5
1964	Arco	Bennett State#1	19-5N-18E	3749	8960-9006	197	4479	.50	25.1
1963	Arco	Smith Marion#1&2	20-5N-18E	3879	8504-10688	222	4579	.43	36.4
1963	Arco	Paschal#1	21-5N-18E	3836	8327-8425	187	4540	.54	29.7
1963	Arco	MCalister#1	22-5N-18E	3855	8288-8328	186	4554	.55	12.9
1963	Anadarko	Williams#1	23-5N-18E	3615	8811-8831	193	4364	.49	14.0
1963	Arco	James#A1	24-5N-18E	3718	9000-9060	197	4455	.49	13.2
1966	Texaco	Varnum Guy#1	25-5N-18E	3645	10461-10478	219	4449	.43	2.5
1964	Arco	Watts-Jones#1	26-5N-18E	3003	10308-10352	217	3845	.37	2.2
1964	Arco	Enis EV#1	27-5N-18E	3766	9764-9783	152	4537	.46	6.0
1963	Arco	State#C1	28-5N-18E	3815	8946-8986	196	4534	.51	24.6
1963	Arco	Dobbs State#1	29-5N-18E	3829	8707-8754	193	4543	.52	16.3
1964	Ar-La Gas	Bennett Jessie#1&2	30-5N-18E	3313	9132-9832	209	4098	.42	3.0
1964	Arco	Watts M#1	33-5N-18E	3397	11371-11399	233	4221	.37	4.0

1965	Amoco	Reusch#1	3-5N-19E	4062	11476-11492	235	4900	.43	20.5
1966	Amoco	Choctow#T3	4-5N-19E	4012	11302-11326	232	4829	.43	9.4
1966	Amoco	Choctow T#T4	5-5N-19E	4055	11371-11393	233	4863	.43	18.4
1966	Amoco	USA McTiernan J#1	6-5N-19E	3963	11325-11333	232	4790	.42	11.8
1966	Amoco	Quaid#1	7-5N-19E	4020	11836-11842	239	4845	.41	11.6
1963	JMC	College 100#1	18-5N-19E	3975	11866-11892	241	4763	.40	7.6
1964	Exxon	Sparks Charles#1	19-5N-19E	3582	12310-12320	247	4465	.36	4.2
1965	Exxon	Ray JA#1	20-5N-19E	3800	12265-12286	247	4624	.38	5.0
1967	Oryx	Diamond 1	30-5N-19E	3325	11102-11127	229	4148	.37	1.4

1969	BHP	Wildlife#1	24-6N-18E	4014	11506-11518	235	4807	.42	1.6
1968	Amoco	Anderson Prich#1-12	25-6N-18E	3917	11579-11599	236	4757	.41	6.7
1964	Arco	Michell Unit #1	32-6N-18E	3736	11646-11664	237	4605	.40	1.2
1967	Amoco	Wilson 1	35-6N-18E	2484	11548-11556	236	3271	.28	.09(82)
1967	Oryx	Federal Church#1	36-6N-18E	3830	11033-11060	228	4614	.42	8.2

1968	Sun	Bratton 1	2-6N-19E	3341	10120-10150	214	4173	.41	2.2
1966	Exxon	Clay Brown 1	3-6N-19E	3500	10237-10261	216	4345	.42	8.9
1967	Exxon	Coblentz LM	4-6N-19E	3488	10156-10174	215	4307	.42	2.3
1967	Mobil	Weaver D 1C	5-6N-19E	2765	10175-10185	215	3562	.35	.40(INA)
1967	Arco	Dept of Wildlife Co#2	7-6N-19E	3217	10218-10232	215	4056	.40	1.6(INA)
1968	Mobil	Weaver 1F	8-6N-19E	3038	9982-9994	212	3906	.39	2.3
1969	Mobile	Fred Clawson Unit1	9-6N-19E	3430	10040-10060	213	4279	.43	10.5
1969	Mobil	Browne C 1	10-6N-19E	3340	10367-10390	218	4204	.41	10.8
1969	Oxley	Weaver	16-6N-19E	3453	10426-10446	219	4252	.41	.80(INA)
1969	BHP	Cave 1	19-6N-19E	3827	11438-11454	234	4626	.40	10.6
1967	Mobile	Weaver D#1B	20-6N-19E	3731	11174-11208	230	4563	.41	3.7
1968	Mobile	Weaver D#1E	21-6N-19E	3723	11245-11272	231	4555	.40	2.9
1969	Mobil	Harrison 1	22-6N-19E	3978	10906-10928	226	4765	.44	COM94
1966	Samson	Young R#1	27-6N-19E	3880	11169-11191	230	4687	.42	3.0
1986	Samson	Young R 2	27-6N-19E	1807	11090-11110	229	2440	.22	1.8
1966	Samson	Young R 1	28-6N-19E	3960	11392-11422	234	4757	.42	13.0
1966	Shell	Kilpatrick 1	29-6N-19E	4013	11678-11694	238	4813	.41	18.6
1967	Mobil	Hackney 1	30-6N-19E	3900	11714-11732	238	4717	.40	8.9
1966	Amoco	E Okla A&M#1	31-6N-19E	3990	10990-11018	227	4800	.44	10.9
1966	Amoco	Quaid B1	32-6N-19E	4024	10991-11006	227	4829	.44	13.7
1966	Amoco	Adams C1	33-6N-19E	4079	11030-11062	228	4874	.44	15.2
1966	Williford	Young 1	34-6N-19E	3708	11425-11445	234	4550	.40	.60(INA)

1969	Shell	Jankowsky 1	5-6N-20E	2694	10954-10980	227	3557	.32	.10(73)
1965	Mobil	Parks P 1	33-6N-20E	3875	13089-?		4685		.08(70)

1963	Amoco	Free Unit 1	11-6N-21E	3985	11832-11887	241	4846	.41	12.1
1963	Sun	Norris 1	12-6N-21E	3892	11828-11904	241	4794	.40	10.1
1963	Amoco	Gallagher 1	13-6N-21E	3989	11877-11933	241	4849	.41	13.9
1963	Sun	Gallagher Wm 1	14-6N-21E	3843	11951-11990	242	4678	.39	16.6
1963	Amoco	Booth 1	15-6N-21E	3976	12110-12152	245	4874	.40	6.1(INA)
1964	Amoco	Brewer 1	16-6N-21E	3990	12156-12180	245	4883	.41	4.3
1966	Amoco	White 1	18-6N-21E	4024	12640-12725	253	4925	.39	17.1(INA )
1965	Exxon	Erwin WD 1	23-6N-21E	3734	11982-12001	242	4666	.39	3.3(INA)
1965	Amoco	Cecil 1	24-6N-21E	3945	11757-11831	240	4839	.41	7.4

PRESSURE DATA TABLE OF 24 HOUR TEST  
FOR WELLS COMPLETED AND PRODUCING 1960-1979  
ARKOMA BASIN OKLAHOMA  
(source DWIGHTS)

COMP - YEAR PRODUCTION BEGAN  
WHISP - WELL HEAD SHUT IN PRESSURE (PSI)  
BHT - BOTTOM HOLE TEMPERATURE ( DEG F)  
IBHP - INITIAL BOTTOM HOLE PRESSURE (PSI)  
PGR - PRESSURE GRADIENT(PSI / FT)  
PROD - CUMULATIVE PRODUCTION AS OF 1979 IN MMCF (MILLION CUBIC FEET)

COMP	OPERATOR	WELL	LOCATION	WHSIP	PERF	BHT	IBHP	PGR	PROD
1970	Arkoma	Pattison NW #1	1-4N-17E	3336	11399-11448	238	4168	.36	.40
1970	Arkoma	McCasin 1	2-4N-17E	2580	11371-11405	233	3408	.30	3.3
1970	Arkoma	Layden#1	3-4N-17E	3100	11750-11792	239	3975	.34	1.9
1970	Arkoma	Stine 1-4	4-4N-17E	3726	10909-10941	226	4585	.42	.20
1970	Arkoma	Rock Island 1-5	5-4N-17E	3878	11132-11164	230	4686	.42	7.1
1971	Arkoma	Hartshome 1	6-4N-17E	3740	10892-10926	226	4595	.42	6.7
1973	Amoco	Rock Isl Imp 60 1-7	7-4N-17E	3810	11302-11338	232	4721	.42	.30

1964	Arco	Dunagan ASE#A1	13-5N-17E	3859	8434-8455	188	4560	.54	12.0
1966	Mobile	Kent Heirs#1	14-5N-17E	2503	9975-10017	212	3291	.14	.70
1978	Samson	Kent#1	15-5N-17E	2944	8925-9054	198	3756	.42	3.5
1978	Samson	Bobo 1	16-5N-17E	2587	9634-9648	207	3437	.36	.20
1968	Arco	Bowman Pauline 1	20-5N-17E	3662	9270-9317	202	4494	.31	11.7
1967	Arco	Bowman Pauline 1	21-5N-17E	3732	9630-9668	207	4588	.12	5.4
1966	Mobil	Sivil Gol 1	22-5N-17E	3558	9177-9221	200	4320	.24	7.8
1965	Mobile	Darby UN#1	23-5N-17E	3787	9946-9986	212	4529	.19	7.5
1964	Marathon	Fabro NW SE	24-5N-17E	3846	9126-9150	199	4591	.27	6.3
1965	Arco	Henley JL#1	25-5N-17E	3756	10022-10052	213	4536	.20	5.0
1965	Amoco	Caudron U#1	26-5N-17E	3542	9774-9788	209	4347	.14	1.2
1966	Arco	Parker Alfred#1	27-5N-17E	3804	9121-9140	198	4557	.35	6.9
1967	Arco	USA 1	28-5N-17E	3640	9707-9757	208	4428	.16	3.4
1968	Arco	Bowman 1	29-5N-17E	3650	10553-10606	221	4512	.17	1.8
1969	Arco	Richards Edith 1	30-5N-17E	3786	11030-11055	228	4636	.11	3.5
1970	Arkoma	Pettit 1	31-5N-17E	3908	10353-10390	218	4720	.45	8.5
1968	Oryx	Casteel 1	32-5N-17E	3786	11380-11420	233	4674	.41	2.6
1969	Arkoma	Potichny 1	33-5N-17E	3784	11054-11098	229	4635	.42	3.1
1969	Arkoma	Whitney#1	34-5N-17E	3450	11162-11268	231	4291	.38	1.9
1970	Arco	Kurliko Andrew#1	35-5N-17E	3760	11074-11134	229	4556	.41	4.0
1966	Arco	Lerblance#1	36-5N-17E	3577	10554-10572	221	4338	.41	.30

1964	Arco	USA Jarq Anderson#1	1-5N-18E	3965	11414-11435	234	4764	.42	8.1
1963	Arco	Davis James#1	2-5N-18E	3621	11682-11710	238	4481	.38	2.2
1963	Arco	Pate Kinnikin#1	3-5N-18E	3800	11660-11700	238	4632	.40	3.3
1963	Arco	#1 Edgar S Woods	4-5N-18E	3360	11671-11684	238	4251	.36	1.2
1963	Arco	Sawyer Lela#1	5-5N-18E	3527	11646-11686	237	4425	.38	.97
1963	Arco	Gardner 1	7-5N-18E	3288	11998-12033	243	4227	.35	.08(69)
1963	Arco	Raunika 1	8-5N-18E	2918	11653-11691	238	3753	.32	.20(70)
1963	Arco	State Topping#1	9-5N-18E	3691	11712-11739	238	4542	.39	.97
1963	Arco	MCalister A#1	10-5N-18E	3840	11757-11793	239	4670	.40	1.9
1963	Arco	Davis A#1&2A	11-5N-18E	3528	11912-12132	244	4406	.36	.50
1963	Arco	Robinson#1	12-5N-18E	4015	11980-12004	242	4824	.40	9.3
1963	Arco	Austin Wayne	13-5N-18E	3975	9083-9136	198	4669	.51	11.5
1963	Arco	Costilow PE#1	14-5N-18E	3701	8568-8605	190	4432	.52	.76
1963	Arco	Yourman#1	15-5N-18E	3830	8754-8802	193	4573	.52	9.1
1963	Arco	Kilpatrick#1	16-5N-18E	3766	8576-8614	190	4488	.52	4.6
1963	Arco	Fazekas Steve#1	17-5N-18E	3862	8784-8833	193	4597	.52	17.0
1963	Arco	Hampton Bub#1	18-5N-18E	3867	9030-9069	197	4581	.51	13.4
1964	Arco	Bennett State#1	19-5N-18E	3749	8960-9006	197	4479	.50	18.7
1963	Arco	Smith Marion#1&2	20-5N-18E	3879	8504-10688	222	4579	.43	26.2
1963	Arco	Paschall#1	21-5N-18E	3836	8327-8425	187	4540	.54	23.0
1963	Arco	MCalister#1	22-5N-18E	3855	8288-8328	186	4554	.55	11.8
1963	Arco	Williams#1	23-5N-18E	3615	8811-8831	193	4364	.49	10.6
1963	Arco	James#A1	24-5N-18E	3718	9000-9060	197	4455	.49	10.9
1966	Texaco	Varnum Guy#1	25-5N-18E	3645	10461-10478	219	4449	.43	1.5
1964	Arco	Watts-Jones#1	26-5N-18E	3003	10308-10352	217	3845	.37	1.8
1964	Arco	Enis EV#1	27-5N-18E	3766	9764-9783	152	4537	.46	5.2
1963	Arco	State#C1	28-5N-18E	3815	8946-8986	196	4534	.51	19.4
1963	Arco	Dobbs State#1	29-5N-18E	3829	8707-8754	193	4543	.52	13.1
1964	Ar-La Gas	Bennett Jessie#1&2	30-5N-18E	3313	9132-9832	209	4098	.42	2.2
1976	Hazelwood	Hunter Tucker#1	31-5N-18E	2864	10095-10120	214	3725	.37	1.2
1971	Arkoma	Kennedy#1	32-5N-18E	3561	10903-10918	226	4385	.40	.50
1964	Arco	Watts M#1	33-5N-18E	3397	11371-11399	233	4221	.37	3.3
1976	Coquina	Mose Watts 1	34-5N-18E	1777	11512-11532	235	2408	.21	.46

1965	Amoco	Reusch#1	3-5N-19E	4062	11476-11492	235	4900	.43	16.0
1966	Amoco	Choclow#T3	4-5N-19E	4012	11302-11326	232	4829	.43	5.6

1966	Amoco	Choctow T#T4	5-5N-19E	4055	11371-11393	233	4863	.43	15.2
1966	Amoco	USA MCTiernan J#1	6-5N-19E	3963	11325-11333	232	4790	.42	10.2
1966	Amoco	Quaid#1	7-5N-19E	4020	11836-11842	239	4845	.41	10.0
1963	JMC	College 100#1	18-5N-19E	3975	11866-11892	241	4763	.40	6.4
1964	Exxon	Sparks Charles#1	19-5N-19E	3582	12310-12320	247	4465	.36	3.5
1965	Exxon	Ray JA#1	20-5N-19E	3800	12265-12286	247	4624	.38	3.9
1967	Oryx	Diamond 1	30-5N-19E	3325	11102-11127	229	4148	.37	1.0

1979	Mustang	Booth 1-2	2-5N-20E	3632	12586-12592	251	4489	.36	---
1979	Mustang	Cathy 1-13	3-5N-20E	4083	12646-12704	253	4873	.38	---

1978	Samson	Cicar 1	26-6N-17E	1600	8127-8163	184	2099	.26	.003
------	--------	---------	-----------	------	-----------	-----	------	-----	------

1970	Oxley	Galaxy1	12-6N-18E	2854	10067-10090	213	3714	.37	1.5
1969	BHP	Wildlife#1	24-6N-18E	4014	11506-11518	235	4807	.42	1.3
1968	Amoco	Anderson Prich#1-12	25-6N-18E	3917	11579-11599	236	4757	.41	4.3
1964	Arco	Michell Unit #1	32-6N-18E	3736	11646-11664	237	4605	.40	1.0
1967	Amoco	Wilson 1	35-6N-18E	2484	11548-11556	236	3271	.28	.08
1967	Oryx	Federal Church#1	36-6N-18E	3830	11033-11060	228	4614	.42	6.7

1968	Sun	Bratton 1	2-6N-19E	3341	10120-10150	214	4173	.41	1.7
1966	Exxon	Clay Brown 1	3-6N-19E	3500	10237-10261	216	4345	.42	7.0
1967	Exxon	Coblentz LM	4-6N-19E	3488	10156-10174	215	4307	.42	1.7
1967	Mobil	Weaver D 1C	5-6N-19E	2765	10175-10185	215	3562	.35	.40(INA)
1967	Arco	Dept of Wildlife Co#2	7-6N-19E	3217	10218-10232	215	4056	.40	1.2
1968	Mobil	Weaver 1F	8-6N-19E	3038	9982-9994	212	3906	.39	1.3
1969	Mobile	Fred Clawson Unit1	9-6N-19E	3430	10040-10060	213	4279	.43	8.1
1969	Mobil	Browne C 1	10-6N-19E	3340	10367-10390	218	4204	.41	8.2
1970	Mobil	Wilburton 1	11-6N-19E	3395	10051-10077	213	4220	.42	4.7
1979	Prospective	Shaw 1-LT	14-6N-19E	506	10939-10957	227	644	.06	---
1970	Mobil	Johnson H 1	15-6N-19E	3409	10290-10317	217	4267	.41	2.6
1969	Oxley	Weaver	16-6N-19E	3453	10426-10446	219	4252	.41	.85(INA)
1974	Samson	Robbers Cave 1	18-6N-19E	3062	10564-10592	221	3941	.37	1.1
1969	BHP	Cave 1	19-6N-19E	3827	11438-11454	234	4626	.40	7.4
1967	Mobile	Weaver D#1B	20-6N-19E	3731	11174-11208	230	4563	.41	2.9
1968	Mobile	Weaver D#1E	21-6N-19E	3723	11245-11272	231	4555	.40	2.0
1969	Mobil	Harrison 1	22-6N-19E	3978	10906-10928	226	4765	.44	10.1
1966	Samson	Young R#1	27-6N-19E	3880	11169-11191	230	4687	.42	2.2
1966	Samaon	Young R 1	28-6N-19E	3960	11392-11422	234	4757	.42	11.3
1966	Shell	Kilpatrick 1	29-6N-19E	4013	11678-11694	238	4813	.41	15.1
1967	Mobil	Hackney 1	30-6N-19E	3900	11714-11732	238	4717	.40	7.6
1966	Amoco	E Okia A&M#1	31-6N-19E	3990	10990-11018	227	4800	.44	9.1
1966	Amoco	Quaid B1	32-6N-19E	4024	10991-11006	227	4829	.44	11.4
1966	Amoco	Adams C1	33-6N-19E	4079	11030-11062	228	4874	.44	13.2
1966	Williford	Young 1	34-6N-19E	3708	11425-11445	234	4550	.40	.50

1969	Shell	Jankowsky 1	5-6N-20E	2694	10954-10980	227	3557	.32	.10(73)
1970	Texas Intl	Jankowsky 1	6-6N-20E	2849	9784-9831	209	3705	.38	1.4
1965	Mobil	Parks P 1	33-6N-20E	3875	13089-?		4685		.08(70)

1963	Amoco	Free Unit 1	11-6N-21E	3985	11832-11887	241	4846	.41	10.2
1963	Sun	Norris 1	12-6N-21E	3892	11828-11904	241	4794	.40	5.0
1963	Amoco	Gallagher 1	13-6N-21E	3989	11877-11933	241	4849	.41	9.3
1963	Sun	Gallagher Wm 1	14-6N-21E	3843	11951-11990	242	4678	.39	13.7
1963	Amoco	Booth 1	15-6N-21E	3976	12110-12152	245	4874	.40	5.4 INA
1964	Amoco	Brewer 1	16-6N-21E	3990	12156-12180	245	4883	.41	3.5
1966	Amoco	White 1	18-6N-21E	4024	12640-12725	253	4925	.39	11.8
1975	Mustang	Foster 1	19-6N-21E	2182	12656-12710	253	3058	.24	.72
1965	Exxon	Erwin WD 1	23-6N-21E	3734	11982-12001	242	4666	.39	2.8
1965	Amoco	Cecil 1	24-6N-21E	3945	11757-11831	240	4839	.41	6.6
1976	Mustang	Lyon 1-27	27-6N-21E	3255	12135-12184	245	3255	.27	.42
1976	Mustang	Smallwood 1	28-6N-21E	2332	12181-12298	247	3131	.26	.27

PRESSURE DATA TABLE OF 24 HOUR TEST  
FOR WELLS COMPLETED AND PRODUCING 1960-1989  
ARKOMA BASIN OKLAHOMA  
(source DWIGHTS)

COMP - YEAR PRODUCTION BEGAN  
WHISP - WELL HEAD SHUT IN PRESSURE (PSI)  
BHT - BOTTOM HOLE TEMPERATURE ( DEG F)  
IBHP - INITIAL BOTTOM HOLE PRESSURE (PSI)  
PGR - PRESSURE GRADIENT(PSI / FT)  
PROD - CUMULATIVE PRODUCTION AS OF 1989 (MMCF- MILLION CUBIC FEET)

COMP	OPERATOR	WELL	LOCATION	WHISP	PERF	BHT	IBHP	PGR	PROD
1970	Arkoma	Pattison NW #1	1-4N-17E	3336	11399-11448	238	4168	.36	.60
1970	Arkoma	McCasin 1	2-4N-17E	2580	11371-11405	233	3408	.30	4.6
1987	Arkoma	McCasin#2-2	2-4N-17E	2986	11304-11340	232	3792	.33	2.3
1987	Arkoma	Sparks 1	3-4N-17E	1332	11626-11666	177	1718	.15	1.1
1970	Arkoma	Layden#1	3-4N-17E	3100	11750-11792	239	3975	.34	2.9
1970	Arkoma	Stine 1-4	4-4N-17E	3726	10909-10941	226	4585	.42	.33
1970	Arkoma	Rock Island 1-5	5-4N-17E	3878	11132-11164	230	4686	.42	8.3
1971	Arkoma	Hartshorne 1	6-4N-17E	3740	10892-10926	226	4595	.42	9.8
1973	Amoco	Rock Isl Imp 60 1-7	7-4N-17E	3810	11302-11338	232	4721	.42	.42
1989	Texaco	Wallace Wayne 1-21	21-4N-17E	2086	13258-13308	262	3075	.23	2.9

1964	Arco	Dunagan ASE#A1	13-5N-17E	3859	8434-8455	188	4560	.54	14.6
1966	Mobile	Kent Heirs#1	14-5N-17E	2503	9975-10017	212	3291	.33	.96
1982	Arkoma	Kent Heirs B-1	14-5N-17E	1869	8747-8966	196	2459	.27	11.5
1978	Samson	Kent#1	15-5N-17E	2944	8925-9054	198	3756	.42	13.1
1978	Samson	Bobo 1	16-5N-17E	2587	9634-9648	207	3437	.36	.85
1968	Arco	Bowman Pauline 1	20-5N-17E	3662	9270-9317	202	4494	.48	16.8
1988	Arco	Bowman Pauline 3	20-5N-17E	2248	9270-9317	202	3019	.32	4.6
1967	Arco	Bowman Pauline 1	21-5N-17E	3732	9630-9668	207	4588	.48	7.4
1966	Mobil	Sivil Gol 1	22-5N-17E	3558	9177-9221	200	4320	.47	9.3
1986	Samson	Sams 1	22-5N-17E	1131	9526-9570	206	1478	.15	.50
1965	Mobile	Darby UN#1	23-5N-17E	3787	9946-9986	212	4529	.45	9.1
1964	Marathon	Fabro NW SE	24-5N-17E	3846	9126-9150	199	4591	.50	8.1
1965	Arco	Henley JL#1	25-5N-17E	3756	10022-10052	213	4536	.45	6.6
1965	Amoco	Caudron U#1	26-5N-17E	3542	9774-9788	209	4347	.44	1.6
1966	Arco	Parker Alfred#1	27-5N-17E	3804	9121-9140	198	4557	.50	9.5
1967	Arco	USA 1	28-5N-17E	3640	9707-9757	208	4428	.45	4.8
1968	Arco	Bowman 1	29-5N-17E	3650	10553-10606	221	4512	.43	2.4
1969	Arco	Richards Edith 1	30-5N-17E	3786	11030-11055	228	4636	.42	4.6
1969	Arco	Richards Edith 3	30-5N-17E	2617	9566-9596	205	3468	.36	1.2
1970	Arkoma	Pettit 1	31-5N-17E	3908	10353-10390	218	4720	.45	10.1
1988	Arkoma	Petite 3C	31-5N-17E	3010	10325-10371	218	3880	.37	.15
1968	Oryx	Casteel 1	32-5N-17E	3786	11380-11420	233	4674	.41	.12
1989	Oryx	Casteel 2	32-5N-17E	924	11011-11051	228	1299	.12	.25INA
1969	Arkoma	Potichny 1	33-5N-17E	3784	11054-11098	229	4635	.42	4.4
1987	Arkoma	Potichny 33t	33-5N-17E	2220	10670-10705	223	3011	.28	1.8
1985	Arkoma	Whitney#3	34-5N-17E	3001	10710-10750	223	3852	.36	5.0
1969	Arkoma	Whitney#1	34-5N-17E	3450	11162-11268	231	4291	.38	2.6
1970	Arco	Kurilko Andrew#1	35-5N-17E	3760	11074-11134	229	4556	.41	6.0
1986	Arco	Lerblance#2	36-5N-17E	3171	11062-11090	229	4031	.36	1.8
1966	Arco	Lerblance#1	36-5N-17E	3577	10554-10572	221	4338	.41	.92

1964	Arco	USA Jarq Anderson#1	1-5N-18E	3965	11414-11435	234	4764	.42	8.6
1963	Arco	Davis James#1	2-5N-18E	3621	11682-11710	238	4481	.38	2.6
1963	Arco	Pate Kinnikin#1	3-5N-18E	3800	11660-11700	238	4632	.40	4.1
1963	Arco	#1 Edgar S Woods	4-5N-18E	3360	11671-11684	238	4251	.36	1.4
1963	Arco	Sawyer Lela#1	5-5N-18E	3527	11646-11686	237	4425	.38	1.2
1963	Arco	Gardner 1	7-5N-18E	3288	11998-12033	243	4227	.35	.08(69)
1963	Arco	Raunika 1	8-5N-18E	2918	11653-11691	238	3753	.32	.20(70)
1963	Arco	State Topping#1	9-5N-18E	3691	11712-11739	238	4542	.39	1.2
1963	Arco	MCalister A#1	10-5N-18E	3840	11757-11793	239	4670	.40	2.2
1988	Arco	MCAlester 2A	10-5N-18E	2136	10395-10442	219	2901	.28	.60
1963	Arco	Davis A#1&2A	11-5N-18E	3528	11912-12132	244	4406	.36	.57
1963	Arco	Robinson#1	12-5N-18E	4015	11980-12004	242	4824	.40	10.0
1963	Arco	Austin Wayne	13-5N-18E	3975	9083-9136	198	4669	.51	14.5
1963	Arco	Costilow PE#1	14-5N-18E	3701	8568-8605	190	4432	.52	.90
1986	Samson	Costilow#2	14-5N-18E	3689	10503-10528	219	4489	.43	9.3
1963	Arco	Yourman#1	15-5N-18E	3830	8754-8802	193	4573	.52	10.3
1989	Arco	Kilpatrick#3 UT	16-5N-18E	1302	8706-8730	192	1709	.20	.03
1963	Arco	Kilpatrick#1	16-5N-18E	3766	8576-8614	190	4488	.52	5.6
1963	Arco	Fazekas Steve#1	17-5N-18E	3862	8784-8833	193	4597	.52	21.5
1963	Arco	Hampton Bub#1	18-5N-18E	3867	9030-9069	197	4581	.51	15.5
1964	Arco	Bennett State#1	19-5N-18E	3749	8960-9006	197	4479	.50	23.2
1963	Arco	Smith Marion#1&2	20-5N-18E	3879	8504-10688	222	4579	.43	32.6
1963	Arco	Paschall#1	21-5N-18E	3836	8327-8425	187	4540	.54	27.6
1963	Arco	MCalister#1	22-5N-18E	3855	8288-8328	186	4554	.55	12.8 INA

1987	Arco	MCalister RF#2-X	22-5N-18E	3820	10933-10975	225	4601	.42	1.2
1963	Anadarko	Williams#1	23-5N-18E	3615	8811-8831	193	4364	.49	12.1
1987	Anadarko	Williams#2-23	23-5N-18E	3011	11487-11531	234	3909	.34	.54
1963	Arco	James#A1	24-5N-18E	3718	9000-9060	197	4455	.49	13.0
1966	Texaco	Varnum Guy#1	25-5N-18E	3645	10461-10478	219	4449	.43	2.1
1987	Zinke&Trumbo	Malitz 1-25	25-5N-18E	1059	10730-10762	224	1366	.13	.36
1964	Arco	Watts-Jones#1	26-5N-18E	3003	10308-10352	217	3845	.37	2.1
1964	Arco	Enis EV#1	27-5N-18E	3766	9764-9783	152	4537	.46	5.9
1963	Arco	State#C1	28-5N-18E	3815	8946-8986	196	4534	.51	22.8
1963	Arco	Dobbs State#1	29-5N-18E	3829	8707-8754	193	4543	.52	15.5
1964	Ar-La Gas	Bennett Jessie#1&2	30-5N-18E	3313	9132-9832	209	4098	.42	2.8
1988	Ebony	Hunter Tucker 3-31	31-5N-18E	1908	10614-10644	222	2546	.24	.45
1988	Arkoma	Hunter Tucker#2	31-5N-18E	2880	10480-10504	220	3724	.36	.27
1976	Hazelwood	Hunter Tucker#1	31-5N-18E	2864	10095-10120	214	3725	.37	4.1
1971	Arkoma	Kennedy#1	32-5N-18E	3561	10903-10918	226	4385	.40	.65
1984	Arkoma	Kennedy 2B	32-5N-18E	2397	10930-10950	226	3181	.29	1.0
1964	Arco	Watts M#1	33-5N-18E	3397	11371-11399	233	4221	.37	3.9
1976	Coquina	Mose Watts 1	34-5N-18E	1777	11512-11532	235	2408	.21	1.3
1985	Samson	Mose#1	35-5N-18E	1385	11592-11626	237	1786	.15	.51

1965	Amoco	Reusch#1	3-5N-19E	4062	11476-11492	235	4900	.43	18.9
1966	Amoco	Choctaw#T3	4-5N-19E	4012	11302-11326	232	4829	.43	6.6
1987	Amoco	Choctaw T3 #2	4-5N-19E	1245	11720-11755	239	1684	.14	.71
1966	Amoco	Choctaw T#T4	5-5N-19E	4055	11371-11393	233	4863	.43	17.1
1966	Amoco	USA Mctiernan J#1	6-5N-19E	3963	11325-11333	232	4790	.42	10.9
1966	Amoco	Quaid#1	7-5N-19E	4020	11836-11842	239	4845	.41	10.8
1986	Vintage	Denton#1-16	16-5N-19E	2034	10769-10792	224	2880	.27	.04
1985	Willford	Burger 1-16	16-5N-19E	3319	10800-10876	225	4169	.38	.75
1963	JMC	College 100#1	18-5N-19E	3975	11866-11892	241	4763	.40	7.1
1964	Exxon	Sparks Charles#1	19-5N-19E	3582	12310-12320	247	4465	.36	3.9
1965	Exxon	Ray JA#1	20-5N-19E	3800	12265-12286	247	4624	.38	4.6
1967	Oryx	Diamond 1	30-5N-19E	3325	11102-11127	229	4148	.37	1.4

1979	Mustang	Booth 1-2	2-5N-20E	3632	12586-12592	251	4489	.36	1.2 INA
1979	Mustang	Cathy 1-13	3-5N-20E	4083	12646-12704	253	4873	.38	2.4 INA

1978	Samson	Cicar 1	26-6N-17E	1600	8127-8163	184	2099	.26	.01(82)
------	--------	---------	-----------	------	-----------	-----	------	-----	---------

1970	Oxley	Galaxy1	12-6N-18E	2854	10067-10090	213	3714	.37	2.0
1969	BHP	Wildlife#1	24-6N-18E	4014	11506-11518	235	4807	.42	1.4
1968	Amoco	Anderson Prich#1-12	25-6N-18E	3917	11579-11599	236	4757	.41	5.8
1964	Arco	Michell Unit #1	32-6N-18E	3736	11646-11664	237	4605	.40	1.2 INA
1967	Amoco	Wilson 1	35-6N-18E	2484	11548-11556	236	3271	.28	.09(82)
1986	Samson	Sunflower 1-35	35-6N-18E	1431	11277-11309	232	1909	.17	.60
1989	Oryx	Federal Church#2	36-6N-18E	1092	11415-11423	233	1451	.13	.04
1967	Oryx	Federal Church#1	36-6N-18E	3830	11033-11060	228	4614	.42	8.2

1982	Samson	Choctaw Unit1	1-6N-19E	1560	9802-9832	209	2059	.21	.08
1968	Sun	Bratton 1	2-6N-19E	3341	10120-10150	214	4173	.41	2.1
1966	Exxon	Clay Brown 1	3-6N-19E	3500	10237-10261	216	4345	.42	8.7
1989	Exxon	Clayton Brown 2	3-6N-19E	750	9998-10018	212	942	.09	---
1967	Exxon	Coblentz LM	4-6N-19E	3488	10156-10174	215	4307	.42	2.2
1967	Mobil	Weaver D 1C	5-6N-19E	2765	10175-10185	215	3562	.35	.40(INA)
1967	Arco	Dept of Wildlife Co#2	7-6N-19E	3217	10218-10232	215	4056	.40	1.6(INA)
1968	Mobil	Weaver 1F	8-6N-19E	3038	9982-9994	212	3906	.39	2.0
1969	Mobile	Fred Clawson Unit1	9-6N-19E	3430	10040-10060	213	4279	.43	9.8
1969	Mobil	Browne C 1	10-6N-19E	3340	10367-10390	218	4204	.41	9.7
1970	Mobil	Wilburton 1	11-6N-19E	3395	10051-10077	213	4220	.42	5.3
1979	Prospective	Shaw 1-LT	14-6N-19E	506	10939-10957	227	644	.06	.34
1970	Mobil	Johnson H 1	15-6N-19E	3409	10290-10317	217	4267	.41	3.2
1989	Mobil	Johnson H 2	15-6N-19E	1531	10615-10648	222	2049	.19	.21
1969	Oxley	Weaver	16-6N-19E	3453	10426-10446	219	4252	.41	.80(INA)
1986	Oxley	Weaver 2	16-6N-19E	1900	10753-10795	224	1416	.13	.12
1984	Samson	Mollie 1	17-6N-19E	1404	10724-10744	223	1859	.17	.11
1974	Samson	Robbers Cave 1	18-6N-19E	3062	10564-10592	221	3941	.37	2.0
1969	BHP	Cave 1	19-6N-19E	3827	11438-11454	234	4626	.40	9.4
1967	Mobile	Weaver D#1B	20-6N-19E	3731	11174-11208	230	4563	.41	3.4
1968	Mobile	Weaver D#1E	21-6N-19E	3723	11245-11272	231	4555	.40	2.5
1969	Mobil	Harrison 1	22-5N-19E	3978	10906-19028	226	4765	.44	15.2
1982	Samson	Golightly#1	24-6N-19E	3271	13722-13753	269	4189	.31	.41(85)
1985	Sante Fe	Arkansas Kraft#1-25	25-6N-19E	3349	13848-13889	271	4265	.31	.17
1984	Sante Fe	Arkansas Kraft#1-26	26-6N-19E	4095	13951-13972	272	5359	.38	1.8
1966	Samson	Young R#1	27-6N-19E	3880	11169-11191	230	4687	.42	2.9
1986	Samson	Young R 2	27-6N-19E	1807	11090-11110	229	2440	.22	.73
1966	Samaon	Young R 1	28-6N-19E	3960	11392-11422	234	4757	.42	12.5
1966	Shell	Kilpatrick 1	29-6N-19E	4013	11678-11694	238	4813	.41	17.1
1967	Mobil	Hackney 1	30-6N-19E	3900	11714-11732	238	4717	.40	8.2
1989	Mobil	Hackney 2	30-6N-19E	723	11796-11830	240	950	.10	.02



1966	Amoco	E Okla A&M#1	31-6N-19E	3990	10990-11018	227	4800	.44	10.1
1966	Amoco	Quaid B1	32-6N-19E	4024	10991-11006	227	4829	.44	12.9
1966	Amoco	Adams C1	33-6N-19E	4079	11030-11062	228	4874	.44	14.3
1986	Amoco	Adams C2	33-6N-19E	860	11146-11182	230	1134	.10	.70
1966	Williford	Young 1	34-6N-19E	3708	11425-11445	234	4550	.40	.55
1983	Williford	Young 2-34	34-6N-19E	954	11099-11124	230	1268	.11	.50
1984	Santa Fe	Arkansas Kraft 1-35	35-6N-19E	3974	13929-13950	272	4849	.35	.63
1986	Sante Fe	Shaw 1-36	36-6N-19E	4906	14112-14153	275			.20

1969	Shell	Jankowsky 1	5-6N-20E	2694	10954-10980	227	3557	.32	.10(73)
1970	Texas Intl	Jankowsky 1	6-6N-20E	2849	9784-9831	209	3705	.38	1.6
1984	Santa Fe	Jankowsky 1-18	18-6N-20E	3742	14444-14506	281	4607	.32	.90
1982	Santa Fe	Cecil 1-19	19-6N-20E	3958	13598-13652	267	4743	.35	3.3
1984	Santa Fe	Swart 1-20	20-6N-20E	4357	13859-13911	272	5099	.37	.96
1981	Mustang	Young&Cooper 1-26	26-6N-20E	2439	13646-13701	268	3293	.24	.34
1982	Sante Fe	Pierce 1-30	30-6N-20E	3537	13840-13873	271	4379	.32	.40
1965	Mobil	Parks P 1	33-6N-20E	3875	13089-?		4685		.08(70)
1981	Mustang	Metcalf 1-34	34-6N-20E	3390	12697-12714	253	4276	.34	3.5
1980	Mustang	Fisherman 1	34-6N-20E	2151	13071-13353	263	2924	.22	.03(86)
1980	Mustang	Foster#1-35	35-6N-20E	3371	12630-12703	253	4257	.34	.50(INA)

1986	Samson	Circle F Ranch	10-6N-21E	1113	11927-12002	242	1362	.11	.63
1963	Amoco	Free Unit 1	11-6N-21E	3985	11832-11887	241	4846	.41	12.1 INA
1963	Sun	Norris 1	12-6N-21E	3892	11828-11904	241	4794	.40	8.6
1963	Amoco	Gallagher 1	13-6N-21E	3989	11877-11933	241	4849	.41	12.7
1963	Sun	Gallagher Wm 1	14-6N-21E	3843	11951-11990	242	4678	.39	16.6
1986	Oryx	Gallagher 2	14-6N-21E	1454	11995-12080	244	1954	.16	.04
1963	Amoco	Booth 1	15-6N-21E	3976	12110-12152	245	4874	.40	6.1(INA)
1986	Amoco	Booth 2	15-6N-21E	1570	12068-12120	244	2134	.18	.30
1964	Amoco	Brewer 1	16-6N-21E	3990	12156-12180	245	4883	.41	4.2
1966	Amoco	White 1	18-6N-21E	4024	12640-12725	253	4925	.39	16.2
1975	Mustang	Foster 1	19-6N-21E	2182	12656-12710	253	3058	.24	1.3
1985	Mustang	Strother 1-20	20-6N-21E	1366	13253-13310	262	1935	.15	1.4
1988	JMC	Oxley 3	22-6N-21E	984	12152-12214	246	1304	.11	.28
1965	Exxon	Erwin WD 1	23-6N-21E	3734	11982-12001	242	4666	.39	3.2
1965	Amoco	Cecil 1	24-6N-21E	3945	11757-11831	240	4839	.41	7.2
1980	Texas	Gallagher 1	26-6N-21E	1222	12510-12570	251	1655	.13	.40(83)
1976	Mustang	Lyon 1-27	27-6N-21E	3255	12135-12184	245	3255	.27	1.2
1976	Mustang	Smallwood 1	28-6N-21E	2332	12181-12298	247	3131	.26	.56
1982	Whitmar	McCreery 1-30	30-6N-21E	1948	13412-13471	265	2671	.20	.97

PRESSURE DATA TABLE OF 24 HOUR TEST  
FOR WELLS COMPLETED AND PRODUCING 1960-1994  
ARKOMA BASIN OKLAHOMA  
(source DWIGHTS)

COMP - YEAR PRODUCTION BEGAN  
WHISP - WELL HEAD SHUT IN PRESSURE (PSI)  
BHT - BOTTOM HOLE TEMPERATURE ( DEG F)  
IBHP - INITIAL BOTTOM HOLE PRESSURE (PSI)  
PGR - PRESSURE GRADIENT(PSI / FT)  
PROD - CUMULATIVE PRODUCTION AS OF 1994 (MMCF- MILLION CUBIC FEET)

COMP	OPERATOR	WELL	LOCATION	WHISP	PERF	BHT	IBHP	PGR	PROD
1990	Exxon	Szenasy 1	1-3N-16E	4235	14088-14154	275	5066	.36	.96
1989	Amoco	Tschappat A-1	3-3N-16E	2910	9616-9648	207	3791	.39	1.6

1990	Amoco	Watts 1	6-3N-17E	2390	12810-12985	257	3243	.25	1.5
------	-------	---------	----------	------	-------------	-----	------	-----	-----

1992	H&H Star	Hope 1-4	4-3N-20E	3127	18742-18818	346	4424	.23	.60
------	----------	----------	----------	------	-------------	-----	------	-----	-----

1973	Marathon	Slaughter 1	1-4N-16E	3720	10652-10696	223	4573	.43	20.2
1987	Marathon	Slaughter 2LT	1-4N-16E	2031	11955-12001	249	2791	.23	1.4
1974	Marathon	Madden 1	2-4N-16E	3468	10462-10480	219	4350	.41	22.1
1983	Whitmar	Smallwood 2-3	3-4N-16E	2690	11575-11620	241	3598	.31	.31NA
1973	Marathon	Needham 1	11-4N-16E	2502	11120-11171	235	3455	.31	6.61NA
1988	Marathon	Needham 2-11	11-4N-16E	1673	12097-12118	244	2296	.19	2.2
1974	Marathon	Lewis	12-4N-16E	3094	11382-11404	233	4053	.35	1.2
1988	Marathon	Lewis 3	12-4N-16E	2502	12411-12420	254	3587	.29	1.6
1979	Whitmar	Cope 1	13-4N-16E	1995	11876-11937	241	2740	.23	3.7
1985	Samson	Tex 1	14-4N-16E	1500	11852-11866	240	2046	.17	1.6
1974	Zinke&Trumbo	Lynn 1	15-4N-16E	1522	11531-11552	236	2072	.18	.151NA
1987	NJRE	Lynn 1-15	15-4N-16E	1471	10934-10967	232	2006	.18	1.4
1991	Texaco	Dromgold D 1-35	35-4N-16E	4895	13108-13147	260	5537	.42	1.5
1991	Texaco	Silva D 1-36	36-4N-16E	4350	14658-14708	283	5352	.36	.12

1970	Arkoma	Pattison NW #1	1-4N-17E	3336	11399-11448	238	4168	.36	.70
1970	Arkoma	McCasin 1	2-4N-17E	2580	11371-11405	233	3408	.30	5.3
1987	Arkoma	McCasin#2-2	2-4N-17E	2986	11304-11340	232	3792	.33	3.3
1987	Arkoma	Sparks 1	3-4N-17E	1332	11626-11666	177	1718	.15	2.2
1970	Arkoma	Layden#1	3-4N-17E	3100	11750-11792	239	3975	.34	3.6
1970	Arkoma	Stine 1-4	4-4N-17E	3726	10909-10941	226	4585	.42	.65
1986	Arkla	Stine 2-UT	4-4N-17E	2344	10823-10856	230	4145	.38	2.2
1970	Arkoma	Rock Island 1-5	5-4N-17E	3878	11132-11164	230	4686	.42	9.1
1987	Arkla	Rock Island 2-5	5-4N-17E	1060	11290-11320	237	1424	.13	.27
1971	Arkoma	Hartshorne 1	6-4N-17E	3740	10892-10926	226	4595	.42	10.4
1987	Arkla	Hartshorne 3-6	6-4N-17E	1145	10551-10587	226	1496	.14	1.6
1989	JMC	Belusko 1	6-4N-17E	1662	12146-12186	250	2282	.19	.35
1973	Amoco	Rock Isl Imp 60 1-7	7-4N-17E	3810	11302-11338	232	4721	.42	.48
1993	Tide	Wallace 1	16-4N-17E	3445	13405-13491	270	4374	.32	.25
1989	Texaco	Wallace Wayne 1-21	21-4N-17E	2086	13258-13308	262	3075	.23	2.9
1991	JMC	Blue Mountain 1-1	22-4N-17E	3016	13660-13750	269	3933	.29	2.6
1990	Amoco	Retherford 1-A	25-4N-17E	4480	12142-12170	245	5144	.42	21.5
1990	Amoco	Mose Watts 1	36-4N-17E	2398	13410-13440	264	3212	.24	2.8

1990	BTA	Amason 1	24-4N-18E	2384	13649-13696	268	3198	.23	1.8
1993	Anadarko	Robe A 1-25	25-4N-18E	3604	15163-15274	292	5198	.34	.20
1990	Exxon	Garrett A-1	26-4N-18E	1514	14814-14878	286	2081	.14	.60
1991	Exxon	Watts Bros. C-1	29-4N-18E	651	13107-13450	264	854	.06	.90
1990	Exxon	Retherford B-1	31-4N-18E	4035	13338-13365	263	4826	.36	7.1
1990	Exxon	Garrett C-1	33-4N-18E	5355	14435-14474	280	5818	.40	5.9

1991	Mobil	EM Lawless 1	1-4N-19E	4627	14846-14929	287	5360	.36	1.7
1991	Arco	James 1-17	17-4N-19E	2636	14597-14644	283	3510	.24	3.6
1992	H&H Star	Swindle 1-18	20-4N-19E	5222	12122-12204	245	5657	.46	.40
1992	H&H Star	Colony 1-23	23-4N-19E						.30

1991	An son	Smallwood 1-3	3-4N-20E	2059	16313-16327	308	2879	.18	.40
1992	H&H Star	Dipping Vat 1-4	4-4N-20E	6902	16066-16180	306	6801	.42	2.3
1992	H&H Star	Lucky Strike 1-5	5-4N-20E	1980	12748-?		2670		.35
1992	Mobil	Kiamichi 1-6	6-4N-20E	3340	14730-14750	284	4279	.29	.90
1991	Anadarko	Barnes A1-9	9-4N-20E	5889	16305-16364	309	6238	.38	4.8
1991	An son	Golden 1	10-4N-20E	5860	15978-16060	304	6267	.39	11.5
1993	An son	Lamb 1-10	10-4N-20E	3011	15018-15088	289	4020	.27	.06
1993	Arco	Borne 1-12	12-4N-20E	5780	15626-15756	300	5768	.37	.50
1993	H&H Star	Berkley Hills 1-15	15-4N-20E	5431	16914-17130	320	6009	.35	1.0
1993	H&H Star	Coopers Hollow 1-16	16-4N-20E		17217-17313	323			.70

1993	H&H Star	Eight Mile Mt 1-21	21-4N-20E		17600-17679	329			.05
------	----------	--------------------	-----------	--	-------------	-----	--	--	-----

1982	Sante Fe	Moss A1-13	13-5N-16E	2866	8937-9111	198	3726	.41	8.1
1977	Samson	Mcbee 1	23-5N-16E	2675	9001-9017	197	3707	.41	12.1
1970	Oryx	Peden 1	24-5N-16E	3583	9255-9330	202	4450	.48	5.3
1986	Amoco	Peden 2	24-5N-16E	1365	9084-9124	204	1800	.20	4.3
1984	Marathon	Mass 2	25-5N-16E	2093	9737-9766	208	2851	.29	.89INA
1971	Arco	King RA 1	26-5N-16E	3782	9340-9364	202	4564	.49	15.8
1980	Arco	USA 2-27	27-5N-16E	2332	9412-9446	204	3185	.34	2.7
1981	Samson	Monroe 1	28-5N-16E	1600	10808-10846	225	2187	.20	.43
1973	NJRE	Marlangeli 1	34-5N-16E	3105	10674-10696	228	4076	.38	.03(73)
1989	Price	Almerito 1	34-5N-16E	1679	10398-10514	220	2248	.21	.32
1971	Marathon	Woods Prospect 1	36-5N-16E	3529	11256-11275	231	4481	.40	1.3

1964	Arco	Dunagan ASE#A1	13-5N-17E	3859	8434-8455	188	4560	.54	16.0
1966	Mobile	Kent Heirs#1	14-5N-17E	2503	9975-10017	212	3291	.33	1.1
1982	Arkoma	Kent Heirs B-1	14-5N-17E	1869	8747-8966	196	2459	.27	13.2
1978	Samson	Kent#1	15-5N-17E	2944	8925-9054	198	3756	.42	15.7
1978	Samson	Bobo 1	16-5N-17E	2587	9634-9648	207	3437	.36	1.2
1968	Arco	Bowman Pauline 1	20-5N-17E	3662	9270-9317	202	4494	.48	18.1
1988	Arco	Bowman Pauline 3	20-5N-17E	2248	9270-9317	202	3019	.32	15.7
1992	Vastar	Bowman Pauline 5	20-5N-17E	2006	9852-9876	215	2684	.27	1.7
1967	Arco	Bowman Pauline 1	21-5N-17E	3732	9630-9668	207	4588	.48	8.4
1990	Vastar	Bowman Pauline 2	21-5N-17E	1366	10736-10750	228	1834	.17	.21
1966	Mobil	Sivil Gol 1	22-5N-17E	3558	9177-9221	200	4320	.47	9.3
1986	Samson	Sams 1	22-4N-17E	1131	9526-9570	206	1478	.15	.80
1965	Mobile	Darby UN#1	23-5N-17E	3787	9946-9986	212	4529	.45	9.5
1964	Marathon	Fabro NW SE	24-5N-17E	3846	9126-9150	199	4591	.50	8.9
1965	Arco	Henley JL#1	25-5N-17E	3756	10022-10052	213	4536	.45	7.4
1965	Amoco	Caudron U#1	26-5N-17E	3542	9774-9788	209	4347	.44	1.8
1991	JMC	Caudron 3	26-5N-17E	1166	9310-9328	202	1509	.16	.40
1966	Arco	Parker Alfred#1	27-5N-17E	3804	9121-9140	198	4557	.50	10.4
1967	Arco	USA 1	28-5N-17E	3640	9707-9757	208	4428	.45	5.1
1968	Arco	Bowman 1	29-5N-17E	3650	10553-10606	221	4512	.43	2.6
1990	Arco	Bowman 2	29-5N-17E	1366	10736-10750	222	1834	.17	
1969	Arco	Richards Edith 1	30-5N-17E	3786	11030-11055	228	4636	.42	5.3
1969	Arco	Richards Edith 3	30-5N-17E	2617	9566-9596	205	3468	.36	2.4
1970	Arkoma	Pettit 1	31-5N-17E	3908	10353-10390	218	4720	.45	10.8
1988	Arkoma	Petite 3C	31-5N-17E	3010	10325-10371	218	3880	.37	.38
1968	Oryx	Casteel 1	32-5N-17E	3786	11380-11420	233	4674	.41	4.2
1989	Oryx	Casteel 2	32-5N-17E	924	11011-11051	228	1299	.12	.25INA
1969	Arkoma	Potichny 1	33-5N-17E	3784	11054-11098	229	4635	.42	5.0
1987	Arkoma	Potichny 33t	33-5N-17E	2220	10670-10705	223	3011	.28	4.0
1985	Arkoma	Whitney#3	34-5N-17E	3001	10710-10750	223	3852	.36	7.5
1969	Arkoma	Whitney#1	34-5N-17E	3450	11162-11268	231	4291	.38	2.8
1970	Arco	Kuriko Andrew#1	35-5N-17E	3760	11074-11134	229	4556	.41	6.6
1986	Arco	Lerblance#2	36-5N-17E	3171	11062-11090	229	4031	.36	3.7
1966	Arco	Lerblance#1	36-5N-17E	3577	10554-10572	221	4338	.41	1.2

1964	Arco	USA Jarq Anderson#1	1-5N-18E	3965	11414-11435	234	4764	.42	8.7
1963	Arco	Davis James#1	2-5N-18E	3621	11682-11710	238	4481	.38	2.8
1963	Arco	Pate Kinnikin#1	3-5N-18E	3800	11660-11700	238	4632	.40	4.3
1963	Arco	#1 Edgar S Woods	4-5N-18E	3360	11671-11684	238	4251	.36	1.5
1963	Arco	Sawyer Lela#1	5-5N-18E	3527	11646-11686	237	4425	.38	1.4
1963	Arco	Gardner 1	7-5N-18E	3288	11998-12033	243	4227	.35	.08(69)
1963	Arco	Raunika 1	8-5N-18E	2918	11653-11691	238	3753	.32	.20(70)
1963	Arco	State Topping#1	9-5N-18E	3691	11712-11739	238	4542	.39	1.3
1963	Arco	MCalister A#1	10-5N-18E	3840	11757-11793	239	4670	.40	2.4
1988	Arco	McAlester 2A	10-5N-18E	2136	10395-10442	219	2901	.28	1.1
1963	Arco	Davis A#1&2A	11-5N-18E	3528	11912-12132	244	4406	.36	.60
1963	Arco	Robinson#1	12-5N-18E	4015	11980-12004	242	4824	.40	10.2
1963	Arco	Austin Wayne	13-5N-18E	3975	9083-9136	198	4669	.51	15.0
1963	Arco	Costilow PE#1	14-5N-18E	3701	8568-8605	190	4432	.52	.90
1986	Samson	Costilow#2	14-5N-18E	3689	10503-10528	219	4489	.43	15.6
1990	Samson	Costilow#4	14-5N-18E	544	8543-8587	190	665	.08	1.5
1963	Arco	Yourman#1	15-5N-18E	3830	8754-8802	193	4573	.52	10.8
1989	Arco	Kilpatrick#3 UT	16-5N-18E	1302	8706-8730	192	1709	.20	.90
1963	Arco	Kilpatrick#1	16-5N-18E	3766	8576-8614	190	4488	.52	5.9
1963	Arco	Fazekas Steve#1	17-5N-18E	3862	8784-8833	193	4597	.52	22.5
1963	Arco	Hampton Bub#1	18-5N-18E	3867	9030-9069	197	4581	.51	16.5
1964	Arco	Bennett State#1	19-5N-18E	3749	8960-9006	197	4479	.50	25.1
1991	Arco	Bennett State 3U	19-5N-18E	899	9271-9301	201	1151	.12	.40
1963	Arco	Smith Marion#1&2	20-5N-18E	3879	8504-10688	222	4579	.43	36.4
1963	Arco	Paschall#1	21-5N-18E	3836	8327-8425	187	4540	.54	29.7
1963	Arco	MCalister#1	22-5N-18E	3855	8288-8328	186	4554	.55	12.9
1987	Arco	MCalister RF#2-X	22-5N-18E	3820	10933-10975	225	4601	.42	2.2
1963	Anadarko	Williams#1	23-5N-18E	3615	8811-8831	193	4364	.49	14.0
1987	Anadarko	Williams#2-23	23-5N-18E	3011	11487-11531	234	3909	.34	.50

1963	Arco	James#A1	24-5N-18E	3718	9000-9060	197	4455	.49	13.2
1966	Texaco	Varnum Guy#1	25-5N-18E	3645	10461-10478	219	4449	.43	2.5
1987	Zinke&Trumbo	Malitz 1-25	25-5N-18E	1059	10730-10762	224	1366	.13	.50
1964	Arco	Watts-Jones#1	26-5N-18E	3003	10308-10352	217	3845	.37	2.2
1964	Arco	Enis EV#1	27-5N-18E	3766	9764-9783	152	4537	.46	6.0
1963	Arco	State#C1	28-5N-18E	3815	8946-8986	196	4534	.51	24.6
1963	Arco	Dobbs State#1	29-5N-18E	3829	8707-8754	193	4543	.52	16.3
1964	Ar-La Gas	Bennett Jessie#1&2	30-5N-18E	3313	9132-9832	209	4098	.42	3.0
1988	Ebony	Hunter Tucker 3-31	31-5N-18E	1908	10614-10644	222	2546	.24	1.7
1988	Arkoma	Hunter Tucker#2	31-5N-18E	2880	10480-10504	220	3724	.36	.60
1976	Hazelwood	Hunter Tucker#1	31-5N-18E	2864	10095-10120	214	3725	.37	4.8
1971	Arkoma	Kennedy#1	32-5N-18E	3561	10903-10918	226	4385	.40	.80
1984	Arkoma	Kennedy 2B	32-5N-18E	2397	10930-10950	226	3181	.29	1.3
1964	Arco	Watts M#1	33-5N-18E	3397	11371-11399	233	4221	.37	4.0
1976	Coquina	Mose Watts 1	34-5N-18E	1777	11512-11532	235	2408	.21	1.3
1985	Samson	Mose#1	35-5N-18E	1385	11592-11626	237	1786	.15	.70

1965	Amoco	Reusch#1	3-5N-19E	4062	11476-11492	235	4900	.43	20.5
1966	Amoco	Choctaw#T3	4-5N-19E	4012	11302-11326	232	4829	.43	9.4
1987	Amoco	Choctaw T3 #2	4-5N-19E	1245	11720-11755	239	1684	.14	1.5
1966	Amoco	Choctaw T#T4	5-5N-19E	4055	11371-11393	233	4863	.43	18.4
1966	Amoco	USA MCTiernan J#1	6-5N-19E	3963	11325-11333	232	4790	.42	11.8
1966	Amoco	Quaid#1	7-5N-19E	4020	11836-11842	239	4845	.41	11.6
1986	Vintage	Denton#1-16	16-5N-19E	2034	10769-10792	224	2880	.27	.12
1985	Willford	Burger 1-16	16-5N-19E	3319	10800-10876	225	4169	.38	1.7
1963	JMC	College 100#1	18-5N-19E	3975	11866-11892	241	4763	.40	7.6
1964	Exxon	Sparks Charles#1	19-5N-19E	3582	12310-12320	247	4465	.36	4.2
1965	Exxon	Ray JA#1	20-5N-19E	3800	12265-12286	247	4624	.38	5.0
1991	Texaco	HM Jennings No23-1	23-5N-19E	3875	13796-14004	273	4788	.34	.40
1967	Oryx	Diamond 1	30-5N-19E	3325	11102-11127	229	4148	.37	1.4
1990	Oryx	Diamond#2	30-5N-19E	1952	11288-11336	232	2641	.23	1.4
1991	Chaparral	VFW 1-29	32-5N-19E	1374	11908-12427	249	1829	.15	.50
1992	Amoco	Erlain Wheeler25-1	36-5N-19E	3080	14798-14918	287	4085	.27	.20

1979	Mustang	Booth 1-2	2-5N-20E	3632	12586-12592	251	4489	.36	1.2
1979	Mustang	Cathy 1-13	3-5N-20E	4083	12646-12704	253	4873	.38	2.1
1991	Anson	Buzzard Gap 1-19	19-5N-20E	2700	13833-13892	271	3656	.26	.45
1991	Anson	Hardcastle 1-20	20-5N-20E	2400	13988-14053	273	3256	.23	.13
1990	Anson	Cindy 1-21	21-5N-20E	4710	13584-13616	272	5405	.40	4.9
1991	Amoco	Raymond Smith 1-7	26-5N-20E	4154	10762-10936	226	5289	.48	
1990	Amoco	Raymond Smith#1	26-5N-20E	5595	13332-13374	263	5954	.45	13.6
1991	Amoco	Jack Bauman Unit1	27-5N-20E	5408	13784-13834	270	5897	.43	21.0
1991	Anson	Turney 1-28	28-5N-20E	3563	14093-14250	277	4439	.31	4.5
1991	Anson	Clear Creek1-29	29-5N-20E	2326	14184-14198	276	3140	.22	1.7
1991	Anadarko	H&H Cattle A1-31	31-5N-20E	4921	15250-15330	293	5653	.37	.11
1992	Anson	Cox 1-28	33-5N-20E	2661	14221-14271	277	3562	.25	2.9
1992	Anson	Turner1-33	33-5N-20E	3485	15346-15417	294	4658	.30	1.4
1991	Arco	Norman 1-34	34-5N-20E	7390	14556-14626	282	6951	.48	10.3
1992	Anson	Long Creek 1-25	36-5N-20E	2340	15644-15666	298	3306	.21	.15

1978	Samson	Cicar 1	26-6N-17E	1600	8127-8163	184	2099	.26	.01(82)
------	--------	---------	-----------	------	-----------	-----	------	-----	---------

1970	Oxley	Galaxy1	12-6N-18E	2854	10067-10090	213	3714	.37	2.4
1969	BHP	Wildlife#1	24-6N-18E	4014	11506-11518	235	4807	.42	1.6
1968	Amoco	Anderson Prich#1-12	25-6N-18E	3917	11579-11599	236	4757	.41	6.7
1964	Arco	Michell Unit #1	32-6N-18E	3736	11646-11664	237	4605	.40	1.2
1967	Amoco	Wilson 1	35-6N-18E	2484	11548-11556	236	3271	.28	.09(82)
1986	Samson	Sunflower 1-35	35-6N-18E	1431	11277-11309	232	1909	.17	1.0
1989	Oryx	Federal Church#2	36-6N-18E	1092	11415-11423	233	1451	.13	.04
1967	Oryx	Federal Church#1	36-6N-18E	3830	11033-11060	228	4614	.42	8.2

1982	Samson	Choctaw Unit1	1-6N-19E	1560	9802-9832	209	2059	.21	.11(INA)
1968	Sun	Bratton 1	2-6N-19E	3341	10120-10150	214	4173	.41	2.2
1966	Exxon	Clay Brown 1	3-6N-19E	3500	10237-10261	216	4345	.42	8.9
1989	Exxon	Clayton Brown 2	3-6N-19E	750	9998-10018	212	942	.09	.12
1967	Exxon	Coblentz LM	4-6N-19E	3488	10156-10174	215	4307	.42	2.3
1967	Mobil	Weaver D 1C	5-6N-19E	2765	10175-10185	215	3562	.35	.40(INA)
1967	Arco	Dept of Wildlife Co#2	7-6N-19E	3217	10218-10232	215	4056	.40	1.6(INA)
1968	Mobil	Weaver 1F	8-6N-19E	3038	9982-9994	212	3906	.39	2.3
1969	Mobile	Fred Clawson Unit1	9-6N-19E	3430	10040-10060	213	4279	.43	10.5
1990	Eberly&Meade	Clawson 2-9	9-6N-19E	797	10167-10195	215	1019	.10	.61
1969	Mobil	Browne C 1	10-6N-19E	3340	10367-10390	218	4204	.41	10.8
1970	Mobil	Wilburton 1	11-6N-19E	3395	10051-10077	213	4220	.42	6.0
1979	Prospective	Shaw 1-LT	14-6N-19E	506	10939-10957	227	644	.06	.50
1970	Mobil	Johnson H 1	15-6N-19E	3409	10290-10317	217	4267	.41	3.6
1989	Mobil	Johnson H 2	15-6N-19E	1531	10615-10648	222	2049	.19	1.8
1969	Oxley	Weaver	16-6N-19E	3453	10426-10446	219	4252	.41	.80(INA)

1986	Oxley	Weaver 2	16-6N-19E	1900	10753-10795	224	1416	.13	.12(INA)
1984	Samson	Mollie 1	17-6N-19E	1404	10724-10744	223	1859	.17	.20
1974	Samson	Robbers Cave 1	18-6N-19E	3062	10564-10592	221	3941	.37	2.4
1969	BHP	Cave 1	19-6N-19E	3827	11438-11454	234	4626	.40	10.6
1991	BHP	Cave 2	19-6N-19E	1068	11036-11058	228	1402	.13	.27
1967	Mobile	Weaver D#1B	20-6N-19E	3731	11174-11208	230	4563	.41	3.7
1968	Mobile	Weaver D#1E	21-6N-19E	3723	11245-11272	231	4555	.40	2.9
1969	Mobil	Harrison 1	22-6N-19E	3978	10906-10928	226	4765	.44	COM91
1982	Samson	Golightly#1	24-6N-19E	3271	13722-13753	269	4189	.31	.41(85)
1985	Sante Fe	Arkansas Kraft#1-25	25-6N-19E	3349	13848-13889	271	4265	.31	.25
1984	Sante Fe	Arkansas Kraft#1-26	26-6N-19E	4095	13951-13972	272	5359	.38	2.3
1966	Samson	Young R#1	27-6N-19E	3880	11169-11191	230	4687	.42	3.0
1986	Samson	Young R 2	27-6N-19E	1807	11090-11110	229	2440	.22	1.8
1966	Samaon	Young R 1	28-6N-19E	3960	11392-11422	234	4757	.42	13.0
1966	Shell	Kilpatrick 1	29-6N-19E	4013	11678-11694	238	4813	.41	18.6
1967	Mobil	Hackney 1	30-6N-19E	3900	11714-11732	238	4717	.40	8.9
1989	Mobil	Hackney 2	30-6N-19E	723	11796-11830	240	950	.10	.60
1966	Amoco	E Okla A&M#1	31-6N-19E	3990	10990-11018	227	4800	.44	10.9
1966	Amoco	Quaid B1	32-6N-19E	4024	10991-11006	227	4829	.44	13.7
1966	Amoco	Adams C1	33-6N-19E	4079	11030-11062	228	4874	.44	15.2
1986	Amoco	Adams C2	33-6N-19E	860	11146-11182	230	1134	.10	1.2
1966	Williford	Young 1	34-6N-19E	3708	11425-11445	234	4550	.40	.60(INA)
1983	Williford	Young 2-34	34-6N-19E	954	11099-11124	230	1268	.11	.65
1984	Santa Fe	Arkansas Kraft 1-35	35-6N-19E	3974	13929-13950	272	4849	.35	.80
1986	Sante Fe	Shaw 1-36	36-6N-19E	4906	14112-14153	275			.60

1969	Shell	Jankowsky 1	5-6N-20E	2694	10954-10980	227	3557	.32	.10(73)
1970	Texas Intl	Jankowsky 1	6-6N-20E	2849	9784-9831	209	3705	.38	1.8
1984	Santa Fe	Jankowsky 1-18	18-6N-20E	3742	14444-14506	281	4607	.32	1.2
1982	Santa Fe	Cecil 1-19	19-6N-20E	3958	13598-13652	267	4743	.35	4.6
1984	Santa Fe	Swart 1-20	20-6N-20E	4357	13859-13911	272	5099	.37	2.2
1981	Mustang	Young&Cooper 1-26	26-6N-20E	2439	13646-13701	268	3293	.24	.34(INA)
1982	Sante Fe	Pierce 1-30	30-6N-20E	3537	13840-13873	271	4379	.32	.50
1965	Mobil	Parks P 1	33-6N-20E	3875	13089-?		4685		.08(70)
1981	Mustang	Metcalf 1-34	34-6N-20E	3390	12697-12714	253	4276	.34	4.2
1980	Mustang	Fisherman 1	34-6N-20E	2151	13071-13353	263	2924	.22	.03(86)
1980	Mustang	Foster#1-35	35-6N-20E	3371	12630-12703	253	4257	.34	.50(INA)

1986	Samson	Circle F Ranch	10-6N-21E	1113	11927-12002	242	1362	.11	1.2
1963	Amoco	Free Unit 1	11-6N-21E	3985	11832-11887	241	4846	.41	12.1
1963	Sun	Norris 1	12-6N-21E	3892	11828-11904	241	4794	.40	10.1
1963	Amoco	Gallagher 1	13-6N-21E	3989	11877-11933	241	4849	.41	13.9
1963	Sun	Gallagher Wm 1	14-6N-21E	3843	11951-11990	242	4678	.39	16.6
1986	Oryx	Gallagher 2	14-6N-21E	1454	11995-12080	244	1954	.16	1.1
1963	Amoco	Booth 1	15-6N-21E	3976	12110-12152	245	4874	.40	6.1(INA)
1986	Amoco	Booth 2	15-6N-21E	1570	12068-12120	244	2134	.18	.30(INA)
1964	Amoco	Brewer 1	16-6N-21E	3990	12156-12180	245	4883	.41	4.3
1966	Amoco	White 1	18-6N-21E	4024	12640-12725	253	4925	.39	17.1(INA)
1975	Mustang	Foster 1	19-6N-21E	2182	12656-12710	253	3058	.24	1.4
1991	Mustang	Gillespie 2-20	20-6N-21E	916	12515-12536	250	1215	.10	1.0
1985	Mustang	Strother 1-20	20-6N-21E	1366	13253-13310	262	1935	.15	1.7
1988	JMC	Oxley 3	22-6N-21E	984	12152-12214	246	1304	.11	.80(INA)
1965	Exxon	Erwin WD 1	23-6N-21E	3734	11982-12001	242	4666	.39	3.3(INA)
1965	Amoco	Cecil 1	24-6N-21E	3945	11757-11831	240	4839	.41	7.4
1980	Texas	Gallagher 1	26-6N-21E	1222	12510-12570	251	1655	.13	.40(83)
1976	Mustang	Lyon 1-27	27-6N-21E	3255	12135-12184	245	3255	.27	1.2
1976	Mustang	Smallwood 1	28-6N-21E	2332	12181-12298	247	3131	.26	.60(INA)
1982	Whitmar	McCreery 1-30	30-6N-21E	1948	13412-13471	265	2671	.20	1.4

1988	Amoco	Lewis 3	4-6N-22E	1121	11205-11280	232	1512	.13	.6INA
1964	Amoco	Foster 1	7-6N-22E	3928	11670-11716	238	4823	.41	1.7INA
1964	Amoco	Orr 1	8-6N-22E	3400	11514-11568	236	4339	.38	2.9(90)
1987	Amoco	Orr 2	8-6N-22E	2962	11380-11444	234	3884	.34	.75(93)
1988	Amoco	Lyons 2	9-6N-22E	2340	11360-11420	234	3208	.28	.16(93)
1964	Amoco	Maxey 1	10-6N-22E	3588	11397-11406	233	4505	.40	1.5(90)
1987	Amoco	Ramer 2	14-6N-22E	2060	11718-11796	239	2797	.24	.11(90)
1964	Amoco	Rider 1	17-6N-22E	3300	11961-11969	242	4227	.35	1.7(89)
1987	Amoco	Rider 2	17-6N-22E	2550	11546-11612	236	3465	.30	.6(93)
1963	Oxley	Hulsey 1	18-6N-22E	3520	11662-11728	238	4448	.38	10.1
1986	Oryx	Hulsey 2	18-6N-22E	1796	11723-11756	239	2419	.21	1.7
1966	Amoco	Martin 1	20-6N-22E	2982	12306-12322	247	3984	.32	.79
1987	Amoco	Parks 2B	27-6N-22E	2220	12226-12302	247	3101	.25	.31(92)

1965	Mobil	LB Burreis 2	15-7N-19E	2894	10259-10300	217	3845	.37	7.7
1976	Samson	Powell 1	19-7N-19E	2023	10339-10403	218	2796	.27	.66
1964	Arco	Farmers Union 1	25-7N-19E	2970	10010-10060	213	3836	.38	2.9(80)
1964	Arco	Delamater Ray 1	26-7N-19E	2925	9686-9732	208	3783	.39	3.1
1964	Mobil	Coblentz 1	27-7N-19E	3322	10218-10234	216	4184	.41	6.2

1988	Mobil	Coblentz 2-27	27-7N-19E	1990	10224-10244	216	2648	.26	.03
1964	Oxley	Schwegman 1	28-7N-19E	3253	10134-10156	214	4117	.41	5.4
1967	Mobil	Butler 1	29-7N-19E	3227	10296-10312	217	4070	.40	4.0
1980	Samson	Golden A1-30	30-7N-19E	1188	10420-10436	219	1557	.15	1.8
1966	Arco	Parks Pete 1	32-7N-19E	3467	10555-10584	221	4324	.41	9.7
1965	Mobil	Schwegman 1	33-7N-19E	3431	10487-10502	220	4289	.41	7.0
1965	Shell	Stevenson 1	34-7N-19E	3600	10408-10429	219	4411	.42	12.9

1982	Marathon	Walker 1	10-7N-20E	1066	8035-8058	182	1349	.17	.6(89)
1983	Grand	Walker 1-11	11-7N-20E	846	8033-8077	183	1074	.13	.66(NA)
1964	Samson	Rose 1	12-7N-20E	1174	8454-8496	189	1528	.18	5.5
1973	Sante Fe	Bryant 1	13-7N-20E	1111	8712-8794	193	1466	.17	2.4
1970	Cotton Pet	Burris 1	15-7N-20E	1223	9412-9462	204	1618	.17	.31(77)
1969	Sante Fe	Falconer Alva 1	16-7N-20E	1553	9197-9245	200	2118	.23	3.5
1965	Samson	Mason 1	18-7N-20E	2510	9848-9878	210	3439	.35	1.8
1964	Mobil	Murphy 1	19-7N-20E	3057	9372-9423	203	3991	.42	11.8
1989	Mobil	Murphy 2	19-7N-20E	690	9576-9636	206	884	.10	1.3
1967	Shell	Jankowsky 1	29-7N-20E	2871	9611-9636	207	3694	.38	5.9
1965	Exxon	Rowe Perry 1	30-7N-20E	3036	9868-9926	211	3901	.39	6.7
1966	Mobil	Dipple 1	31-7N-20E	2546	9735-9793	209	3364	.34	.93
1967	Shell	Jankowsky 1-32	32-7N-20E	3150	9796-9852	210	3984	.40	11.0

1970	Faulconer	Nix Loyd 1	1-7N-21E	1081	7080-7110	168	1373	.19	4.7
1982	Arkoma	Horton 1	2-7N-21E	491	7146-7199	169	592	.08	.68
1978	Price	Wright 1-A	3-7N-21E	880	7233-7244	169	1109	.15	.25(89)
1966	Zinke&Trumbo	Wright 1	3-7N-21E	1163	7370-7414	172	1517	.21	1.5(85)
1966	Samson	Slater 1	4-7N-21E	1150	7371-7400	172	1485	.20	3.4
1987	D Pex	Martin O A-1	5-7N-21E	347	7642-7716	177	418	.05	.003(89)
1964	Texaco	Hulsey Robert 1C	5-7N-21E	1168	7413-7513	174	1512	.20	4.6
1966	Amoco	Sloan 1	6-7N-21E	1152	7776-7788	178	1484	.19	.69(86)
1964	Mobil	Vaughn 1	7-7N-21E	1145	8064-8081	183	1490	.18	1.4(92)
1969	Samson	Bowen 1	8-7N-21E	1025	7850-7934	180	1318	.17	1.6
1974	Coquina	Holt 1	10-7N-21E	783	7706-7726	177	985	.13	.16(77)
1978	Samson	Kennedy 2	10-7N-21E	754	7490-7530	174	943	.13	2.0
1988	Mustang	Kamphaus 1-12	12-7N-21E	3083	9694-9738	207	3996	.41	7.2
1976	Mustang	Martin 1	12-7N-21E	906	7192-7234	169	1144	.16	1.5
1982	Vintage	Snow 1-13	13-7N-21E	2702	11944-11990	242	3841	.32	7.3
1981	Unit Pet	Panther Hollow U	14-7N-21E	3060	12216-12248	245	4100	.34	3.7
1987	Unit Pet	Panther Hollow 2	14-7N-21E	2588	11966-11995	242	3712	.31	.88
1991	Unit Pet	Panther Hollwow 3	14-7N-21E	1582	11262-11280	231	2210	.20	.73
1981	Unit Pet	Turkey Flat 1	16-7N-21E	949	7950-7990	181	1216	.15	.66
1964	Getty	Madden 1	17-7N-21E	1035	7856-7864	179	1332	.17	.27(82)
1973	Mobil	Duncan 1	19-7N-21E	2117	8982-9030	197	2860	.32	.51(83)
1980	Samson	Furrow 1	22-7N-21E	207	12258-12296	247	3059	.25	1.3
1987	Samson	Steven 1UT	22-7N-21E	1310	11956-12005	242	2893	.24	.20(91)
1981	Cheyenne	Kirkwood 1	23-7N-21E	2854	12248-12290	247	3853	.31	3.9
1980	Cheyenne	James 1-28	28-7N-21E	1087	12244-12304	247	1459	.12	.81

1982	Whit Mar	Nunn 1-4	4-7N-22E	465	6632-6644	160	555	.08	.01(85)
1978	Samson	Bush 1	5-7N-22E	855	6846-6896	164	1069	.16	1.8
1987	Tucker	Murchinson 1-6	6-7N-22E	386	6902-6931	165	463	.07	.30
1982	Whit Mar	Arkansas Kraft 1-10	10-7N-22E	1841	13155-13178	260	2578	.20	.14(90)
1982	Whit Mar	Saddlebach 1-15	15-7N-22E	1866	13210-13246	261	2644	.20	.84

1976	Eberly&Meade	Thompson 1-8	8-7N-23E	2920	11414-11465	234	3849	.34	6.4
1976	Eberly&Meade	Reed 1-9	9-7N-23E	2538	11283-11309	232	3423	.30	4.8
1978	Arco	Hollie Estate Unit 1-X	20-7N-23E	2401	11406-11656	237	3351	.29	3.5
1977	Arco	Roy Reed Unit 1	21-7N-23E	2301	11576-11709	238	3231	.28	7.9

1964	Exxon	Terrel WM 1	36-8N-19E	1350	5819-5834	149	1710	.29	5.2
------	-------	-------------	-----------	------	-----------	-----	------	-----	-----

1964	Snee-Eberly	Drain 1-A	21-8N-20E	1138	5551-5561	144	1417	.26	1.6
1984	Howden	Kaisner 1-22	22-8N-20E	347	5439-5465	143	405	.07	.87
1981	DMS	Roye 1	25-8N-20E	850	6613-6666	166	1046	.16	.18
1965	JMC	Anderson 1	29-8N-20E	1150	5626-5648	151	1434	.25	.48(93)
1965	Redstone	Smith 1	30-8N-20E	1242	5702-5712	152	1560	.27	2.5(93)
1964	Mobil	Kinta 1	31-8N-20E	1295	5627-5642	151	1643	.29	4.5
1961	Mobil	Davenport 1	33-8N-20E	1253	5542-5570	150	1572	.28	1.6
1973	Wytex	Scott Estate 1	35-8N-20E	1627	6720-6744	162	2132	.32	2.3
1990	JMC	Jeffery 1	35-8N-20E	452	6720-6744	167	540	.08	.42
1980	Samson	Slaon 1	36-8N-20E	947	6662-6712	167	1176	.17	.64

1972	Red Wine	Blackman 1	2-8N-21E	1192	6585-6590	160	1505	.23	.04(73)
1989	Red Wine	Tyler 1	2-8N-21E	719	5310-5340	146	858	.16	1.1
1969	Sante Fe	Hall Jim 1	3-8N-21E	1721	5525-5549	149	2218	.40	.60
1991	Sante Fe	Hall Jim 2	3-8N-21E	500	5320-5330	146	596	.11	4.8
1980	National	Hall 1-9	9-8N-21E	1437	5260-5348	141	1836	.34	.52(92)



1969	Kaiser	Kerr McGee 1	12-8N-21E	1111	6372-6384	162	1403	.22	1.2(84)
1983	Kaiser	Kerr McGee 2	12-8N-21E	429	6356-6366	162	509	.08	.54
1966	Samson	Fields Farm A-1	13-8N-21E	1153	6464-6496	159	1463	.23	3.3
1965	Amoco	Robertson 1	14-8N-21E	429	6404-6431	163	1463	.23	8.1
1982	Bogert	Rees 1-15	15-8N-21E	1154	5662-5674	151	1118	.20	.54
1980	Red Wine	Abbath 1	16-8N-21E	1154	5352-5434	143	1444	.27	.24(83)
1983	Roye	Roye 1-19	19-8N-21E	1333	5467-5482	148	1694	.31	.11NA
1965	Humble	J Fred Dittman 1	21-8N-21E	1180	5876-5964	150	1340	.23	.37(92)
1967	Humble	Eva McDaniel 1	23-8N-21E	1125	6526-6544	159	1425	.22	4.6
1971	Rife Oil	State Hightower 1	24-8N-21E	1078	6466-6490	159	1361	.21	.91
1991	Williford	Hightower 2-24	24-8N-21E	322	6392-6424	163	377	.06	.28
1969	Samson	Hightower 1	25-8N-21E	1225	6612-6646	166	1566	.24	2.8
1965	Exxon	Oliver Heirs 1000 1	26-8N-21E	1140	6676-6715	167	1140	.17	1.0(89)
1965	Exxon	Oliver 1	28-8N-21E	1127	6602-6630	166	1429	.21	1.7
1965	Exxon	Roye 1	29-8N-21E	1575	6124-6204	154	2046	.33	1.7(92)
1989	Exxon	Roye Claude 2	30-8N-21E	910	6500-6570	165	1132	.17	1.4
1966	Exxon	Burge 1	31-8N-21E	1525	6609-6632	161	1968	.30	2.2

1965	Monsanto	Lone Star 1	8-8N-22E	1168	6286-6348	156	1480	.23	14.9
1965	Exxon	Cummings Est 1	9-8N-22E	1220	6105-6191	154	1549	.25	16.3
1969	Headington	Greenwood 1	11-8N-22E	1063	5746-5776	148	1328	.23	7.2
1964	Stevens	Fitzger 1	12-8N-22E	1014	5287-5391	142	1240	.23	.67
1965	Stephens	Patterson 1	13-8N-22E	1170	5652-5681	151	1449	.25	2.9
1984	Arkla	Patterson 2	13-8N-22E	429	5620-5658	151	501	.09	4.8
1965	Oryx	Federal College 1	15-8N-22E	1172	5840-6016	151	1480	.25	20.8
1965	Exxon	Hightower 1	17-8N-22E	1200	6125-6229	155	1522	.24	7.7
1965	Exxon	McCurtain 1	22-8N-22E	1175	5734-5918	150	1482	.25	22.4
1965	Exxon	Rees lizabeil 1	23-8N-22E	1165	5594-5680	151	1464	.26	18.3
1987	Oryx	Fed Langford 2	24-8N-22E	357	5560-5685	151	414	.07	5.3
1968	Amoco	Krisher 1	25-8N-22E	1169	5402-5554	144	1455	.26	15.8
1966	Amoco	McCaferty 1	26-8N-22E	1150	5617-5644	146	1445	.26	18.3
1966	Arco	Wantland 1	27-8N-22E	1169	5784-5817	148	1461	.25	11.9
1965	D Pex	Thompson 1	29-8N-22E	1101	6352-6394	157	1390	.22	1.5(90)
1977	P Sec	Farmer 1	31-8N-22E	907	6915-6933	170	1135	.16	2.7
1968	Amoco	White C-1	34-8N-22E	1022	6067-6072	152	1260	.21	.35(73)
1976	Samson	Ramirez Etal 1	36-8N-22E	615	5904-6006	151	740	.12	7.4

1966	Exxon	Wallen Heirs 1	4-8N-23E	1025	5353-5368	142	1257	.23	3.3
1965	Exxon	McBee 1	7-8N-23E	1050	5581-5593	145	1292	.23	.98(76)
1986	Kaiser	Kennedy 2-18	18-8N-23E	284	5440-5475	143	325	.06	.34
1968	Amoco	Bowen 1	23-8N-23E	1023	5256-5264	140	1243	.24	.91(78)
1979	Amoco	Tanksley 1	24-8N-23E	707	5062-5066	137	838	.17	.73
1968	Amoco	Birckel 1	29-8N-23E	1160	5347-5646	146	1425	.25	5.8
1968	Amoco	Miller 1	30-8N-23E	1147	5696-5700	147	1412	.25	.7

Potentiometric Data Table  
for selected wells producing from  
single Spiro completions

<u>#</u>	<u>LOCATION</u>	<u>WELL</u>	<u>YEAR</u>	<u>Z=POTEN</u>	<u>X</u>	<u>Y</u>
1	20-4N-19E	Swindle 1-18	1992	812	99	45.5
2	13-5N-17E	DunaganA-1	1964	1963	76.5	76.5
3	22-5N-17E	Sivil Gol #1	1965	733	50	71.5
4	23-5N-17E	Darby #1	1965	577	54	72
5	24-5N-17E	Fabbro #1	1964	1550	59	72.5
6	25-5N-17E	Henley #1	1964	499	58.5	68
7	26-5N-17E	Caudron #1	1965	314	53.5	67
8	27-5N-17E	Parker #1	1966	1377	47.5	69
9	13-5N-18E	Austin #1	1962	1591	87.5	83.5
10	14-5N-18E	Costilow #1	1963	1592	85	83
11	15-5N-18E	Yourman #1	1963	1692	80.5	85
12	16-5N-18E	Kilpatrick #1	1963	1680	75	84
13	17-5N-18E	Fazekas #1	1963	1703	65.5	82.5
14	18-5N-18E	BHampton #1	1963	1408	61.5	82.5
15	19-5N-18E	Bennett #1	1964	1242	63	77
16	20-5N-18E	Smith #1	1963	1935	68	77
17	21-5N-18E	Paschall #1	1963	2014	75.5	77
18	22-5N-18E	MCalester #1	1963	2115	80	76
19	23-5N-18E	Williams #1	1963	1230	85	78.5
20	24-5N-18E	James #1	1963	1181	88	77
21	27-5N-18E	Enis #1	1964	673	79.5	73
22	29-5N-18E	Dobbs #1	1963	1642	68.5	74.5
23	30-5N-18E	Bennett #1	1964	290	64.5	72.5
24	26-5N-20E	Smith #!	1990	50	143	72
25	26-5N-20E	Smith 1-7	1991	1039	143	73
26	34-5N-20E	Norman #1	1991	1222	141	65.5
27	22-6N-19E	Harrison #1	1969	349	108.5	102
28	27-6N-19E	Young #1	1966	89	109	96
29	33-6N-19E	Adams C-1	1966	70	103	93



APPENDIX B

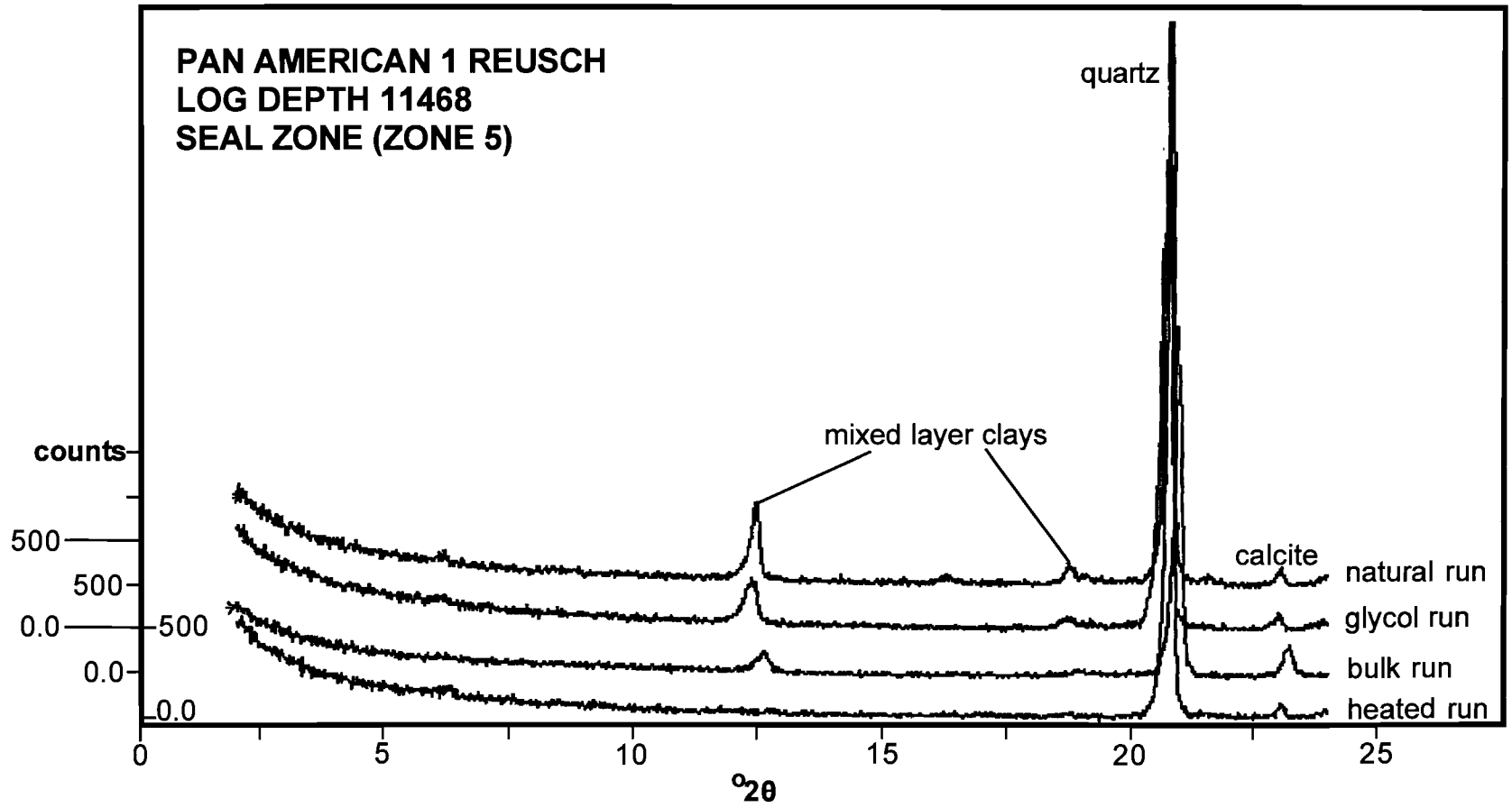
X-RAY DIFFRACTOGRAMS  
FLUID INCLUSION DATA

X-RAY DIFFRACTION DATA TABLE  
PAN AMERICAN 1 REUSCH

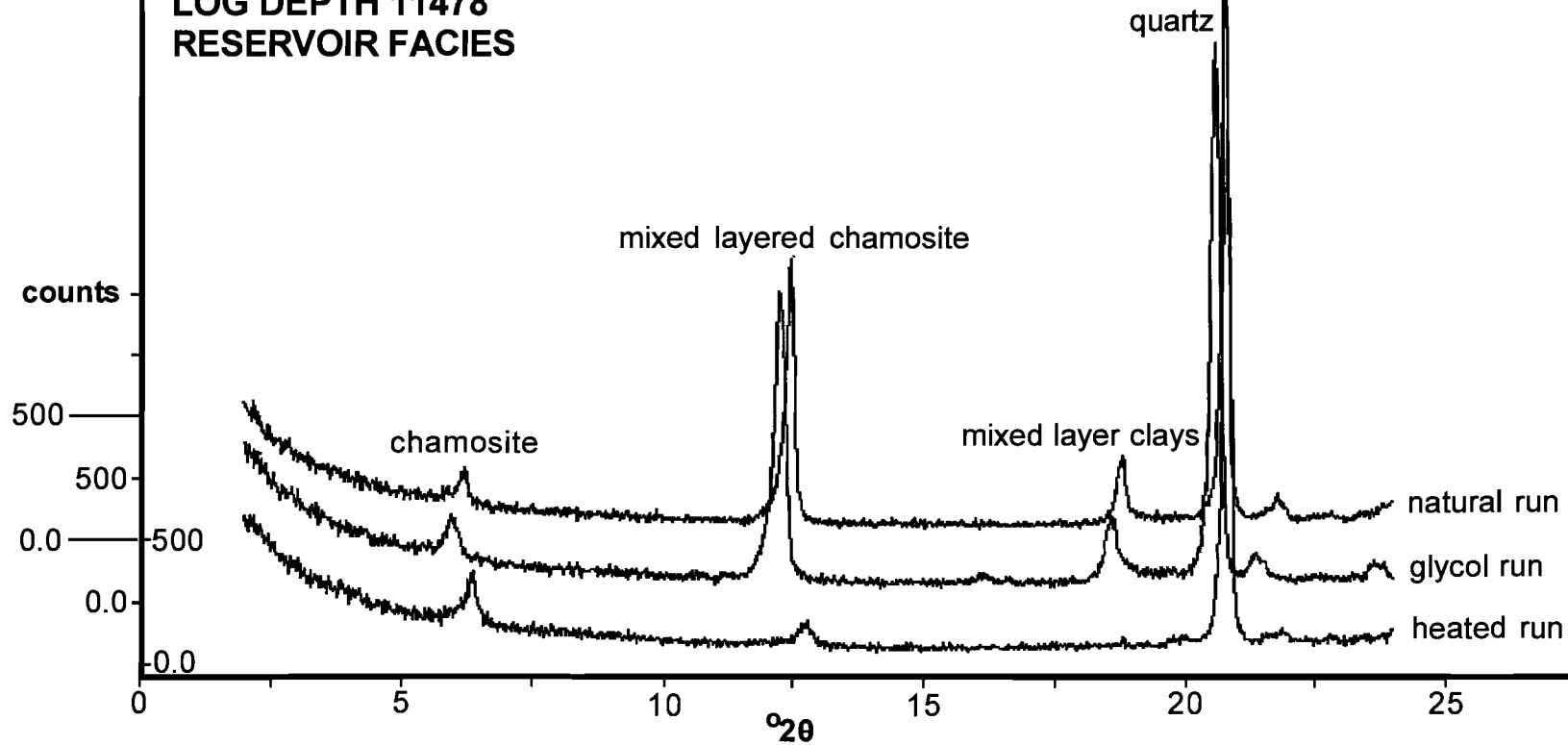
	<u>Angle <math>\frac{1}{2} 2\theta</math></u>	<u>d-value (<math>\text{\AA}</math>)</u>	<u>d-value (<math>\text{\AA}^2</math>)</u>	<u>pk width <math>\frac{1}{2} 2\theta</math></u>	<u>counts</u>
<u>P11468</u>	12.625	7.0058	7.0231	0.100	102
	18.910	4.6891	4.7007	0.240	27
	20.940	4.2389	4.2494	0.120	1980
	23.220	3.8276	3.8370	0.160	180
<u>P11468N</u>	2.045	43.1660	43.2722	0.240	246
	6.205	14.2326	14.2676	0.240	26
	8.540	10.3456	10.3711	0.480	8
	12.465	7.0954	7.1129	0.120	412
	16.285	5.4386	5.4520	0.160	38
	18.760	4.7263	4.7379	0.160	86
	20.805	4.2661	4.2766	0.160	3672
	21.590	4.1128	4.1229	0.200	35
	23.030	3.8538	3.8633	0.060	94
<u>P11468G</u>	4.430	19.9304	19.9795	0.200	14
	6.105	14.4655	14.5010	0.240	13
	12.460	7.0982	7.1157	0.120	180
	18.730	4.7338	4.7454	0.200	52
	20.645	4.2988	4.3094	0.060	2144
	20.785	4.2702	4.2807	0.100	2490
	22.985	3.8662	3.8757	0.080	81
<u>P11468H</u>	2.215	39.8534	39.9515	0.320	219
	6.300	14.0182	14.0526	0.240	36
	16.975	5.2191	5.2319	0.960	7
	18.715	4.7376	4.7492	0.480	8
	20.805	4.2661	4.2766	0.160	3181
	23.055	3.8546	3.8641	0.100	71
<u>P11478N</u>	6.210	14.2211	14.2561	0.160	110
	12.510	7.0700	7.0874	0.120	967
	18.825	4.7101	4.7217	0.140	262
	20.835	4.2600	4.2705	0.120	2470
	21.765	4.0801	4.0901	0.100	83
<u>P11478G</u>	5.990	14.7429	14.7792	0.160	146
	12.255	7.2165	7.2343	0.200	1156
	14.870	5.9528	5.9674	0.560	4
	16.110	5.4973	5.5108	0.200	28
	18.580	4.7717	4.7834	0.100	250
	18.675	4.7476	4.7593	0.080	225
	20.620	4.3040	4.3146	0.220	2172
	21.350	4.1584	4.1687	0.200	104
	23.610	3.7652	3.7745	0.200	59
<u>P11478H</u>	6.370	13.8643	13.8984	0.080	213
	12.735	6.9456	6.9627	0.240	79
	18.810	4.7139	4.7254	0.060	22

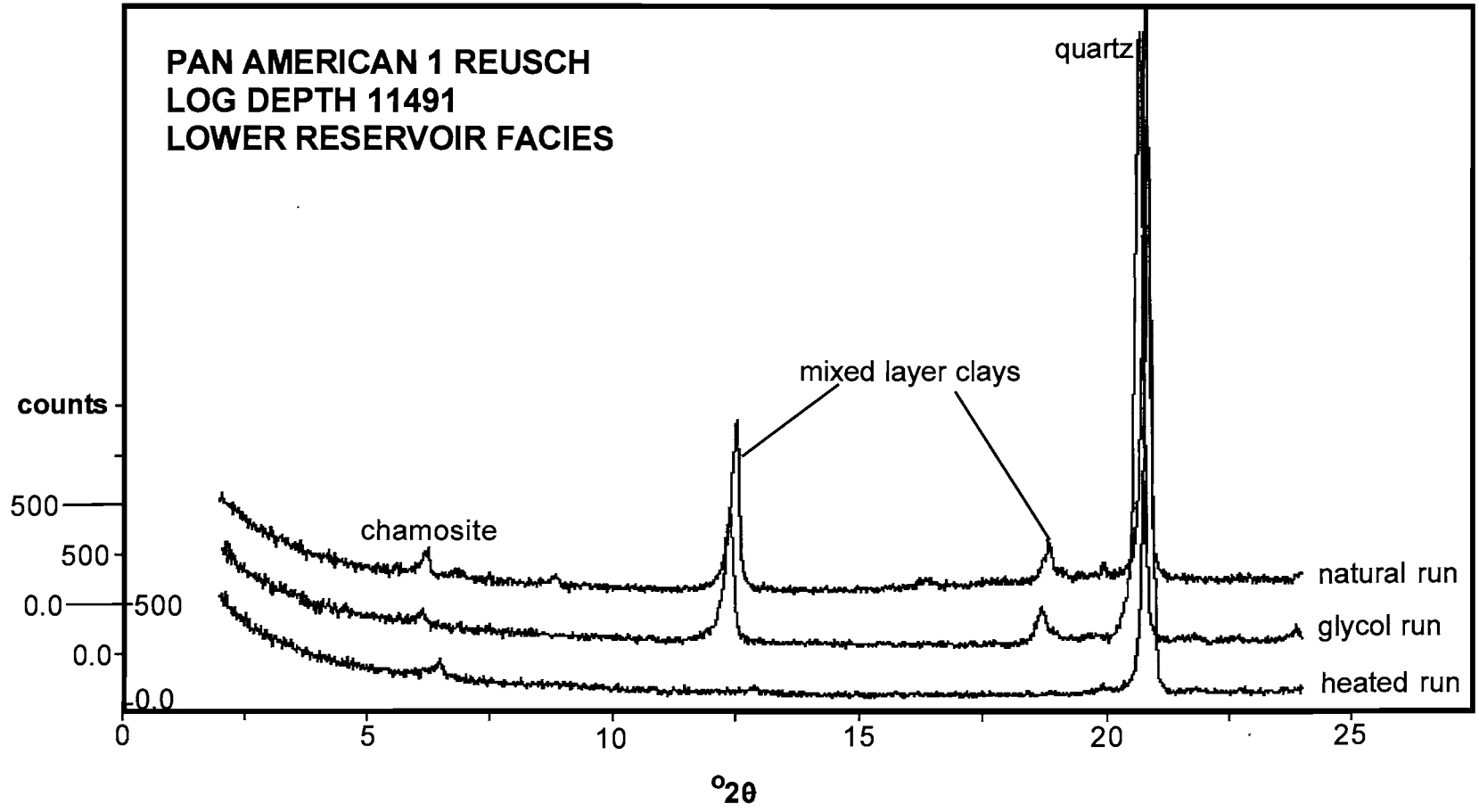
	<u>Angle <math>\frac{1}{2} 2\theta</math></u>	<u>d-value (Å1)</u>	<u>d-value (Å2)</u>	<u>pk width <math>\frac{1}{2} 2\theta</math></u>	<u>counts</u>
	19.870	4.4647	4.4757	0.320	27
	20.840	4.2590	4.2695	0.120	2788
	21.915	4.0525	4.0625	0.160	48
	22.810	3.8955	3.9050	0.160	32
<u>P11491</u>	12.835	6.8917	6.9086	0.160	61
	19.180	4.6237	4.6351	0.320	10
	21.150	4.1973	4.2076	0.140	462
	23.390	3.8002	3.8095	0.240	4
	25.715	3.4616	3.4701	0.320	31
	26.730	3.3324	3.3406	0.060	339
	27.120	3.2854	3.2935	0.180	1927
<u>P11491N</u>	2.105	41.9358	42.0390	0.320	210
	6.260	14.1076	14.1423	0.080	130
	8.845	9.9896	10.0141	0.120	40
	12.535	7.0559	7.0733	0.160	824
	16.345	5.4188	5.4321	0.240	35
	18.840	4.7064	4.7180	0.100	185
	19.935	4.4503	4.4612	0.060	96
	20.840	4.2590	4.2695	0.140	3226
<u>P11491G</u>	6.130	14.4065	14.4420	0.120	55
	12.410	7.1267	7.1443	0.180	605
	17.840	4.9679	4.9801	0.320	1
	18.705	4.7401	4.7517	0.100	177
	20.600	4.3081	4.3187	0.060	1866
	20.720	4.2834	4.2940	0.140	3036
	21.830	4.0681	4.0781	0.480	22
	22.630	3.9260	3.9357	0.320	14
<u>P11491H</u>	6.500	13.5873	13.6207	0.160	62
	12.830	6.8944	6.9113	0.320	22
	20.880	4.2510	4.2614	0.140	2862
<u>P11500</u>	12.670	6.9811	6.9982	0.200	28
	19.080	4.6477	4.6592	0.800	7
	21.060	4.2150	4.2254	0.080	231
	21.170	4.1934	4.2037	0.080	146
	23.310	3.8130	3.8224	0.120	204
	23.420	3.7954	3.8047	0.060	231
<u>P11500N</u>	12.515	7.0672	7.0846	0.120	106
	18.785	4.7201	4.7317	0.160	25
	20.825	4.2621	4.2726	0.100	199
	23.055	3.8546	3.8641	0.140	576
<u>P11500G</u>	2.120	41.6391	41.7415	0.240	219
	12.440	7.1096	7.1271	0.200	58
	13.205	6.6994	6.7159	0.240	4
	18.745	4.7300	4.7417	0.480	11
	20.630	4.3019	4.3125	0.080	144
	20.785	4.2702	4.2807	0.120	182

	<u>Angle <math>\frac{1}{2} 2\theta</math></u>	<u>d-value (<math>\text{\AA}</math>1)</u>	<u>d-value (<math>\text{\AA}</math>2)</u>	<u>pk width <math>\frac{1}{2} 2\theta</math></u>	<u>counts</u>
	23.040	3.8571	3.8666	0.140	424
<u>P11500H</u>	2.120	41.6391	41.7415	0.480	219
	6.250	14.1302	14.1649	0.320	21
	20.650	4.2978	4.3084	0.200	142
	21.295	4.1691	4.1793	0.200	23
	22.870	3.8854	3.8949	0.060	538
	22.965	3.8695	3.8790	0.080	497
<u>P11507</u>	8.900	9.9279	9.9524	0.320	27
	12.440	7.1096	7.1271	0.160	72
	17.680	5.0125	5.0248	0.200	32
	18.805	4.7151	4.7267	0.240	29
	19.760	4.4893	4.5004	0.280	121
	20.685	4.2906	4.3012	0.140	807
	20.815	4.2641	4.2746	0.080	942
	22.035	4.0307	4.0406	0.240	36
	22.890	3.8820	3.8916	0.480	35
<u>P11507N</u>	6.170	14.3132	14.3484	0.200	36
	8.860	9.9727	9.9972	0.120	228
	12.520	7.0644	7.0817	0.120	462
	16.350	5.4171	5.4305	0.200	19
	17.740	4.9957	5.0080	0.100	213
	18.805	4.7151	4.7267	0.200	108
	19.305	4.4792	4.4902	0.100	228
	20.865	4.2540	4.2645	0.120	2228
	22.040	4.0298	4.0397	0.160	66
	22.905	3.8795	3.8891	0.240	58
	23.535	3.7771	3.7864	0.120	76
<u>P11500G</u>	2.070	42.6448	42.7497	0.320	243
	6.095	14.4892	14.5248	0.480	15
	8.760	10.0863	10.1111	0.060	156
	12.380	7.1439	7.1615	0.180	335
	16.155	5.4821	5.4956	0.120	18
	17.595	5.0365	5.0489	0.080	119
	18.685	4.7451	4.7568	0.080	112
	19.570	4.5325	4.5436	0.280	142
	20.700	4.2875	4.2981	0.180	2237
	21.345	4.1594	4.1696	0.200	58
	21.815	4.0708	4.0809	0.200	67
	22.715	3.9115	3.9212	0.160	40
<u>P11507H</u>	6.270	14.0852	14.1198	0.360	81
	8.660	10.2025	10.2276	0.200	207
	17.550	5.0493	5.0618	0.320	166
	19.585	4.5290	4.5402	0.100	335
	20.690	4.2896	4.3001	0.220	2162
	21.835	4.0672	4.0772	0.160	71
	22.635	3.9252	3.9348	0.320	108
	23.435	3.7930	3.8023	0.240	146



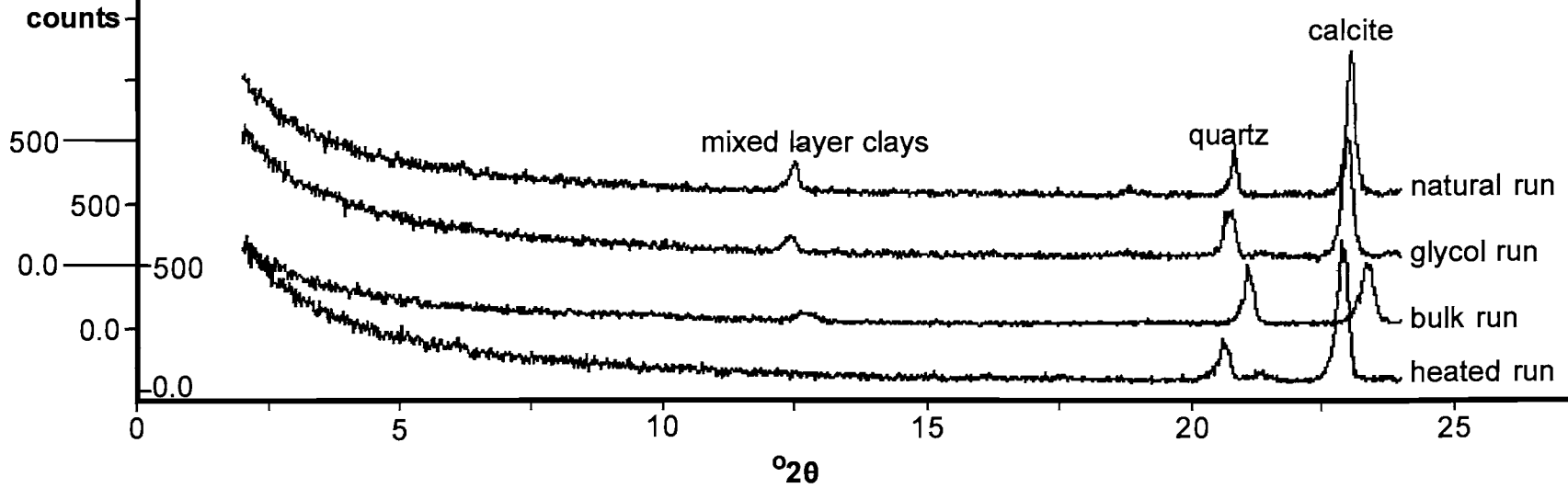
PAN AMERICAN 1 REUSCH  
LOG DEPTH 11478  
RESERVOIR FACIES





PAN AMERICAN 1 REUSCH  
LOG DEPTH 11500  
LOWER SEAL ZONE (ZONE 1)

97





PAN AMERICAN 1 REUSCH  
LOG DEPTH 11507  
LOWER SEAL ZONE (ZONE 1)

quartz

mixed layer clays

illite

chlorite

illite

natural run

glycol run

bulk run

heated run

counts

500

500

0.0

0.0

0

5

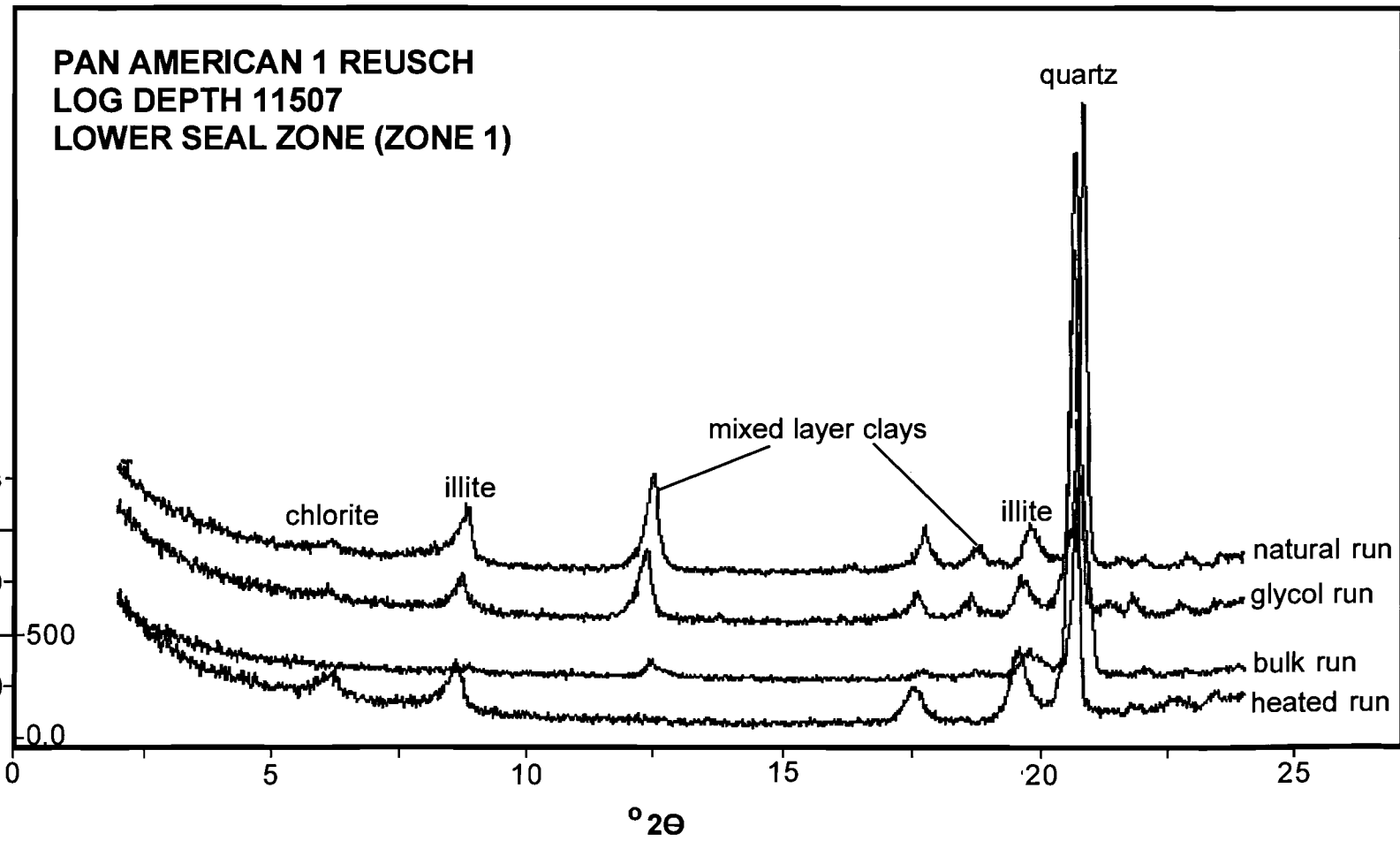
10

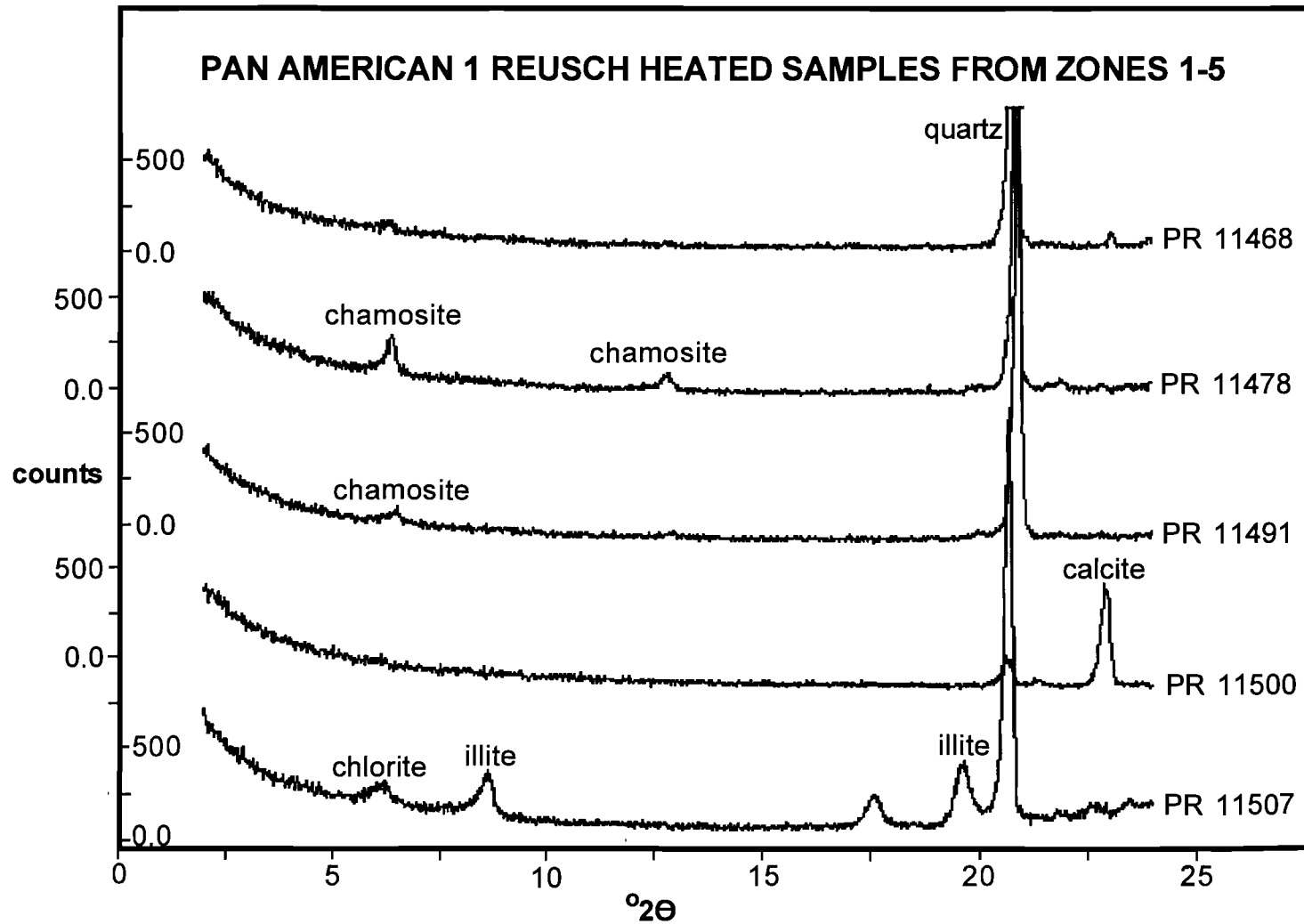
15

20

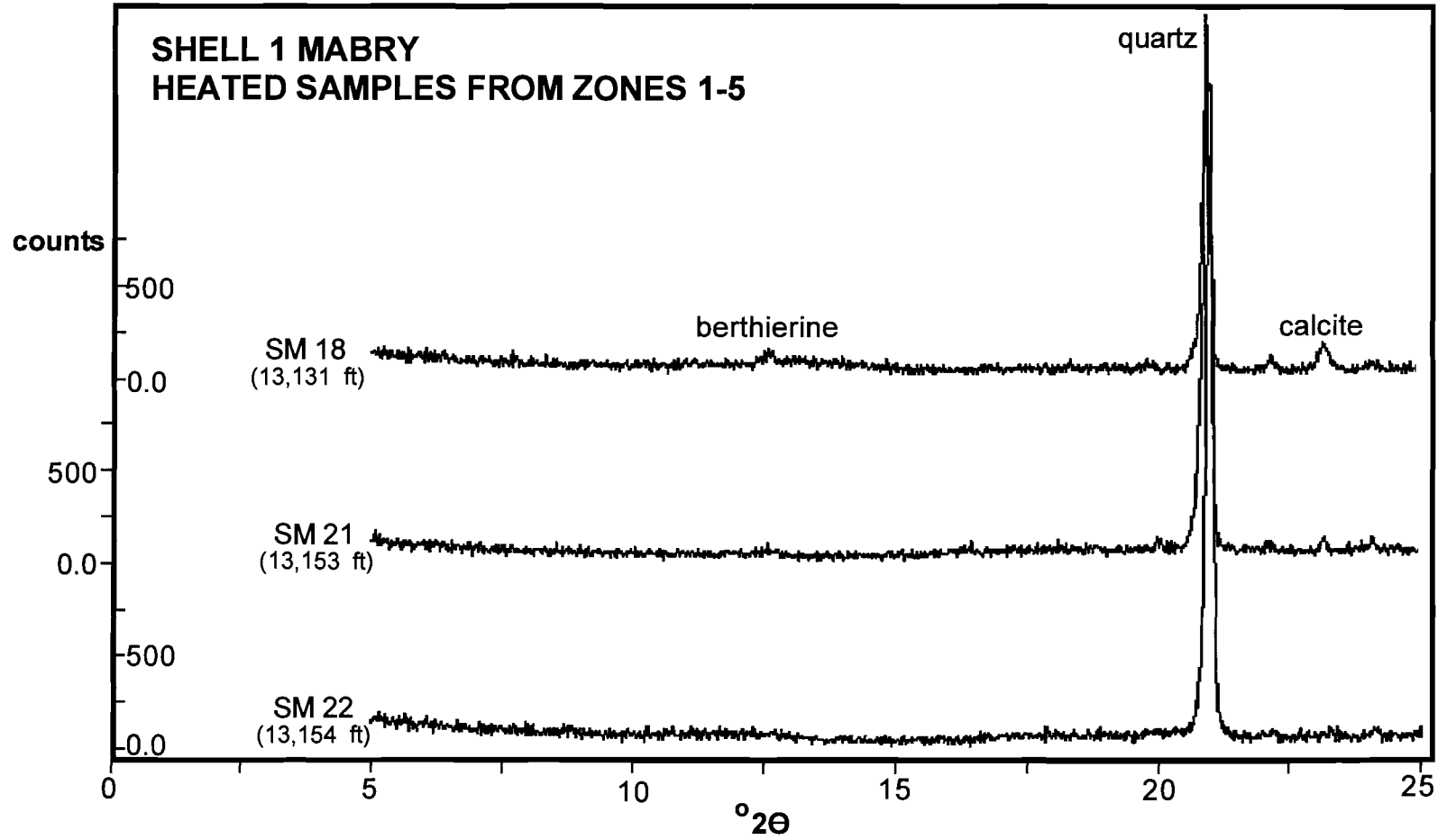
25

$^{\circ}2\theta$


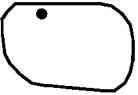
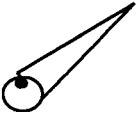


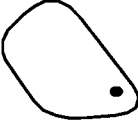





**SHELL 1 MABRY  
HEATED SAMPLES FROM ZONES 1-5**



**FLUID-INCLUSION DATA SUMMARY  
FOR THE PAN AMERICAN 1 REUSCH TYPE LOG-CORE**

SKETCH	TYPE OF INCLUSION	TH (°C)	SAMPLE DEPTH	OBSERVATIONS
	Primary homogeneous	140.0 136.6	11,505 ft	Quartz overgrowth dust-rim inclusion
	Primary homogeneous	140.9 136.6	11,505 ft	Quartz overgrowth dust-rim inclusion
	Primary homogeneous	140.9 141.2	11,505 ft	Silica replacement within fossil frag
	Primary homogeneous	140.9 141.3	11,505 ft	Silica replacement within fossil frag
	Primary homogeneous	114.4 114.3	11,505 ft	Remnant calcite within fossil frag
	Primary homogeneous	120.1 118.5	11,473 ft	Diagenetic calcite cement zone
	Primary homogeneous	119.1 117.4	11,473 ft	Diagenetic calcite cement zone

APPENDIX C

WELL-LOG DATA  
PETROLOGS  
FORMATION DATA

SPIRO SANDSTONE ZONES FROM WELL LOG EVALUATION  
THICKNESS AND POROSITY

WELL	ZONES	THICKNESS(ft)	AVE POROSITY
Arkoma Pattison 1 1-4N-17E	Zone 5	28	2.69 (bulk den)
	Zone 4	14	2.64
	Zone 3	14	2.61
	Zone 2	20	2.55
	Zone 1	8	2.70
Arkoma McCaslin 1 2-4N-17E	Zone 5	14	2.58 (bulk den)
	Zone 4	14	2.54
	Zone 3	12	2.50
	Zone 2	10	2.45
	Zone 1	36	2.70
Arkoma McCaslin 2 2-4N-17E	Zone 5	24	2.65 (bulk den)
	Zone 4	12	2.42
	Zone 3	12	2.55
	Zone 2	8	2.55
	Zone 1	12	2.69
Arkoma Sparks 1 3-4N-17E (TYPE LOG I)	Zone 5	14	2.59 (bulk den)
	Zone 4	12	2.54
	Zone 3	14	2.50
	Zone 2	12	2.57
	Zone 1	40	2.65
Arkoma Layden 1-3 3-4N-17E	Zone 5	10	2.62 (bulk den)
	Zone 4	14	2.56
	Zone 3	14	2.50
	Zone 2	10	2.45
	Zone 1	36	2.67
Whitmar Silver Bullet 1 11-4N-17E	Zone 5	18	5 (den por)
	Zone 4	10	8
	Zone 3	16	9
	Zone 2	12	6
	Zone 1	68?	4
JMC Blue Mt 1-1 22-4N-17E	Zone 5	26	2 (spec den)
	Zone 4	24	7
	Zone 3	20	4
	Zone 2	24	10
	Zone 1	22	5
Amoco Retherford 1A 25-4N-17E	Zone 5	18	3 (spec den)
	Zone 4	16	3
	Zone 3	20	15
	Zone 2	14	8
	Zone 1	24	4
BTA Amason 1 24-4N-18E	Zone 5	18	2 (den por)
	Zone 4	14	2
	Zone 3	18	4
	Zone 2	14	11
	Zone 1	12	2
Exxon Retherford 1B 31-4N-18E	Zone 5	24	2 (den por)
	Zone 4	16	2
	Zone 3	14	18
	Zone 2	16	10
	Zone 1	32	3
An son Golden 1-10 10-4N-20E	Zone 5	22	4 (den por)
	Zone 4	30	6
	Zone 3	28	3
	Zone 2	15	6
	Zone 1	37	4
Pan Am Caudron 1 26-5N-17E ?	Zone 5	12	50 (sonic)
	Zone 4	14	51
	Zone 3	12	58
	Zone 2	10	59
	Zone 1	12	52
Arkoma Whitney 3 34-5N-17E	Zone 5	14	5 (den por)
	Zone 4	12	12
	Zone 3	11	6
	Zone 2	14	5
	Zone 1	9	1

WELL	ZONES	THICKNESS (ft)	AVE POROSITY
Arco Kurilko Andrew 35-5N-17E	Zone 5	13	5 ( porosity)
	Zone 4	16	8
	Zone 3	21	13
	Zone 2	22	8
	Zone 1	23	6
Arco Lerblanc 2 36-5N-17E	Zone 5	9	3 (den por)
	Zone 4	8	14
	Zone 3	8	13
	Zone 2	10	2
	Zone 1	23	2
Arco Davis A-2 11-5N-18E	Zone 5	12	2 (den por)
	Zone 4	12	6
	Zone 3	8	7
	Zone 2	7	6
	Zone 1	16	2
Samson Costilow 2 14-5N-18E	Zone 5	6	7 (den por)
	Zone 4	10	7
	Zone 3	9	14
	Zone 2	10	6
	Zone 1	23	6
Arco Kilpatrick 3 16-5N-18E	Zone 5	11	6 (den por)
	Zone 4	9	7
	Zone 3	7	7
	Zone 2	6	9
	Zone 1	14	7
Skelly Guy Varnum 1 25-5N-18E	Zone 5	9	2.70 (bulk den)
	Zone 4	14	2.62
	Zone 3	11	2.52
	Zone 2	10	2.65
	Zone 1	31	2.70
Arco Jessie Bennett 2 30-5N-18E	Zone 5	6	3 (den por)
	Zone 4	12	5
	Zone 3	12	14
	Zone 2	8	4
	Zone 1	22	3
Trigg HunterTucker1-31 31-5N-18E	Zone 5	8	0 (porosity)
	Zone 4	12	0
	Zone 3	12	13
	Zone 2	12	2
	Zone 1	20	0
Arkoma HunterTucker 2 31-5N-18E	Zone 5	10	3 (den por)
	Zone 4	10	10
	Zone 3	12	9
	Zone 2	10	6
	Zone 1	20	3
Arkoma Kennedy b-2 32-5N-18E	Zone 5	11	7 (den por)
	Zone 4	10	8
	Zone 3	11	19
	Zone 2	7	11
	Zone 1	26	6
Coquina Watts 1 34-5N-18E	Zone 5	14	2.67 (bulk den)
	Zone 4	15	2.65
	Zone 3	17	2.5
	Zone 2	18	2.67
	Zone 1	7	2.62
Samson Mose 1 35-5N-18E	Zone 5	17	1 (den por)
	Zone 4	13	5
	Zone 3	18	4
	Zone 2	14	4
	Zone 1	14	1
Pan Am Reusch 1 3-5N-19E	Zone 5	9	52 (sonic)
	Zone 4	15	65
	Zone 3	8	78
	Zone 2	6	70
	Zone 1	16	55
Amoco Choctaw T-3 2 4- 5N- 19E	Zone 5	10	6 (den por )
	Zone 4	10	13
	Zone 3	10	17
	Zone 2	7	12
	Zone 1	13	4

WELL	ZONES	THICKNESS (ft)	AVE POROSITY
Pan Am Choctaw T-3 1 4- 5N- 19E	Zone 5	6	59 (sonic)
	Zone 4	10	68
	Zone 3	9	70
	Zone 2	12	73
	Zone 1	10	58
Pan Am Choctaw T-4 1 5- 5N- 19E	Zone 5	6	52 (sonic)
	Zone 4	8	70
	Zone 3	9	70
	Zone 2	6	73
	Zone 1	12	9
Pan Am McEtieran 1 6- 5N- 19E	Zone 5	12	51 (sonic)
	Zone 4	7	67
	Zone 3	10	75
	Zone 2	8	70
	Zone 1	11	56
Pan Am Quaid 1 7- 5N- 19E	Zone 5	10	53 (sonic)
	Zone 4	8	55
	Zone 3	14	75
	Zone 2	8	64
	Zone 1	10	60
Hadson College 1-8 8-5N- 19E	Zone 5	10	2.70 (bulk den)
	Zone 4	8	2.65
	Zone 3	14	2.5
	Zone 2	14	2.42
	Zone 1	14	2.70
Williford Burger 1-16 16- 5N- 19E	Zone 5	14	4 (den por)
	Zone 4	18	4
	Zone 3	22	10
	Zone 2	18	10
	Zone 1	20	4
Texaco Jennings 23-1 23- 5N- 19E	Zone 5	6	0 (den por)
	Zone 4	14	3
	Zone 3	16	9
	Zone 2	8	2
	Zone 1	16	0
Austrial Diamond 1-30 30- 5N- 19E	Zone 5	8	2.69 (bulk den)
	Zone 4	8	2.47
	Zone 3	18	2.39
	Zone 2	13	2.60
	Zone 1	21	2.69
Mustang Cathy 1 3- 5N- 20E	Zone 5	7	3 (den por)
	Zone 4	6	5
	Zone 3	10	10
	Zone 2	12	6
	Zone 1	30	3
An son Hardcastle 1-20 20- 5N- 20E	Zone 5	20	2.68 (bulk den)
	Zone 4	20	2.68
	Zone 3	23	2.45
	Zone 2	19	2.55
	Zone 1	30	2.75
An son Cindy 1-21 21- 5N- 20E	Zone 5	16	4 (den por)
	Zone 4	20	4
	Zone 3	20	14
	Zone 2	14	4
	Zone 1	46	2
Amoco Smith 1 26- 5N- 20E	Zone 5	20	2 (den por)
	Zone 4	24	2
	Zone 3	16	10
	Zone 2	16	14
	Zone 1	24	2
Amoco Bauman 1 27- 5N- 20E	Zone 5	20	2 (den por)
	Zone 4	18	1
	Zone 3	18	7
	Zone 2	18	19
	Zone 1	18	0
An son Turney 1-28 28- 5N- 20E	Zone 5	20	2 (den por)
	Zone 4	20	2
	Zone 3	22	15
	Zone 2	18	16
	Zone 1	38	0







**FORMATION DATA FOR BURIAL AND THERMAL HISTORY CURVES OF THE  
ARKOMA BASIN, LATIMER CO., OKLAHOMA**

	FORMATION	THICKNESS	TOT SS (%)	TOT SHALE (%)	TOT LMST (%)	TOT DOL (%)	
PENNSYLVANIAN	Boggy Creek	1090 ft	828 ft (76)	262 ft (24)			
	Savanna	2411 ft	676 ft (28)	1735 ft (72)			
	McAl	Cameron	1018 ft	105 ft (10)	913 ft (90)		
	Booch	872 ft	87 ft (10)	785 ft (90)			
	Hartshorne	218 ft		218 ft (100)			
	Atoka U.	694 ft		694 ft (100)			
	M	648 ft		648 ft (100)			
	L	920 ft		920 ft (100)			
	K	365 ft		365 ft (100)			
	J	348 ft		348 ft (100)			
	I	797 ft		797 ft (100)			
	Fanshawe	455 ft	45 ft (10)	410 ft (90)			
	Red Oak	1764 ft	258 ft (15)	1506 ft (85)			
	Panola	725 ft	145 ft (20)	580 ft (80)			
	Brazil	1940 ft		1940 ft (100)			
	C	312 ft		312 ft (100)			
	B	205 ft		205 ft (100)			
A	442 ft	113 ft (25)	329 ft (75)				
Spiro	68 ft	65 ft (97)	3 ft (3)				
MISSISSIPPIAN	Wapanucka	93 ft		12 ft (13)	81 ft (87)		
	Union Valley	400 ft	110 ft (28)	258 ft (64)	32 ft (8)		
	Cromwell	840 ft	598 ft (70)	242 ft (30)			
	Caney U.	135 ft	63 ft (47)	72 ft (53)			
	Caney L.	106 ft		106 ft (100)			
	Mays	209 ft		209 ft (100)			
	Osage	89 ft		89 ft (100)			
	Woodford	132 ft		132 ft (100)			
	Hunton	29 ft			29 ft (100)		
	Sylvan	62 ft		62 ft (100)			
ORDOVICIAN	Viola	126 ft			126 ft (100)		
	Bromide	303 ft			303 ft (100)		
	McLish	118 ft	43 ft (36)	10 ft (9)	65 ft (55)		
	Oil Creek U.	97 ft	28 ft (30)		69 ft (70)		
	Oil Creek L.	168 ft			168 ft (100)		
	Joins	174 ft		10 ft (5)	164 ft (95)		
	West Spr Cr	825 ft			825 ft (100)		
	Kindblade	825 ft			825 ft (100)		
	Cool Creek	825 ft			688 ft (80)	137 ft (20)	
	McKenzie	440 ft			440 ft (100)		
CAMBRIAN	Butterly	165 ft				165 ft (100)	
	Signal Mt.	385 ft			385 ft (100)		
	Royer	165 ft				165 ft (100)	
	Ft. Sill	440 ft			440 ft (100)		
	Honey Creek	100 ft			100 ft (100)		
	Regan SS	100 ft	100 ft (100)				

Estimated 4000 ft missing above the Boggy Creek. Formation data for the Boggy Creek to Cromwell; Samedan 1-9 Gibson, Sec 9, T6N, R20E, Latimer Co, OK.

Morrowan erosional event estimated 29 ft missing Wapanucka.

Formation data for the Cromwell to Arbuckle; Exxon A1 Reutherford, Sec 5, T3N, R18E, Latimer Co., OK.

Pre-Woodford erosional event estimated 250 ft missing strata.

APPENDIX D

PLATES I-IV

## VITA

Rodney B. Feller

Candidate for the Degree of

Master of Science

Thesis: CHARACTERISTICS OF ABNORMALLY-PRESSURED GAS COMPARTMENTS, AND POTENTIAL SEALING MECHANISMS IN THE SPIRO SANDSTONE: ARKOMA BASIN, OKLAHOMA.

Major Field: Geology

### Biography:

Education: Graduated from Moore High School, Moore, Oklahoma in May 1983; recieved Bachelor of Science degree in Geology with a minor in Geography from Oklahoma State University, Stillwater, Oklahoma in December 1993. Completed the requirements for the Master of Science degree with a major in Geology at Oklahoma State University in July 1995.

Experence: Employed by Oklahoma State University, Department of Geology as an undergraduate and as a graduate research assistant; Oklahoma State University, Department of Geology, 1992 to present. Employed as a summer intern by Exxon U. S. A. Production Division, May-August 1994.

Professional Memberships: American Association of Petroleum Geologists, Geological Society of America.

Figure 21 and  
Plates I, II, III,  
IV, and V.

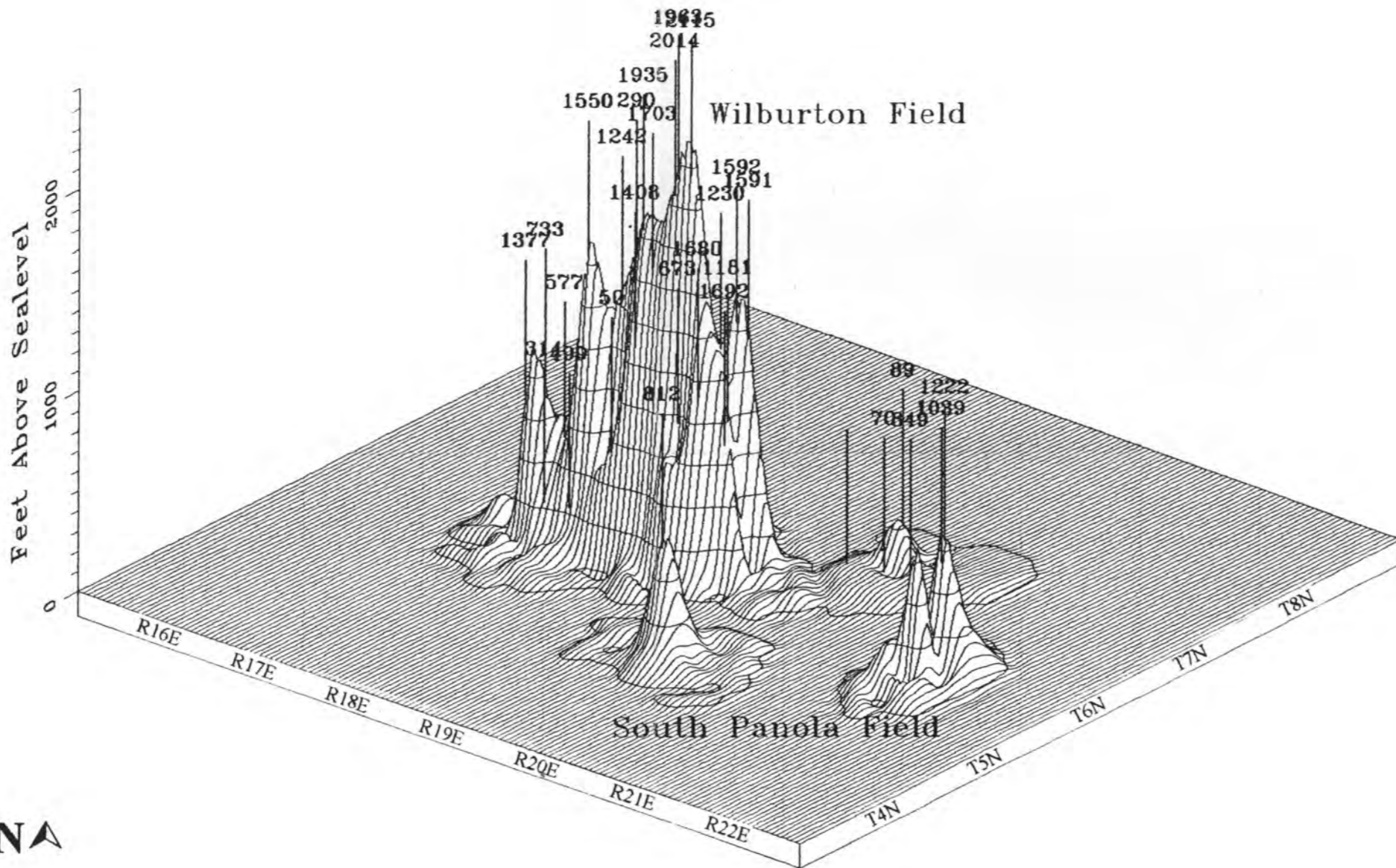


Figure 21. Three-dimentional plot, Spiro Sandstone, Wilburton and South Panola fields



